SPRINGER BRIEFS IN
ELECTRICAL AND COMPUTER ENGINEERING

Christoph Guger
Brendan Allison
Junichi Ushiba *Editors*

Brain-Computer Interface Research

A State-of-the-Art Summary 5

Springer

SpringerBriefs in Electrical and Computer Engineering

More information about this series at http://www.springer.com/series/10059

Christoph Guger · Brendan Allison
Junichi Ushiba
Editors

Brain-Computer Interface Research

A State-of-the-Art Summary 5

Springer

Editors
Christoph Guger
g.tec Guger Technologies OG
Schiedlberg
Austria

Brendan Allison
g.tec Guger Technologies OG
Schiedlberg
Austria

Junichi Ushiba
Biosciences and Informatics
Keio University
Yokohama
Japan

ISSN 2191-8112 ISSN 2191-8120 (electronic)
SpringerBriefs in Electrical and Computer Engineering
ISBN 978-3-319-57131-7 ISBN 978-3-319-57132-4 (eBook)
DOI 10.1007/978-3-319-57132-4

Library of Congress Control Number: 2017938537

Printed on acid-free paper

This Springer imprint is published by Springer Nature
The registered company is Springer International Publishing AG
The registered company address is: Gewerbestrasse 11, 6330 Cham, Switzerland

Contents

Brain-Computer Interface Research: A State-of-the-Art Summary 5

Christoph Guger, Brendan Allison and Junichi Ushiba

1 What Is a BCI?

Brain-computer interface (BCI) technology was first developed as a tool to provide basic communication, such as spelling, without movement. By detecting specific patterns of activity in the brain, BCIs can get a general idea of which messages or commands a user wants to send. For example, a user might pay attention to a flickering icon on a monitor with the letter "A" to spell that letter, or imagine left hand movement to move a cursor, wheelchair, or humanoid robot to the left. BCIs might detect brain activity through sensors outside the head, such as an electrode cap that detects the electroencephalogram (EEG) or sensors inside the head, such as electrocorticography (ECoG) activity that is detected during neurosurgery.

BCIs were initially developed to help patients with very severe motor disabilities, who otherwise could not communicate. The last several years have seen a shift to new patient groups and applications, such as helping stroke patients regain movement or helping neurosurgeons map the brain more accurately to perform surgery more quickly and safely. This book, and the awards from 2015, reflect and extend these trends, including BCIs to help new patient groups such as persons with cerebral palsy or severe brain damage.

C. Guger (✉) · B. Allison
g.tec Guger Technologies OG, 4521 Schiedlberg, Austria
e-mail: guger@gtec.at

B. Allison
e-mail: allison@gtec.at

J. Ushiba
Biosciences and Informatics, Keio University Biosciences and Informatics,
Yokohama, Kazagawa 223-8522, Japan
e-mail: ushiba@bio.keio.ac.jp

C. Guger et al. (eds.), *Brain-Computer Interface Research*,
SpringerBriefs in Electrical and Computer Engineering,
DOI 10.1007/978-3-319-57132-4_1

2 The Annual BCI Research Award

The Annual BCI Research Award is organized by G.TEC, a leading provider of BCI research equipment headquartered in Austria, with branches in Spain and the USA. Because of the growth of BCI research worldwide, G.TEC decided to create an Annual BCI Research Award to recognize new achievements. The international competition is open to any group doing BCI research, regardless of region, hardware or software used, prior publications, or other factors. The first Award was presented in 2010, and followed the same process that has been used in subsequent years:

- G.TEC selects a Chairperson of the Jury from a well-known BCI research institute.
- This Chairperson forms a jury of top BCI researchers who can judge the Award submissions.
- G.TEC publishes information about the BCI Award for that year, including submission instructions, scoring criteria, and a deadline.
- The jury reviews the submissions and scores each one across several criteria. The jury then determines ten nominees and one winner.
- The nominees are announced online, and invited to a Gala Award Ceremony that is attached to a major conference (such as an International BCI Meeting or Conference).
- At this Gala Award Ceremony, the ten nominees each receive a certificate, and the winner is announced. The winner earns $3000 USD and the prestigious trophy. In 2014, we added prizes for the 2nd place winner ($2000 USD) and 3rd place ($1000 USD).

Each year, the juries have scored the submissions based on several award criteria. Given the intensity of the competition, nominated projects typically score high on several of these criteria:

- Does the project include a novel application of the BCI?
- Is there any new methodological approach used compared to earlier projects?
- Is there any new benefit for potential users of a BCI?
- Is there any improvement in terms of speed of the system (e.g. bit/min)?
- Is there any improvement in terms of accuracy of the system?
- Does the project include any results obtained from real patients or other potential users?
- Is the used approach working online/in real-time?
- Is there any improvement in terms of usability?
- Does the project include any novel hardware or software developments?

Fig. 1 This picture shows attendees watching the Award Ceremony in the Cuvée in Chicago

The 2015 jury was:

- *Junichi Ushiba (chair of the jury 2015)*,
- *Msayuki Hirata*
- *Nuri Firat Ince*
- *Zachary Freudenburg*
- *José del R. Millán*
- *Sydney Cash*
- *Tomasz M. Rutkowski (winner 2014)*

Like previous BCI Awards, the jury included the winner from the preceding year (Dr. Rutkowski). The chair of the jury, Dr. Junichi Ushiba, is a top figure in BCI research and leads the well-known BCI lab at Keio University, Japan. Dr. Ushiba said: "I was very fortunate to work with the 2015 jury. All of the jury members that I approached chose to join the jury, and we had an outstanding team."

Also like previous BCI Awards, we held the annual Gala Award Ceremony in tandem with a major conference. In 2015, this was the annual Society for Neuroscience conference in Chicago, Illinois. The ceremony was held at the Cuvée in Chicago and was very well attended. Dr. Guger organized the event, with Dr. Allison acting as moderator. The ceremony began with an introduction of all projects that were nominated, and the recipients came onstage to receive their certificates. Next, we announced the first, second, and third place winners and presented their awards (Figs. 1 and 2).

Fig. 2 Christoph Guger (organizer), Christian Herff (nominee), Kenji Kato (nominee), and Brendan Allison (moderator)

3 The BCI Book Series

Each year, we ask the nominees to write a chapter for this book series. While these chapters mainly present the work that they submitted for the BCI Award, authors are also invited to present newer work, discussion, and related material. The authors who contributed to this book have all remained active since being nominated, and thus they all have newer work from as late as fall 2015.

One of our concerns in editing and managing the chapters is accessibility to non-experts. While chapters present advanced material, we have tried to explain many terms and develop figures and tables to help illustrate the BCI systems and the results. Students and newcomers to BCI research should be able to understand the different BCI advances presented in the chapters and why they matter. Also, like BCI research in general, the chapters here address a wide variety of disciplines, including neuroscience, psychology, engineering, mathematics, and medicine.

The chapters from this year's nominees are consistent with many broader trends in BCIs. Both invasive and noninvasive systems are presented, with a strong focus on online, real-world systems for patients. A few chapters aim to help patient groups that have been prominent in recent BCI research, such as diagnostic BCI tools for patients with disorders of consciousness (DOC) or BCIs to control prosthetic hands. Different chapters present original work that extends BCI technology to new patient groups, such as persons with chronic pain, cerebral palsy, or cerebellar damage. Two chapters show how invasive technology could be used to control finger movement or decode speech, which could lead to "literal" BCIs that

can directly decode imagined words. One chapter even presents BCI-based cockroach control. Overall, these chapters both reflect trends in BCI research and describe several novel directions.

4 Projects Nominated for the BCI Award 2015

In 2015, 60 high quality research projects were submitted from all over the world! The jury, chaired by Junichi Ushiba, carefully scored 10 nominated projects, and then selected the winner for the Annual BCI Research Award 2014. The ten nominees,[4] presented alphabetically by first author, were:

Peter Brunner, Karen Dijkstra, Will Coon, Jürgen Mellinger, Anthony L. Ritaccio, Gerwin Schalk (Albany Medical College and the National Center for Adaptive Neurotechnologies, Wadsworth Center, Albany, US).

An ECoG-Based BCI on Auditory Attention to Natural Speech

R. Chavarriaga[1], L.A. Gheorghe[1,2], H. Zhang[1], Z. Khaliliardali[1], J. d. R. Millán[1] ([1]Defitech Chair in Brain-Machine Interface, Center for Neuroprosthetics, EPFL, Lausanne, CH,[2] Mobility Services Laboratory, Nissan Research Center, Nissan Motor Co., JP).

Easy Riders: Brain-Computer Interfaces for Enhancing Driving Experience

Damien Coyle (School of Computing and Intelligent Systems, Ulster University, UK).

Sensorimotor Modulation Assessment and Brain-Computer Interface Training with Auditory Feedback in Disorders of Consciousness

Christian Herff[1], Dominic Heger[2], Adriana de Pesters[3], Dominic Telaar[2], Peter Brunner[3,4], Gerwin Schalk[3,4], Tanja Schultz[1] ([1]Cognitive Systems Lab, Universität Bremen, Bremen, DE, [2]Cognitive Systems Lab, Karlsruhe Institute of Technology, Karlsruhe, DE, [3]National Resource Center for Adaptive Neurotechnologies, Wadsworth Center, Albany, US, [4]Department of Neurology, Albany Medical College, Albany, US).

Brain-to-Text: Towards Continuous Speech as a Paradigm for BCI

Roni Hogri[1,3], Simeon A. Bamford[2,4], Aryeh H. Taub[1,5] ([1]Psychobiology Research Unit, Tel Aviv University, IL,[2] Complex Systems Modeling Group, Istituto Superiore di Sanità, IT, [3]Department of Neurophysiology, Medical University of Vienna, AT,[4] Inilabs Gmbh, CH,[5] Department of Neurobiology, Wiezmann Institute of Science, IL).

De Novo Experience-Based Learning in Rats Interfaced with a "Cerebellar Chip"

Guy Hotson[1], David P McMullen[2], Matthew S. Fifer[3], Matthew S. Johannes[4], Kapil D. Katyal[4], Matthew P. Para[4], Robert Armiger[4], William S. Anderson[2], Nitish V. Thakor[3], Brock A. Wester[4], Nathan E. Crone[5] ([1]Department of Electrical and Computer Engineering, Johns Hopkins University, US,[2] Department of Neurosurgery, Johns Hopkins University, US, [3]Department of Biomedical Engineering, Johns Hopkins University, US,[4] Applied Neuroscience, JHU Applied Physics Laboratory, US, [5]Department of Neurology, Johns Hopkins University, US).

Individual Finger Control of the Modular Prosthetic Limb Using High-Density Electrocorticography in a Human Subject

Kenji Kato, Masahiro Sawada, Tadashi Isa, Yukio Nishimura (National Institute for Physiological Sciences, Aichi, JP).

Restoration for the Volitional Motor Function via an Artificial Neural Connection

Guangye Li, Dingguo Zhang (Robotics Institute, School of Mechanical Engineering, Shanghai Jiao Tong University, CN).

Brain-Computer Interface Controlling Cyborg: A Functional Brain-to-Brain Interface between Human and Cockroach

N Mrachacz-Kersting[1], L Yao[2], S Gervasio[1], N Jiang[3], BD Ebbesen[1], TS Palsson[1], TG Nielsen[1], R. Xu[2], D. Falla[2], K Dremstrup[1], D Farina[2] ([1]Sensory-Motor Interaction, Aalborg University, DK,[2] University Medical Center, Göttigen, DE, [3]University of Waterloo, CA).

A Brain-Computer-Interface to Combat Musculoskeletal Pain

Sergey D. Stavisky, Jonathan C. Kao, Paul Nuyujukian, Stephen I. Ryu, Krishna V. Shenoy (Stanford University, US).

Increasing the Useful Lifespan of Intracortical BCIs by Decoding Local Field Potentials as an Alternative or Compliment to Spikes

5 Summary

The BCI Research Awards have continued to recognize and promote high quality BCI research worldwide. Our book series have been widely downloaded and have hopefully helped to teach and inspire a new generation of BCI researchers. The ten nominees from 2015 have kept the tradition of top-quality submissions alive, and the chapters that follow present many of the best BCI projects of 2015.

An ECoG-Based BCI Based on Auditory Attention to Natural Speech

Peter Brunner, Karen Dijkstra, William G. Coon, Jürgen Mellinger, Anthony L. Ritaccio and Gerwin Schalk

Abstract People affected by severe neuro-degenerative diseases (e.g., late-stage amyotrophic lateral sclerosis (ALS) or locked-in syndrome) eventually lose all muscular control and are no longer able to gesture or speak. For this population, an auditory BCI is one of only a few remaining means of communication. All currently used auditory BCIs require a relatively artificial mapping between a stimulus and a communication output. This mapping is cumbersome to learn and use. Recent studies suggest electrocorticographic (ECoG) signals in the gamma band (i.e., 70–170 Hz) can be used to infer the identity of auditory speech stimuli, effectively removing the need to learn such an artificial mapping. However, BCI systems that use this physiological mechanism for communication purposes have not yet been described. In this study, we explore this possibility by implementing a BCI2000-based real-time system that uses ECoG signals to identify the attended speaker.

1 Introduction

People affected by severe neuro-degenerative diseases (e.g., late-stage amyotrophic lateral sclerosis (ALS) or locked-in syndrome) eventually lose all muscular control and are no longer able to gesture or speak. They also cannot use traditional assistive communication devices that depend on muscle control, nor typical brain-computer-interfaces (BCIs) that depend on visual stimulation or feedback [1–3]. For this population, auditory [4–8] and tactile BCIs [9, 10] are two of only a few remaining means of communication (see [11] for review).

While visual BCIs typically preserve the identity between the stimulus (e.g., a highlighted 'A') and the symbol the user wants to communicate (e.g., the letter 'A'), all currently used auditory or tactile BCIs require a relatively artificial mapping between a stimulus (e.g., a particular but arbitrary sound) and a communication

P. Brunner · K. Dijkstra · W.G. Coon · J. Mellinger · A.L. Ritaccio · G. Schalk (✉)
New York State Department of Health, Center for Adapt Neurotech,
Wadsworth Center, Albany, NY, USA
e-mail: gerwin.schalk@health.ny.gov

C. Guger et al. (eds.), *Brain-Computer Interface Research*,
SpringerBriefs in Electrical and Computer Engineering,
DOI 10.1007/978-3-319-57132-4_2

output (e.g., a particular letter or word). This mapping is easy to learn when there are only few possible outputs (e.g., a yes or no command). However, with an increasing number of possible outputs, such as with a spelling device, this mapping becomes arbitrary and complex. This makes most current auditory and tactile BCI systems cumbersome to learn and use.

Two avenues are being investigated to overcome this limitation. The first avenue is to directly decode expressive silent speech without requiring any external stimuli. In this approach, linguistic elements at different levels (e.g., phonemes, syllables, words and phrases) are first decoded from brain signals and then synthesized into speech. While recent studies have demonstrated this possibility [12–16], even invasive brain imaging techniques (e.g., ECoG, LFPs, single neuronal recordings) are currently unable to capture the entire complexity of expressive speech. Consequently, silent speech BCIs are limited in the vocabulary that can be decoded directly from the brain signals. The second avenue is to replace unnatural stimuli that require an artificial mapping with speech stimuli that do not. In such a system, the user would communicate simply by directing attention to the speech stimulus that matches his/her intent. Previous studies that explored this avenue required the speech stimuli to be designed (e.g., altered and broken up [17]) such that they elicit a particular and discriminable evoked response. Such evoked responses can be readily detected in scalp-recorded electroencephalography (EEG) to identify the attended speech stimulus. However, such altered speech stimuli are difficult to understand, which makes such a BCI system difficult to use. More importantly, this approach does not scale well beyond two simultaneously presented speech stimuli.

Recent studies suggest that the envelope of attended speech is directly tracked by electrocorticographic (ECoG) signals in the gamma band (i.e., 70–170 Hz) [15, 18–21], effectively removing the need to 'alter' the speech stimuli. Further evidence shows that this approach can identify auditory attention to one speaker in a mixture of speakers, i.e., a 'cocktail-party' situation [22].

However, BCI systems that use this physiological mechanism for communication purposes have not been described yet. In this study, we explore this possibility by implementing a BCI2000-based real-time system that uses ECoG signals to identify the attended speaker.

2 Methods

2.1 Human Subject

The subject in this study was a 49 year old left handed woman with intractable epilepsy who underwent temporary placement of subdural electrode arrays (see Fig. 1a) to localize seizure foci prior to surgical resection. A neuropsychological evaluation [23] revealed normal cognitive function and hearing (full scale IQ = 97, verbal IQ = 91, performance IQ = 99) and a pre-operative Wada test [24] determined left hemispheric language dominance.

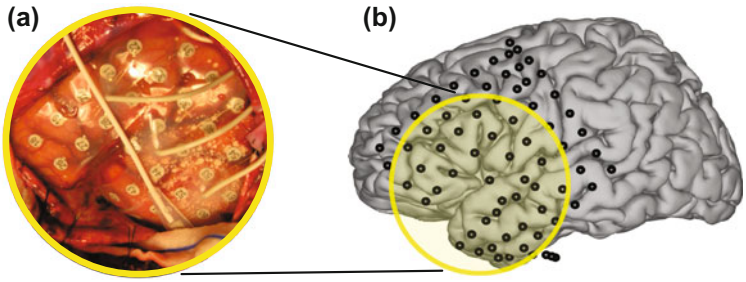

Fig. 1 Implant. The subject had 72 subdural electrodes (1 grid and 3 strips in different configurations) implanted over left frontal, parietal, and temporal regions. **a** Photograph of the craniotomy and the implanted grids in this subject. **b** Cortical model of the subject's brain, showing an 8 × 8 grid over frontal/parietal cortex, and two strips

The subject had a total of 72 subdural electrode contacts (one 8 × 8 64-contact grid with 3 contacts removed, two strips in 1 × 4 configuration, and one strip in 1 × 3 configuration). The grid and strips were placed over the left hemisphere in frontal, parietal and temporal regions (see Fig. 1b for details). The implants consisted of flat electrodes with an exposed diameter of 2.3 mm and an inter-electrode distance of 1 cm, and were implanted for one week. Grid placement and duration of ECoG monitoring were based solely on the requirements of the clinical evaluation, without any consideration of this study. The subject provided informed consent, and the study was approved by the Institutional Review Board of Albany Medical College.

We used post-operative radiographs (anterior-posterior and lateral) and computed tomography (CT) scans to verify the cortical location of the electrodes. We then used Curry software (Neuroscan Inc, El Paso, TX) to create subject-specific 3D cortical brain models from high-resolution pre-operative magnetic resonance imaging (MRI) scans. We co-registered the MRIs by means of the post-operative CT and extracted the electrode coordinates according to the Talairach Atlas [25]. These electrode coordinates are depicted on Talairach template brain in Fig. 1b.

2.2 Data Collection

We recorded ECoG from the implanted electrodes using a g.HIamp amplifier/digitizer system (g.tec, Graz, Austria) and the BCI software platform BCI2000 [26–28], which sampled the data at 1200 Hz. Simultaneous clinical monitoring was implemented using a connector that split the cables coming from the patient into one set that was connected to the clinical monitoring system and another set that was connected to the g.HIamp devices. This ensured that clinical data collection was not compromised at any time. Two electrocorticographically silent electrodes (i.e., locations that were not identified as eloquent cortex by electrocortical stimulation mapping) served as electrical ground and reference, respectively.

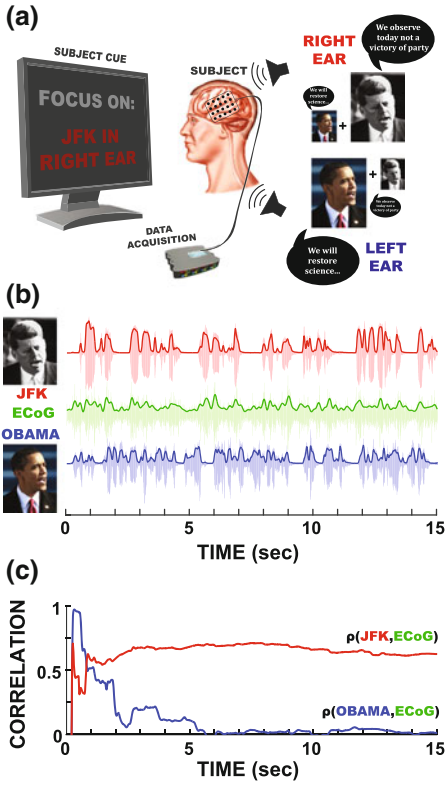

Fig. 2 Experimental setup and methods. **a** Subjects selectively directed auditory attention to one of two simultaneously presented speakers. **b** We extracted the envelope of ECoG signals in the high gamma band, as well as the envelopes of the attended and unattended speech stimuli (i.e., JFK and Obama). **c** The correlation between the envelopes of the ECoG gamma band and the attended speech stimulus, accumulated over time, is markedly larger than the accumulated correlation between the envelopes of the ECoG gamma band and the unattended speech stimulus

2.3 Stimuli and Task

The subject's task was to selectively attend to one of two simultaneously presented speakers in a cocktail party situation (see Fig. 2a). The two speakers were John F. Kennedy and Barack Obama, each delivering his presidential inauguration address. Both speeches were similar in their linguistic features, but were uncorrelated in their sound intensities ($r = -0.02, p = 0.9$). To create a cocktail party situation, we mixed the two (monaural) speeches into a binaural presentation in which the stream presented to each ear contained 20% : 80% of the volume of one speaker and 80% : 20% of the other, respectively. This allowed us to manipulate the aural location of each speaker throughout the task. For the binaural presentation, we used in-ear monitoring earphones (AKP IP2, 12–23500 Hz bandwidth) that isolated the subject from any ambient noise in the room.

To create a trial structure, we broke these combined streams into segments of 15–25 s in length, which resulted in a total of 10 segments of 187 s combined length. In the course of the experiment, we presented each segment four times to counterbalance the aural location (i.e., left and right) and the identity (i.e., JFK and Obama)

of the attended speaker. Thus, over these four trials, the subjects had to attend to each of the two speakers at each of the two aural locations. This resulted in a total of 40 trials (i.e., 10 segments, each presented 4 times).

At the beginning of each trial, an auditory cue indicated the aural location (i.e., left or right) to which the subject should attend. Throughout the trial, a visual stimulus complemented the initial auditory cue to indicate the identity of the aural location (e.g., 'JFK in LEFT ear'). Each trial consisted of a 4 s cue, a 15–25 s stimulus and a 5 s inter-stimulus period. The total length of these 40 trials was 12.5 min. The subject performed these 40 trials in 5 blocks of 8 trials each, with a 3 min break between each block.

2.4 Offline Analysis

In the offline analysis, we characterized the relationship between the neural response (i.e., the ECoG signals) and the attended and unattended speech streams, as shown in Fig. 2b. In particular, we were interested in two parameters of this neural response. The first parameter was the delay between the audio stream and resulting cortical processing, i.e., the time from presentation of the audio stream to the observation of the cortical change. The second parameter was the cortical location that was most selective to the attended speech stream. These two parameters are the only two parameters that were later needed to configure the online BCI system.

To determine these two parameters, we extracted the high gamma band envelope at each cortical location and the envelopes of the covertly attended and unattended speech (i.e., JFK and Obama). We then correlated the high gamma band envelope at each cortical location, once with the attended and once with the unattended speech envelope. This resulted in two Spearman's r-values for each cortical location. An example of this is shown in Fig. 2c. To determine the delay between the audio stream and resulting cortical processing, we measured the neural tracking of the sound intensity across different delays from 0 to 250 ms to identify the deal with the highest r-value.

2.4.1 Signal Processing

We first pre-processed the ECoG signals from the 72 channels to remove external noise. To do this, we high-pass filtered the signals at 0.5 Hz and re-referenced them to a common average reference that we composed from only those channels for which the 60 Hz line noise was within 1.5 standard deviations of the average.

Next, we extracted the signal envelope in the high gamma band using these pre-processed ECoG signals. For this, we applied an 18th order 70–170 Hz Butterworth filter and then extracted the envelope of the filtered signals using the Hilbert transform. Finally, we low-pass filtered the resulting signal envelope at 6 Hz (anti-aliasing) and downsampled the result to 120 Hz.

For each attended and unattended auditory stream, we extracted the time course of the sound intensity, i.e., the envelope of the signal waveform in the speech band. To do this, we applied a 80–6000 Hz Butterworth filter to each audio signal, and then extracted the envelope of the filtered signals using the Hilbert transform. Finally, we low-pass filtered the speech envelopes at 6 Hz and downsampled them to 120 Hz.

2.4.2 Feature Extraction

We extracted features that reflect the neural tracking of the attended and unattended speech stream. We defined neural tracking of speech as the correlation between the gamma envelope (of a given cortical location) and the speech envelope. We calculated this correlation separately for the attended and unattended speech, thereby obtaining two sets of r-values labeled 'attended' and 'unattended,' respectively.

2.4.3 Selection of Cortical Delay and Location

We expected a delay between the audio presentation and resulting cortical processing, i.e., the time from presentation of the audio stimuli to the observation of the cortical change. To account for this delay, we measured the neural tracking of the attended speech stream across different delays (0–250 ms, see Fig. 3) and across all channels. Next, we determined the cortical location that was most selective of the attended speech stream. For this, we selected the cortical location that showed the largest difference between the 'attended' and 'unattended' r-values. Based on these results, we selected a delay of 150 ms and a cortical location over superior temporal gyrus (STG). We corrected for this delay by shifting the speech envelopes relative to the ECoG envelopes prior to calculating the correlation values.

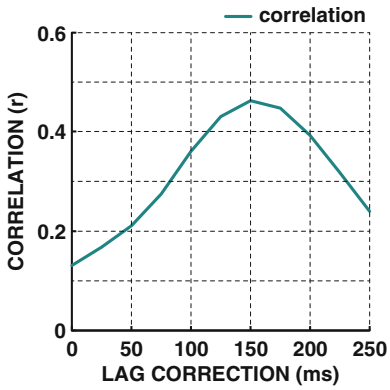

Fig. 3 Lag between speech presentation and neural response. This figure shows the correlation between neural response and the attended speech (*green*) for the most selective cortical location, across corrected lags between 0 and 250 ms. This correlation peaks at 150 ms

2.4.4 Classification

In our approach, we assumed that the extracted features, i.e., the two r-values of the selected cortical location, were directly predictive of the 'attended' conversation. In other words, for the selected cortical location, if the 'attended' r-value was larger than the 'unattended' r-value, the the trial was classified correctly. To determine the performance as a function of the length of attention, we applied our feature extraction and classification procedure to data segments from 0.1 to 15 s in length.

2.5 Real-Time System Verification

In the real-time verification, we evaluated the system performance on the data recorded during the first stage of this study. We configured this system with parameters (i.e., cortical location and delay) determined in the previously detailed offline analysis.

2.5.1 Real-Time System Architecture

We used the BCI software platform BCI2000 [26–28] to implement an auditory attention based BCI. For this, we expanded BCI2000 with the capability to process auditory signals in real time. In detail, we implemented a signal acquisition for audio devices (e.g., a microphone) or pre-recorded files that is synchronized with the acquisition from the neural signals. Further, we implemented a signal correlation filter. For our evaluation, the two (monaural) speeches served as the audio input to the auditory attention based BCI (see Fig. 4).

In this system, BCI2000 filters the audio signals between 80 and 6000 Hz and the ECoG signals between 70 and 170 Hz. Next, a BCI2000 filter extracts the envelopes, decimates them to a common sampling rate of 200 Hz and adjusts their timing for the cortical delay. A signal correlation filter then calculates the correlation values, i.e., the correlation between the two (monaural) speeches and the selected neural envelope, to determine to which speaker the user directs his/her attention. Finally, the feedback augmentation filter increases the volume of the attended speaker and decreases the volume of the unattended speaker to provide feedback to the subject. This processing steps are updated every 50 ms to provide feedback in real-time.

3 Results

3.1 Neural Correlates of Attended and Unattended Speech

First, we were interested in visualizing the cortical areas that track the 'attended' and 'unattended' conversations. The results in Fig. 5 show the neural tracking of

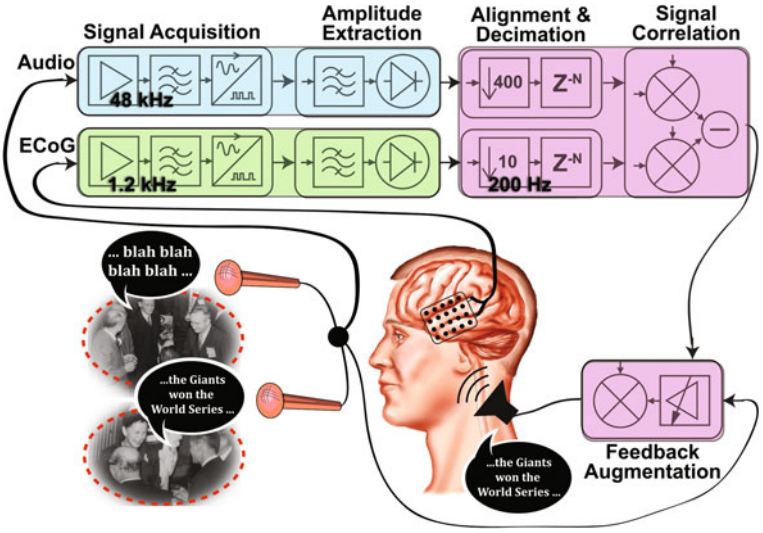

Fig. 4 Real-time system design. The auditory attention BCI is based on BCI2000 and simultaneously acquires and processes **audio** and **ECoG** signals. The audio signals from multiple conversations are sampled at 48 kHz and acquired from a low-latency USB audio-amplifier (Tascam US-122MKII). The ECoG signals from the surface of the brain are sampled at 1200 Hz and acquired from a 256-channel bio-signal amplifier (g.HIamp, g.tec Austria). In the next step, the signals are band-pass filtered (80–6000 Hz for audio, 70–170 Hz for ECoG) and their envelope is extracted. The resulting signal envelopes are decimated to a common sampling rate of 200 Hz and adjusted for timing differences. One channel of the decimated ECoG signal envelope is then selected and correlated with each of the decimated audio signal envelopes. As the human subject perceives the mixture of conversations through ear-phones, the auditory attention BCI then can provide feedback by modifying the volume of the presented mixture of conversations to enhance the volume of the attended and attenuate the volume of the unattended conversation

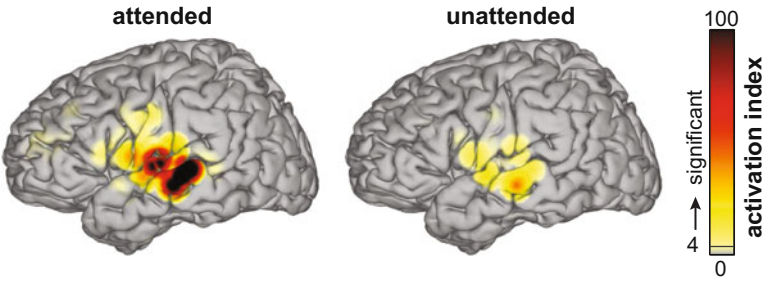

Fig. 5 Neural tracking of attended (*left*) and unattended (*right*) speech. The tracking of the attended speech is both stronger and more widely distributed than the tracking of the unattended speech. In addition, there is only a marginal difference in spatial distribution between attended and unattended stimuli

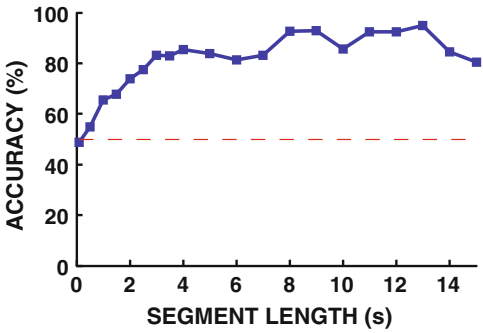

Fig. 6 Accuracy for different segment lengths. The classification accuracy generally increases with segment length. The *red horizontal dashed line* indicates chance accuracy

the 'attended' and 'unattended' speech in the form of an activation index. For each cortical location, this activation index expresses the negative logarithm of the p-value (−log(p)) of the correlation between the high gamma ECoG envelope and the attended or unattended speech envelope. The neural tracking is focused predominantly on areas on or around superior (STG) and middle temporal gyrus (MTG).

3.2 Relationship Between Segment Length and Classification Accuracy

Next, we were interested in determining the duration of attention that is needed to infer the 'attended' speech. For this, we examine the relationship between the segment length and classification accuracy. The results in Fig. 6 show the classification accuracies for variable segment lengths (0.1–15 s). In this graph, the accuracy improvements level off after 5 s, at 80–90% accuracy.

3.3 Interface to the Investigator

Finally, we evaluated the real-time system performance that the determined parameters (i.e., the cortical location and delay) yield on the data recorded during the first stage of this study. The screenshot in Fig. 7 shows interface to the investigator. The interface presents the decimated and aligned ECoG and audio envelopes, their correlation with each other, and the inferred attention. The content of this interface is updated 20 times per second.

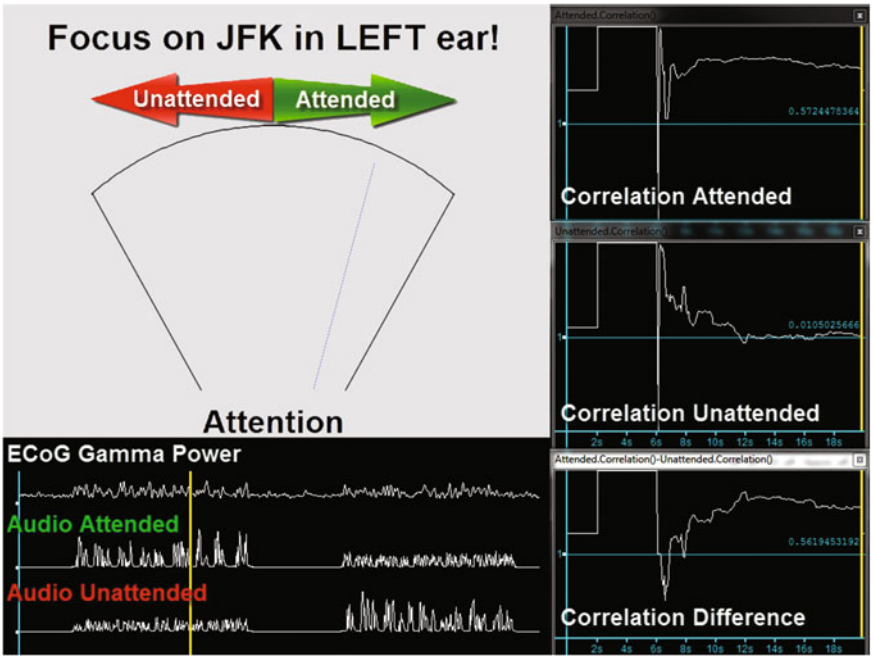

Fig. 7 Interface design. The interface to the investigator presents multiple panels. The *bottom left panel* presents the decimated and aligned ECoG and audio envelopes. The panels on the *right* show the correlation between the ECoG and the attended (*top*), ECoG and unattended (*middle*) and the difference between the two correlation values (*bottom*). The panel on the *top left* shows this correlation difference in form of an analogue instrument where the pointer (i.e., the needle) indicates the direction of attention. In this experiment, the subject was cued to attend to a particular speaker annotated by "Attended" in this panel

4 Discussion

We show the first real-time implementation of an auditory attention BCI that uses ECoG signals and natural speech stimuli. The configuration of this system requires only two parameters: the cortical location and the delay between the audio presentation and the cortical processing. Our results can guide the selection of these parameters. For example, our results indicate that the underlying physiological mechanism is primarily focused on the temporal lobe, specifically the STG and MTG areas. Further, the neural tracking of attended speech is stronger and more widely distributed than that of unattended speech. This confirms results from a previous ECoG study that investigated auditory attention [22]. Further, our study shows that the cortical delay between the audio presentation and the cortical processing is in the range of ∼150 ms.

The presented results indicate that such system could support BCI communication. While being invasive, it may be justified for those affected by severe neurodegenerative diseases (e.g., late-stage ALS, locked-in syndrome) who have lost all muscular control and therefore cannot use conventional assistive devices or BCIs that depend on visual stimulation or feedback. Most importantly, the results suggest that sufficient communication performance (>70%, [29]) could be achieved with a single electrode placed over STG or MTG. This finding is important, because placement of ECoG grids as used in this study requires a large craniotomy. In contrast, a single electrode could be placed through a burr hole [30]. Furthermore, the electrodes in this study were placed subdurally (i.e., the electrodes are placed underneath the dura). Penetration of the dura increases the risk of bacterial infection [31–35]. Epidural electrodes (i.e., electrodes placed on top of the dura) provide signals of approximately comparable fidelity [36, 37]. A single electrode placed epidurally could reduce risk, which should make this approach more clinically practical.

In this study, we focused on demonstrating that one cortical location is sufficient for providing BCI communication. However, it is likely that combining the information from multiple cortical locations could substantially improve the communication performance. Thus, recent advances in clinically practical recordings of ECoG signals from multiple cortical locations [38, 39] could improve the clinical efficacy of the presented approach.

In comparison to many other auditory BCIs, the present approach has the unique advantage of using natural speech without any alteration. This aspect may be particularly relevant for those who are already at a stage where learning how to use a BCI has become difficult.

5 Conclusion

In summary, our study demonstrates the function of an auditory attention BCI that uses ECoG signals and natural speech stimuli. The implementation of this system within BCI2000 lays the groundwork for future studies that investigate the clinical efficacy of this system. Once clinically evaluated, such a system could provide communication without depending on other sensory modalities or a mapping between the stimulus and the communication intent. In the near future, this could substantially benefit people affected by severe motor disabilities that cannot use conventional assistive devices or BCIs that require some residual motor control, including eye movement.

Acknowledgements This work was supported by the NIH (EB006356 (GS), EB00856 (GS) and EB018783 (GS)), the US Army Research Office (W911NF-07-1-0415 (GS), W911NF-08-1-0216 (GS) and W911NF-14-1-0440 (GS)) and Fondazione Neurone.

References

1. J.R. Wolpaw, N. Birbaumer, D.J. McFarland, G. Pfurtscheller, T.M. Vaughan, Clin. Neurophysiol. **113**(6), 767 (2002). doi:10.1016/S1388-2457(02)00057-3
2. P. Brunner, S. Joshi, S. Briskin, J.R. Wolpaw, H. Bischof, G. Schalk, J. Neural Eng. **7**(5), 056013 (2010). doi:10.1088/1741-2560/7/5/056013
3. P. Brunner, G. Schalk, Clin. Neurophysiol. (2010). doi:10.1016/j.clinph.2010.11.014
4. A. Belitski, J. Farquhar, P. Desain, J. Neural Eng. **8**(2), 025022 (2011). doi:10.1088/1741-2560/8/2/025022
5. A. Furdea, S. Halder, D.J. Krusienski, D. Bross, F. Nijboer, N. Birbaumer, A. Kübler, Psychophysiology **46**(3), 617 (2009). doi:10.1111/j.1469-8986.2008.00783.x
6. D.S. Klobassa, T.M. Vaughan, P. Brunner, N.E. Schwartz, J.R. Wolpaw, C. Neuper, E.W. Sellers, Clin. Neurophysiol. **120**(7), 1252 (2009)
7. S. Halder, M. Rea, R. Andreoni, F. Nijboer, E.M. Hammer, S.C. Kleih, N. Birbaumer, A. Kübler, Clin. Neurophysiol. **121**(4), 516 (2010). doi:10.1016/j.clinph.2009.11.087
8. M. Schreuder, B. Blankertz, M. Tangermann, PLoS ONE **5**(4) (2010). doi:10.1371/journal.pone.0009813
9. A.M. Brouwer, J.B. van Erp, Front. Neurosci. **4**, 19 (2010). doi:10.3389/fnins.2010.00019
10. M. van der Waal, M. Severens, J. Geuze, P. Desain, J. Neural Eng. **9**(4), 045002 (2012). doi:10.1088/1741-2560/9/4/045002
11. A. Riccio, D. Mattia, L. Simione, M. Olivetti, F. Cincotti, J. Neural Eng. **9**(4), 045001 (2012). doi:10.1088/1741-2560/9/4/045001
12. X. Pei, D.L. Barbour, E.C. Leuthardt, G. Schalk, J. Neural Eng. **8**(4), 046028 (2011). doi:10.1088/1741-2560/8/4/046028
13. E.C. Leuthardt, C. Gaona, M. Sharma, N. Szrama, J. Roland, Z. Freudenberg, J. Solis, J. Breshears, G. Schalk, J. Neural Eng. **8**(3), 036004 (2011). doi:10.1088/1741-2560/8/3/036004
14. X. Pei, J. Hill, G. Schalk, IEEE Pulse **3**(1), 43 (2012). doi:10.1109/MPUL.2011.2175637
15. S. Martin, P. Brunner, C. Holdgraf, H.J. Heinze, N.E. Crone, J. Rieger, G. Schalk, R.T. Knight, B. Pasley, Front. Neuroeng. **7**(14) (2014). doi:10.3389/fneng.2014.00014
16. F. Lotte, J.S. Brumberg, P. Brunner, A. Gunduz, A.L. Ritaccio, C. Guan, G. Schalk, Front. Hum. Neurosci. **9**, 97 (2015). doi:10.3389/fnhum.2015.00097
17. M.A. Lopez-Gordo, E. Fernandez, S. Romero, F. Pelayo, A. Prieto, J. Neural Eng. **9**(3), 036013 (2012). doi:10.1088/1741-2560/9/3/036013
18. C. Potes, A. Gunduz, P. Brunner, G. Schalk, NeuroImage **61**(4), 841 (2012). doi:10.1016/j.neuroimage.2012.04.022
19. C. Potes, P. Brunner, A. Gunduz, R.T. Knight, G. Schalk, NeuroImage **97**, 188 (2014). doi:10.1016/j.neuroimage.2014.04.045
20. B.N. Pasley, S.V. David, N. Mesgarani, A. Flinker, S.A. Shamma, N.E. Crone, R.T. Knight, E.F. Chang, PLoS Biol. **10**(1), e1001251 (2012). doi:10.1371/journal.pbio.1001251
21. J. Kubanek, P. Brunner, A. Gunduz, D. Poeppel, G. Schalk, PLoS ONE **8**(1), e53398 (2013). doi:10.1371/journal.pone.0053398
22. E.M. Zion Golumbic, N. Ding, S. Bickel, P. Lakatos, C.A. Schevon, G.M. McKhann, R.R. Goodman, R. Emerson, A.D. Mehta, J.Z. Simon, D. Poeppel, C.E. Schroeder, Neuron **77**(5), 980 (2013). doi:10.1016/j.neuron.2012.12.037
23. D. Wechsler, *Weschsler Adult Intelligence Scale-III* (The Psychological Corporation, San Antonio, TX, 1997)
24. J. Wada, T. Rasmussen, J. Neurosurg. **17**, 266 (1960)
25. J. Talairach, P. Tournoux, *Co-Planar Sterotaxic Atlas of the Human Brain* (Thieme Medical Publishers Inc., New York, 1988)
26. G. Schalk, D.J. McFarland, T. Hinterberger, N. Birbaumer, J.R. Wolpaw, IEEE Trans. Biomed. Eng. **51**(6), 1034 (2004)
27. J. Mellinger, G. Schalk, in *Toward Brain-Computer Interfacing*, ed. by G. Dornhege, J. del R. Millan, T. Hinterberger, D. McFarland, K. Müller, (MIT Press, Cambridge, MA, USA, 2007), pp. 359–367

28. G. Schalk, J. Mellinger, *A Practical Guide to Brain-Computer Interfacing with BCI2000*, 1st edn. (Springer, London, UK, 2010)
29. A. Kübler, B. Kotchoubey, J. Kaiser, J.R. Wolpaw, N. Birbaumer, Psychol. Bull. **127**(3), 358 (2001)
30. E.C. Leuthardt, Z. Freudenberg, D. Bundy, J. Roland, Neurosurg. Focus **27**(1), E10 (2009). doi:10.3171/2009.4.FOCUS0980
31. H. Davson, J. Physiol. **255**(1), 1 (1976)
32. H.M. Hamer, H.H. Morris, E.J. Mascha, M.T. Karafa, W.E. Bingaman, M.D. Bej, R.C. Burgess, D.S. Dinner, N.R. Foldvary, J.F. Hahn, P. Kotagal, I. Najm, E. Wyllie, H.O. Lüders, Neurology **58**(1), 97 (2002)
33. K.N. Fountas, J.R. Smith, Stereotact. Funct. Neurosurg. **85**(6), 264 (2007). doi:10.1159/000107358
34. J.J. Van Gompel, G.A. Worrell, M.L. Bell, T.A. Patrick, G.D. Cascino, C. Raffel, W.R. Marsh, F.B. Meyer, Neurosurgery **63**(3), 498 (2008). doi:10.1227/01.NEU.0000324996.37228.F8
35. C.H. Wong, J. Birkett, K. Byth, M. Dexter, E. Somerville, D. Gill, R. Chaseling, M. Fearnside, A. Bleasel, Acta Neurochir. (Wien) **151**(1), 37 (2009). doi:10.1007/s00701-008-0171-7
36. A. Torres Valderrama, R. Oostenveld, M.J. Vansteensel, G.M. Huiskamp, N.F. Ramsey, J. Neurosci. Methods **187**(2). doi:10.1016/j.jneumeth.2010.01.019
37. D.T. Bundy, E. Zellmer, C.M. Gaona, M. Sharma, N. Szrama, C. Hacker, Z.V. Freudenburg, A. Daitch, D.W. Moran, E.C. Leuthardt, J. Neural Eng. **11**(1), 016006 (2014). doi:10.1088/1741-2560/11/1/016006
38. K.A. Sillay, P. Rutecki, K. Cicora, G. Worrell, J. Drazkowski, J.J. Shih, A.D. Sharan, M.J. Morrell, J. Williams, B. Wingeier, Brain Stimul. **6**(5), 718 (2013)
39. T. Stieglitz, *Miniaturized Neural Interfaces and Implants in Neurological Rehabilitation*. In: W. Jensen, O. Andersen, M. Akay (eds.) Replace, Repair, Restore, Relieve–Bridging Clinical and Engineering Solutions in Neurorehabilitation. Biosystems and Biorobotics, vol. 7 Springer, Cham (2014)

Towards Continuous Speech Recognition for BCI

Christian Herff, Adriana de Pesters, Dominic Heger, Peter Brunner, Gerwin Schalk and Tanja Schultz

Abstract For the last two decades, brain-computer interface (BCI) research has worked towards practical and useful applications for communication and control. Yet, many BCI communication approaches suffer from unnatural interaction or time-consuming user training. As continuous speech provides a very natural communication approach, it has been a long standing question whether it is possible to develop BCIs that perform speech recognition from cortical activity. Imagined speech as a BCI paradigm for locked-in patients would mean a large improvement in communication speed and usability without the need for cumbersome spelling using individual letters. We showed for the first time that automatic speech recognition from neural signals is possible. Here, we evaluate the feasibility of speech recognition from neural signals using only temporal offsets associated with speech production and omitting information from speech perception. This analysis provides first insights into the potential usage of imagined speech processes for speech recognition, for which no perceptive activity is present.

Keywords Speech · BCI · Automatic speech recognition · ASR · Brain-computer interface

C. Herff (✉) · D. Heger · T. Schultz
Cognitive Systems Lab, University of Bremen (formerly at Karlsruhe Institute of Technology), Enrique-Schmidt-Str. 5, 28359 Bremen, Germany
e-mail: christian.herff@uni-bremen.de
URL: http://www.csl.uni-bremen.de

A. de Pesters · P. Brunner · G. Schalk
New York State Department of Health, National Resource Center for Adaptive Neurotechnologies, Wadsworth Center, Albany, USA

P. Brunner · G. Schalk
Department of Neurology, Albany Medical College, Albany, USA

C. Guger et al. (eds.), *Brain-Computer Interface Research*,
SpringerBriefs in Electrical and Computer Engineering,
DOI 10.1007/978-3-319-57132-4_3

1 Introduction

Previous neuroscientific studies provided evidence for neural representations of speech, such as phones and phonetic features during speech perception [3, 9, 12]. Other studies classified [1, 8, 10] or investigated the production [4, 18] of limited sets of phones, syllables, and words. A complete set of manually labeled phones was classified in single word production in [13]. However, it was unclear whether the brain encodes a complete repertoire of phonetic representations during the production of continuous speech that allows the decoding of words and phrases.

In a study with 7 participants [6], we showed for the first time that continuously spoken speech is represented in the brain as a sequence of phones. These phones can be decoded from electrocorticographic (ECoG) recordings and allow the composition of the spoken words, which we call *Brain-to-Text*. All participants were undergoing surgery for intractable epilepsy and agreed to participate in our experiment. Electrode locations were determined based solely on clinical needs of the patients. We used electrode grids (Ad-Tech Medical Corp., Racine, WI; PMT Corporation, Chanhassen, MN) with inter-electrode distances of 0.6–1 cm. BCI2000 [16] was used to record ECoG signals from eight 16-channel g.USBamp biosignal amplifiers (g.tec, Graz, Austria).

In our experiment, we recorded ECoG activity and the acoustic waveform simultaneously, while participants read aloud different texts consisting of childrens' literature, fan fiction or political speeches. We time-aligned the neural data to a phone labeling obtained from the acoustic data using our in-house speech recognition toolkit BioKIT [17]. This allowed us to identify the neural activity corresponding to the production of each phone. See Fig. 1 for data recording in our experiment and aligning of ECoG and acoustic data. We segmented the texts into phrases and used the recorded ECoG data of all but one phrase for feature selection and training, then

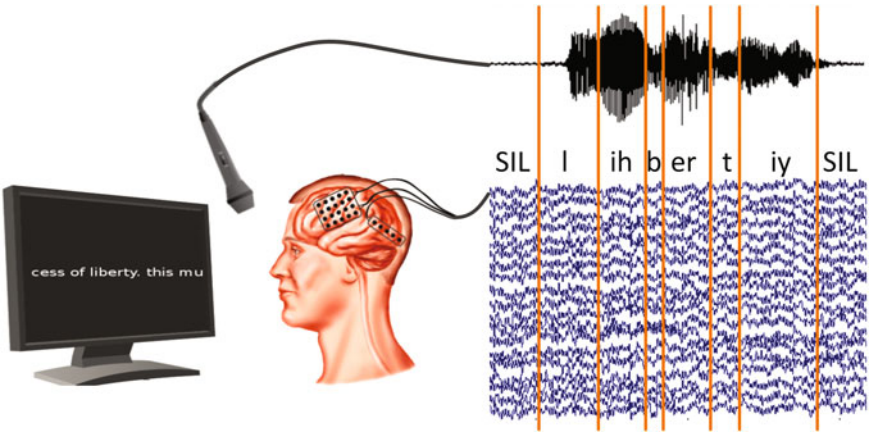

Fig. 1 Synchronized data recording of ECoG data and the acoustic stream

evaluated our approach on the ECoG data of the remaining phrase in a round-robin manner (leave-one-phrase-out validation). We compared the results from temporal offsets associated with speech production to productive and perceptive temporal offsets to analyze the feasibility of continuous speech recognition from imagined speech processes, as perceptive activity is only present when participants hear their own voice.

2 Phone Modeling in ECoG

To model phones in ECoG data, we extracted broadband-gamma (70–170 Hz) activity in 50 ms windows for each channel. The temporal dynamics of speech production were captured by including the features of the four neighboring windows before and after each window in the feature vector, i.e. representing a context of 450 ms length. We modeled each phone with a multivariate Gaussian distribution representing the mean broadband-gamma activity and the corresponding variance for all locations and time lags. We analyzed the discriminability between the different phone models by employing their Kullback-Leibler divergences (KL-div) for every electrode position and time lag. The spatio-temporal distributions of KL-div results give interesting insights into the spatio-temporal dynamics of cortical activity during continuously spoken speech. Figure 2 illustrates discriminability between phones for cortical locations and time offsets on a combined electrode montage of all participants. Phone discriminability can be observed 200 ms prior to phone production in prefrontal areas associated with speech planning (Broca's area). 100 ms prior to phone production, discriminability increases in motor areas and auditory cortex and vanishes in previously observed regions. At phone onset, discriminability peaks in motor cortex, while discriminability is largest in auditory cortex 100 ms after phone production. 200 ms after phone production, phone models can be discriminated in auditory cortex. The activations after the actual phone production are presumably triggered by the participants' perception of their own voice.

We also use the KL-div values to automatically select the best ECoG features for our *Brain-To-Text* system.

To evaluate the feasibility of our system for realistic brain-computer interfaces based on imagined speech production, we performed an analysis that focuses on activity prior to phone onset. By only keeping the temporal offsets between −200 and 0 ms (see Fig. 2), no perceptive activity from hearing one's own voice should remain in the data. This restriction to productive temporal offsets is a first simulation of imagined speech, in which no perceptive activity is present, as participants do not hear their own voice. We refer to these results as *Production* and compare them to those obtained with all temporal offsets, refereed to as *Production and Perception*. This analysis therefore provides a first insight into the feasibility of our system for imagined speech.

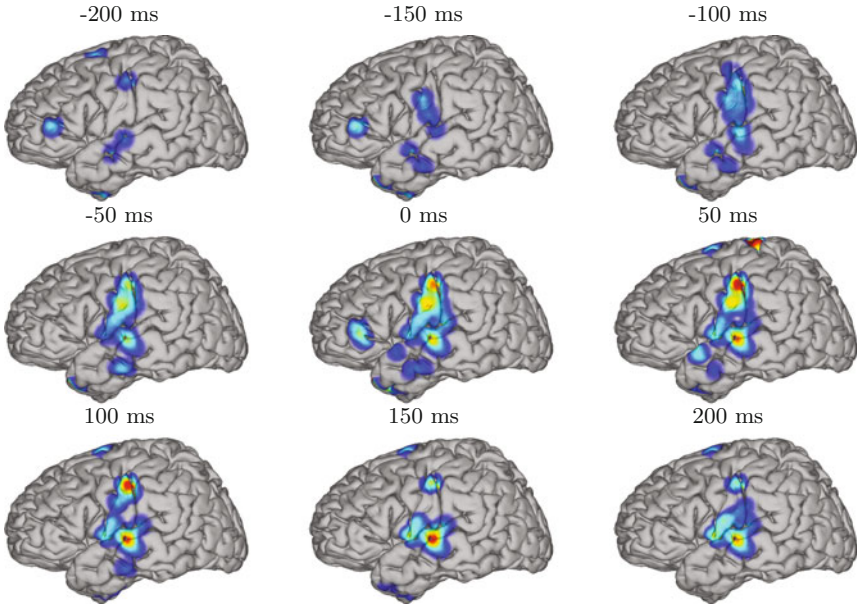

Fig. 2 Discriminability (Mean Kullback-Leibler Divergences) between phones for electrode position of all participants. Color overlays on the rendered average brain show regions of high discriminability (*red*) to lower discriminability (*blue*), all overlays are larger than random discriminability. Early differences can be observed in diverse areas up to 200 ms before phone production. Sensorimotor cortex shows high discriminability 50 ms before production, while discriminability in auditory regions of the superior temporal gyrus peaks 100 ms after production

3 Automatic Speech Recognition for BCI

We combined the phone-based speech representations of cortical activity with language information using automatic speech recognition technology to reconstruct the words in unseen spoken phrases. Language information is included into the decoding process through a language model and a pronunciation dictionary. The pronunciation dictionary contains the mapping of phone sequences to words. The language model statistically models syntactic and semantic information by predicting the next words given the preceding words [7].

Our results show that, with a limited set of words in the dictionary, *Brain-to-Text* is able to reconstruct full sentences. Figure 3 illustrates the different steps of decoding continuously spoken phrases from neural data. *ECoG signals over time* are recorded at every electrode and divided into 50 ms segments. For each 50 ms interval of recorded *broadband gamma activity*, stacked feature vectors are calculated (*Signal processing*). For each *ECoG phone model* calculated on the training data, the likelihood that this model emitted a segment of ECoG features can be calculated, resulting in *phone likelihoods over time*. Combining these Gaussian *ECoG phone models* with

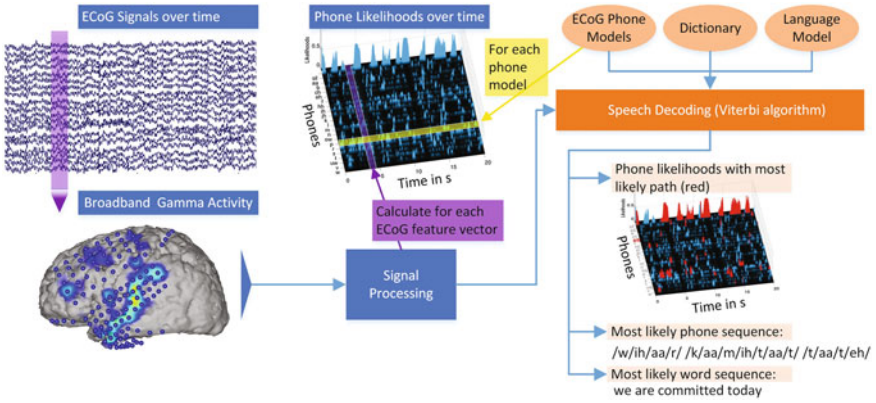

Fig. 3 Overview of the *Brain-to-Text* decoding process

language information in the form of a *dictionary* and an n-gram *language model*, the *Viterbi* algorithm calculates the *most likely word sequence* and corresponding *phone sequence*. To visualize the decoding path, the *most likely phone sequence* can be shown in the *phone likelihoods over time* (red marked areas). The system outputs the decoded word sequence. Once the ECoG phone models are trained, phrases can be decoded in real-time.

4 Results

To evaluate the performance of *Brain-to-Text*, we compared the decoding results of our approach to randomized models (randomization test by shifting the labels of the training data by half the session length). The randomized results illustrate the impact that the language model and dictionary have when no usable neural information is present. Figure 4 shows phone classification accuracies for all participants and sessions. Classification accuracies for combined productive and perceptive areas (purple bars) are better than accuracies achieved with randomized models (yellow bars) for all sessions of all participants. To estimate how well a hypothetical device based on imagined speech production might be, we evaluated our approach only based on productive areas, by excluding all activations from time offsets after phone onset. As the participants cannot hear their own voice prior to the onset of the phone, this ensures that no perceptive activity should be used in this evaluation. Results on productive areas only (turquoise bars) outperform the randomized models for all sessions, but are usually worse than accuracies achieved when using all neural activity.

As *Brain-to-Text* outputs word sequences, we evaluated the Word Error Rate between our predicted word sequence and the reference phrase. One of the major limitations in our study is the small amount of training data per session, with only a

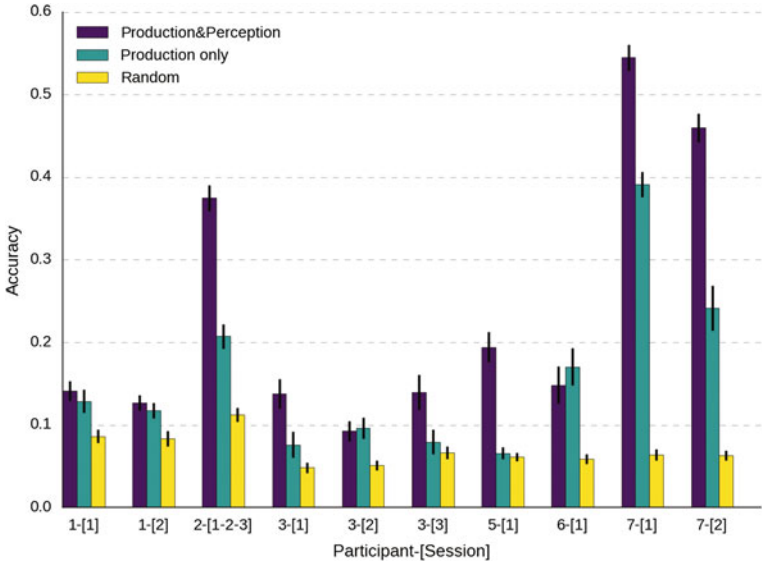

Fig. 4 Phone classification accuracies for all participants and sessions. Error bars depict standard errors. Our system shows significantly better accuracies than random models (*yellow bars*) when using all information (*purple bars*) and when only using productive temporal offsets (*turquoise bars*)

few minutes of data. For comparison, speech recognition systems based on acoustic speech are usually trained on thousands of hours of data. To account for the limited amount of training data, we restricted the amount of recognizable words in the dictionary to a range of 10–100 words. We were able to achieve Word Error Rates as low as 25% when using a dictionary of 10 words. Word Error Rates depending on dictionary size for the best performing participant are shown in Fig. 5. Word Error Rates are lowest (between 25% and just over 60%) when using perceptive and productive (purple line) time offsets. Neural activity only resulting from speech production yields slightly higher Word Error Rates (turquoise line) than perceptive and productive activity, but still outperforms randomized models (yellow line) for all dictionary sizes. Using productive activity only, more than 60% of words are recognized correctly for a dictionary of 10 words.

To ensure that word recognition is not based on the robust recognition of a small subset of phones, we also analyzed average phone true positive rates. For this analysis, we obtained the ground truth of phone timings from the audio alignment described earlier. Bars in Fig. 5 show true positive rates averaged across all phones on window-level. Again, productive and perceptive time offsets (purple) combined yield the best results, but using only productive neural activity (turquoise) still yields high average phone true positive rates above 20%. Both systems using neural activity outperform random true positive rates (yellow). Average phone true positive rates remain rather stable even when dictionary sizes increase.

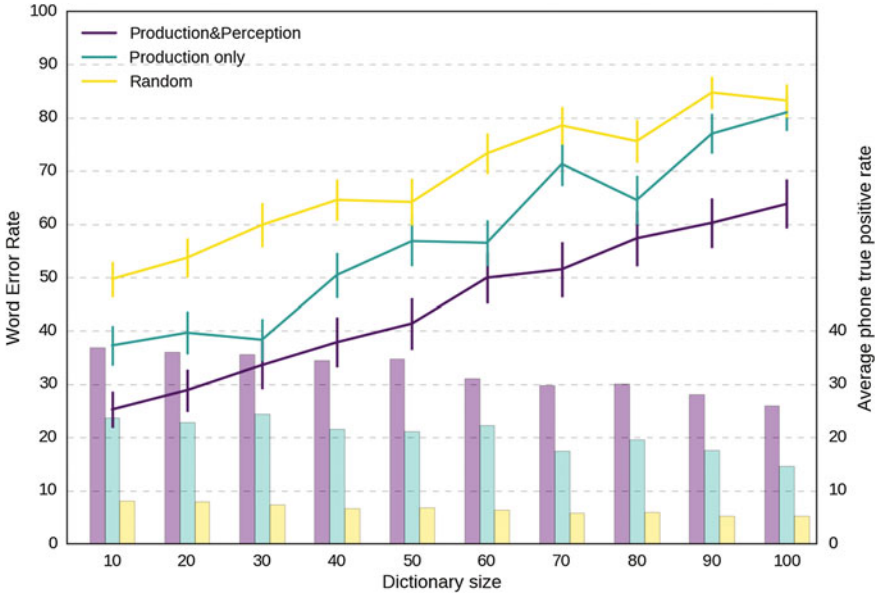

Fig. 5 Word Error Rates over dictionary size (*lines*); average true positive rates across phones depending on dictionary size (*bars*). Error bars depict standard errors. While the full set of temporal offsets performs best (*purple*), information from productive time offsets (*turquoise*) still outperforms random models (*yellow*) for all dictionary sizes both in Word Error Rates and true positive rates

Even though detailed results are only shown for the participant which gave the best recognition results, we found significantly better results than random models in Word Error Rate and single phone true positive rates for all sessions in this study.

5 Conclusion

In summary, our results support the hypothesis that *Brain-to-Text* may eventually allow people to communicate using brain signals associated with continuous spoken language, i.e. without the current limitations of a restricted set of commands or unnatural selection procedures. We showed that participants' neural activity could be used to decode continuously spoken phrases into a textual representation, even when omitting neural activity associated with the perception of their own voice. This illustrates the feasibility of speech recognition from neural activity when participants only imagine to speak. Thus, using continuous speech production for BCIs has the potential to increase naturalness and information transfer rates and the practical utility of current BCI communication approaches. Ultimately, speech processes for BCIs

might lead to information transfer rates similar to that of continuous speech while being more natural to the user.

While the generative models used in this study allow for a good illustration and fast training of phone models, we have shown that more advanced discriminative models can improve results [5].

Recent advances in the modeling of imagined phones [2], reconstruction of imagined speech spectra [11] and investigations in silent reading [14, 15], suggest that covert and overt speech share a neural substrate. Our presented results suggest that neural activity from productive temporal offsets allows reconstruction of a textual form, without the need for perceptive information. These findings highlight the potential of *Brain-to-Text* to be used on imagined continuous speech in the future.

References

1. T. Blakely, K.J. Miller, R.P.N. Rao, M.D. Holmes, J.G. Ojemann, Localization and classification of phonemes using high spatial resolution electrocorticography (ECoG) grids, in *30th Annual International Conference of the IEEE Engineering in Medicine and Biology Society, 2008. EMBS 2008* (IEEE, 2008), pp. 4964–4967
2. S.J. Brumberg, E.J. Wright, D.S. Andreasen, F.H. Guenther, P.R. Kennedy, Classification of intended phoneme production from chronic intracortical microelectrode recordings in speech-motor cortex. Front. Neurosci. **5** (2011)
3. F. Edward, Chang, J.W. Rieger, K. Johnson, M.S. Berger, N.M. Barbaro, R.T. Knight, Categorical speech representation in human superior temporal gyrus. Nat. Neurosci. **13**(11), 1428–1432 (2010)
4. M. Fukuda, R. Rothermel, C. Juhász, M. Nishida, S. Sood, E. Asano, Cortical gamma-oscillations modulated by listening and overt repetition of phonemes. Neuroimage **49**(3), 2735–2745 (2010)
5. D. Heger, C. Herff, A. de Pesters, D. Telaar, P. Brunner, G. Schalk, T. Schultz, Continuous speech recognition from ECoG, in *Sixteenth Annual Conference of the International Speech Communication Association* (2015)
6. C. Herff, D. Heger, A. de Pesters, D. Telaar, P. Brunner, G. Schalk, T. Schultz, Brain-to-text: decoding spoken phrases from phone representations in the brain, Front. Neurosci. **9**(217) (2015)
7. F. Jelinek, *Statistical Methods for Speech Recognition* (MIT Press, 1997)
8. S. Kellis, K. Miller, K. Thomson, R. Brown, P. House, B. Greger, Decoding spoken words using local field potentials recorded from the cortical surface. J. Neural Eng. **7**(5), 056007 (2010)
9. J. Kubanek, P. Brunner, A. Gunduz, D. Poeppel, G. Schalk, The tracking of speech envelope in the human cortex. PLoS ONE **8**(1), e53398 (2013)
10. C.E. Leuthardt, C. Gaona, M. Sharma, N. Szrama, J. Roland, Z. Freudenberg, J. Solis, J. Breshears, G. Schalk, Using the electrocorticographic speech network to control a brain-computer interface in humans. J. Neural Eng. **8**(3), 036004 (2011)
11. S. Martin, P. Brunner, C. Holdgraf, H.-J. Heinze, N.E. Crone, J. Rieger, G. Schalk, R.T. Knight, B. Pasley, Decoding spectrotemporal features of overt and covert speech from the human cortex. Front. Neuroeng. **7**(14) (2014)
12. N. Mesgarani, C. Cheung, K. Johnson, E.F. Chang, Phonetic feature encoding in human superior temporal gyrus. Science 1245994 (2014)
13. M.E. Mugler, J.L. Patton, R.D. Flint, Z.A. Wright, S.U. Schuele, J. Rosenow, J.J. Shih, D.J. Krusienski, M.W. Slutzky, Direct classification of all American English phonemes using signals from functional speech motor cortex. J. Neural Eng. **11**(3), 035015 (2014)

14. M. Perrone-Bertolotti, J. Kujala, J.R. Vidal, C.M. Hamame, T. Ossandon, O. Bertrand, L. Minotti, P. Kahane, K. Jerbi, J.-P. Lachaux, How silent is silent reading? intracerebral evidence for top-down activation of temporal voice areas during reading. J. Neurosci. **32**(49), 17554–17562 (2012)
15. I.C. Petkov, P. Belin, Silent reading: does the brain hear both speech and voices? Curr. Biol. **23**(4), R155–R156 (2013)
16. G. Schalk, D.J. McFarland, T. Hinterberger, N. Birbaumer, J.R. Wolpaw, Bci2000: a general-purpose brain-computer interface (BCI) system. IEEE Trans. Biomed. Eng. **51**(6), 1034–1043 (2004)
17. D. Telaar, M. Wand, D. Gehrig, F. Putze, C. Amma, D. Heger, N.T. Vu, M. Erhardt, T. Schlippe, M. Janke et al., BioKIT—real-time decoder for biosignal processing, in *The 15th Annual Conference of the International Speech Communication Association (Interspeech 2014)* (2014)
18. L.V. Towle, H.-A. Yoon, M. Castelle, J.C. Edgar, N.M. Biassou, D.M. Frim, J.-P. Spire, M.H. Kohrman, ECoG gamma activity during a language task: differentiating expressive and receptive speech areas. Brain **131**(8), 2013–2027 (2008)

Brain-Machine Interface Development for Finger Movement Control

Tessy M. Lal, Guy Hotson, Matthew S. Fifer, David P. McMullen, Matthew S. Johannes, Kapil D. Katyal, Matthew P. Para, Robert Armiger, William S. Anderson, Nitish V. Thakor, Brock A. Wester and Nathan E. Crone

Abstract There have been many developments in brain-machine interfaces (BMI) for controlling upper limb movements such as reaching and grasping. One way to expand the usefulness of BMIs in replacing motor functions for patients with spinal cord injuries and neuromuscular disorders would be to improve the dexterity of upper limb movements performed by including more control of individual finger movements. Many studies have been focusing on understanding the organization of movement control in the sensorimotor cortex of the human brain. Finding the specific mechanisms for neural control of different movements will help focus signal acquisition and processing so as to improve BMI control of complex actions. In a recently published study, we demonstrated, for the first time, online BMI control of individual finger movements using electrocorticography recordings from the hand area of sensorimotor cortex. This study expands the possibilities for combined control of arm movements and more dexterous hand and finger movements.

Keywords Brain-machine interface (BMI) · Brain-computer interface (BCI) · Electrocorticography (ECoG) · Finger movements

T.M. Lal (✉) · M.S. Fifer · N.V. Thakor
Department of Biomedical Engineering, Johns Hopkins University, Baltimore, USA

G. Hotson
Department of Electrical and Computer Engineering, Johns Hopkins University, Baltimore, USA

D.P. McMullen · W.S. Anderson
Department of Neurosurgery, Johns Hopkins University, Baltimore, USA

M.S. Johannes · K.D. Katyal · M.P. Para · R. Armiger · B.A. Wester
JHU Applied Physics Laboratory Applied Neuroscience, Laurel, USA

N.E. Crone
Department of Neurology, Johns Hopkins University, Baltimore, USA

C. Guger et al. (eds.), *Brain-Computer Interface Research*,
SpringerBriefs in Electrical and Computer Engineering,
DOI 10.1007/978-3-319-57132-4_4

1 Introduction

Current upper limb brain-machine interface (BMI) research focuses on developing advanced neurally controlled prosthetics to restore or replace motor function for patients with upper limb paralysis. These advances come as we develop new technologies and expand our understanding of how humans control and execute movements. In order to develop a high performance motor BMI, it is imperative to understand how signals obtained from neural implants encode both gross and fine upper limb movements.

Electrocorticography (ECoG) has been widely studied for motor decoding and BMI control. Compared to other invasive and non-invasive neural recording modalities, ECoG provides a good compromise between coverage extent, signal quality, and signal stability. ECoG electrode grids record from a wide area of cortex, capable of resolving activation corresponding to all five fingers in the hand area of sensorimotor cortex with a single grid [1–3]. This stands in contrast to microelectrode arrays (MEAs), which provide high resolution single neuron activity but only cover a very small patch of cortex, sometimes only spanning two fingers with a single array [4]. ECoG also provides much higher spatial resolution and signal fidelity than electroencephalography (EEG) and better time resolution than functional magnetic resonance imaging (fMRI). Several studies have demonstrated that ECoG grids are implantable for long durations of about 8–12 months [5–8], and provide reliable decoding performance over several months without needing daily calibrations [9]. Furthermore, functional mapping studies provide evidence that power changes in the high gamma frequencies (>70 Hz) of ECoG signals show significant correlation to execution of movements, making them useful tools in mapping motor functions on the cortical surface [10–12]. A paper published recently by our team was the first to demonstrate online control of individual finger movements using ECoG recordings [3]. This chapter will highlight the results of this paper and discuss the impact of the study within the context of the literature on motor BMI development and control for finger movements.

2 Current Motor BMI Control

Neural activity related to motor function can be used for real-time control of devices to help patients with spinal cord injuries (SCI) or neuromuscular disorders regain movement and perform useful actions. ECoG-based control of brain-machine interfaces by epilepsy patients has been demonstrated for 2-D cursor movements using real [13, 14] and imagined [15, 16] movements. A later study by Wang et al. showed that, using similar techniques, a patient with quadriplegia could control 2-D and 3-D cursor movements using ECoG signals during attempted movements [17].

Many groups have shown that it is possible to classify arm movement trajectories and different hand movements from ECoG recordings over sensorimotor

cortex [18–20], allowing paralyzed and able-bodied subjects online control of discrete hand movements with a robotic limb [2, 21]. The somatotopic organization of arm and hand areas has been leveraged to deliver simultaneous, independent control of both reaching and grasping with a robotic limb using ECoG recordings [22]. A tetraplegic patient was able to reach to targets in 3D space with a prosthetic arm using ECoG signals modulated by attempted elbow, wrist, and hand movements [17]. MEA recordings have also been used for online control of multiple prosthetic degrees of freedom [23–26], and for controlling neuromuscular electrical stimulation of forearm muscles in order to restore the ability to produce finger, wrist, and hand movements in a patient with quadriplegia [27].

3 Finger Movement Decoding

Combined control of hand and finger movements can be useful in performing activities of daily living (ADL). It is important to be able to control the finer movements of the hand, because ADLs often require different levels of dexterity, for example drinking from a cup versus brushing your teeth. Previous studies have demonstrated above 90% accuracy in decoding of individual finger movements from single unit activity in the primary motor cortex (M1) of non-human primates [28–30]. Interestingly, significant information about finger movements can still be extracted from lower resolution recordings, like EEG. EEG signals have been shown to correlate with finger kinematics [31, 32], but with large variance from subject to subject. In contrast to EEG, which is recorded on the scalp, ECoG is recorded on the cortical surface where each electrode overlays a more localized group of neurons. The higher spatial resolution provides for more discriminability of the neural signals corresponding to finger movements. Finger positions during slow grasping were predicted from the "local motor potential" (LMP), consisting of the smoothed amplitude in ECoG recordings from motor and sensory areas [33]. The time course of individual finger flexion movements has also been decoded from LMP and high gamma components of ECoG signals in sensorimotor cortex [1, 34–36]. In this study, maximum correlation was achieved when movement was predicted from the neural features preceding the movement by 50–100 ms, suggesting the ECoG features were primarily related to movement rather than sensory feedback alone. Chestek et al. demonstrated classification of finger movements and isometric hand postures, as well as online decoding of grasping movements to control a prosthetic hand, with ECoG signals from sensorimotor cortex in a trial-based manner [2]. In Hotson et al. (2016), our team has shown for the first time that online BMI control of individual finger movements of the Johns Hopkins University Applied Physics Laboratory (JHU/APL) Modular Prosthetic Limb (MPL) is possible using high density ECoG (hd-ECoG) recordings from sensorimotor cortex [3].

4 Neural Representation of Finger Movements

Increased power in certain frequency bands of the ECoG signal, specifically in the high gamma band (70–100 Hz), is known to correspond directly with execution of movements [10]. Some studies have shown that the high gamma band activity in sensorimotor cortex peaks at the onset of each movement phase, for example when the hand begins to move from rest position and when the hand begins to return to rest position, and attenuates to near baseline as the movement progresses between movement phases [10, 18]. The population activity recorded through the high gamma signal has a strong correlation with the speed of movements, and a weaker correlation with the movement direction [37]. Information about movement kinematic parameters can also be extracted from the LMP, in addition to high gamma power of ECoG signals [33, 38, 39]. Most studies describing movement decoding have predicted movement types from analyzing these spectral and temporal components of neural signals recorded over upper limb areas of sensorimotor cortex. While a unifying representation of different hand and finger movements in the motor cortex has not yet been fully agreed upon, various hypotheses have been proposed for cortical movement encoding.

4.1 Somatotopic Representation

Early studies by Penfield and Boldrey suggested that a somatotopic map of different body parts existed on the precentral and postcentral gyri, which make up the sensorimotor cortex [40]. In a somatotopic representation, each part of the upper limb, including each finger, would be represented in a separate area of cortex. A hand movement, such as a specific grasp type, would therefore be characterized by activation of areas corresponding to the hand and each finger. Later studies provide evidence supporting a clear somatotopic organization of the primary somatosensory cortex (S1) as suggested by Penfield and Boldrey. fMRI studies have shown that the somatosensory areas activated by stimulating a specific finger are clearly segregated from areas activated by stimulating other fingers [41, 42]. In addition, a recent study has shown that microstimulation of hand area in S1 through a penetrating microelectrode array induced tactile sensations on individual fingers that a human subject was able to discriminate [4].

In contrast, most research contradicts the idea of an organized somatotopic map in the primary motor cortex (M1). Intracortical microstimulation studies in monkeys have shown that stimulation of multiple sites in M1 can evoke a response from the same muscle, and these sites are distributed and overlapping with sites corresponding to other muscles [43]. Studies with fMRI have also found overlapping and distributed areas in M1 activated for individual finger and wrist movements in

humans [41, 44]. Even though there seems to be little or no separation between the areas representing different parts of the upper limb, fMRI and lesion studies suggest that the overlapping regions still form a somatotopic gradient from one body part to another along M1 [41, 45, 46]. In a recent ECoG study, movements of one finger elicited activation over brain areas corresponding to that particular finger, as well as over areas corresponding to other fingers, providing more evidence that a strict somatotopic map does not exist in human motor cortex [2].

4.2 Synergies

In order to control upper limb movements, the motor cortex needs to code for a large number of degrees of freedom (DOF). One study found that activation of local ensembles of neurons in M1, recorded from MEAs implanted in the arm and hand areas in non-human primates, could be used to reconstruct the joint angles of the arm and hand during reach and grasp movements [47]. However, the study could not conclude that M1 neurons directly encode joint angles. Some studies have suggested that, instead of controlling kinematic parameters of movement, neural populations in the motor cortex may control a lower dimensional representation of upper limb kinematics. Saleh et al. found that the firing rates of M1 neurons in non-human primates correlated more with temporally extensive finger and wrist joint trajectories than with static kinematic parameters of individual joints [48, 49]. Kao et al. found that the predictive power of a BMI was improved when modeling both the binned spike counts and the kinematics as being generated by a low-dimensional latent state [50].

One hypothesis is that, rather than using a large number of DOFs, a smaller number of synergies can be used to characterize upper limb movements. A synergy is a combination of joint angles or muscle activities that commonly occur during natural movements of the arm and hand [51]. Each synergy can summarize the movement in multiple upper limb DOFs. Several studies have found that similar hand postures or similar reach and grasp actions can be represented by a small number of kinematic or muscle synergies [52–57]. Overduin et al. showed that intracortical microstimulation in the motor and premotor cortices in monkeys evoked muscle activations that could be reduced to linear sums of a few basic patterns [58, 59]. The reduced representations of evoked movements corresponded to muscle synergies extracted from EMG recordings of voluntary movements, and stimulated sites correlating to a particular synergy clustered in a non-uniform manner in M1. Direct current stimulation through penetrating microelectrodes in monkeys [60] and surface electrodes in humans [61] has evoked coordinated hand/mouth muscle movements. However, there is not enough evidence to conclude that motor cortex directly encodes synergies. Other studies have found that single neuron activity in M1 correlated more with joint angles and positions during

finger and wrist movements than with kinematic synergies extracted from the movements, suggesting that synergies are not represented more than kinematic parameters in the motor cortex [62, 63].

5 Online Neural Control of Finger Movements

While the principles of representation for hand and finger movements in motor cortex are not fully understood, some degree of separability can be found in the ECoG signals recorded from sensorimotor cortex during individual finger movements. Our recent study extracted these distinguishable ECoG features to perform classification and online control of individual fingers of the MPL [3].

5.1 Subject Info

A high density 8 × 16 ECoG grid (PMT Corp., Chanhassen, MN; 1 mm diameter, 3 mm center-to-center spacing) was implanted subdurally over sensorimotor areas of a 20 year old male suffering from intractable epilepsy. The placement of the electrodes was designed to localize the source of the patient's seizures, which routinely began with a sensation in distal right upper limb, and to map sensorimotor cortex in detail before performing respective surgery. The high density array straddled the central sulcus of the putative hand sensorimotor areas. Figure 1 shows a 3D reconstruction of the electrode locations performed using the BioImage Suite [64]. Not shown are electrode strips over nearby regions and depth electrodes in frontal and parietal opercula, targeting SII. All recordings were re-referenced using a common average reference (CAR) filter, in which the mean across electrodes was subtracted for each sample.

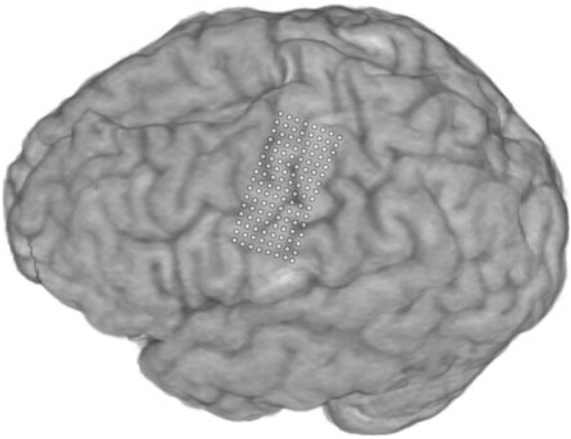

Fig. 1 3D reconstruction showing the location of hd-ECoG grid over hand area of sensorimotor cortex

5.2 Feature Extraction

During training and testing of the online finger classifier, high gamma power was extracted using the Hilbert transform with a bandpass of 72–110 Hz. Baseline activity was estimated using the average of high gamma powers in an 896 ms period before cue onset in each trial. The activation due to each finger movement was estimated using the average of high gamma powers in an 896 ms period during the cued finger movement (see below).

5.3 Preliminary Mapping of Activation

Preliminary mapping of high gamma activation on the hd-ECoG grid was performed using a finger tapping task and passive vibrotactile stimulation. In the motor task, the patient was visually cued to flex and extend a specific finger 5 times repeatedly for each trial, while finger movements were recorded using the Cyberglove II (Cyberglove Systems LLC, San Jose CA). In the sensory task, each finger was stimulated using a vibrational motor taped to the patient's unsupported, isolated fingertips in a pseudorandom order to record cortical activation

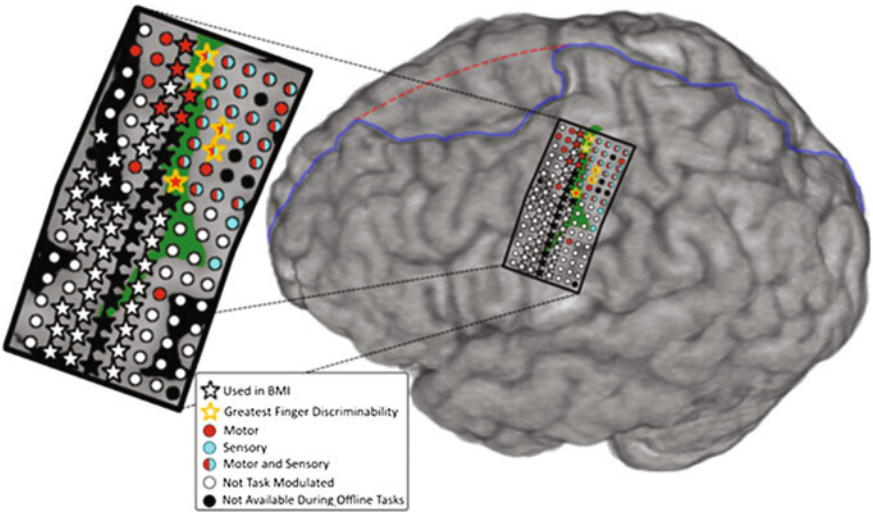

Fig. 2 Distribution of motor and sensory activations among the electrode grid. *Red* electrodes showed significant activation during the finger tapping task. *Blue* electrodes showed significant activation during the vibrotactile stimulation task. *Starred* electrodes were used for online control of finger movements. *Starred* electrodes outlined in *gold* were found to have the most discriminability between fingers. *Green* denotes the central sulcus, and the *purple line* denotes the interhemispheric fissure. The *red dashed line* outlines a previously resected area of the superior frontal gyrus. ([3])

corresponding to the sensory response of individual fingers. Figure 2 shows the distribution of significant motor and sensory activation along the hd-ECoG grid electrodes.

5.4 Decoder Training

A hierarchical classifier trained using linear discriminant analysis (LDA) was used to predict what finger was moving from the high gamma power correlates of finger movements. The decoder was trained using data collected as the patient performed a finger tapping task. The classifier first made the binary classification of whether or not a finger was moving. If a finger movement was occurring, there was then a subsequent 5-way classification of which finger was moving.

When performing online classification, the decoder used a subset of electrodes that avoided the postcentral gyrus (except for two electrodes), and was limited to only electrodes which appeared to have significant activation during preliminary mapping of high gamma activation during the finger tapping task. Some electrodes were excluded for appearing to be primarily activated by sensory feedback during preliminary analysis of activation during vibrotactile stimulation task. Figure 2 shows the location of electrodes chosen for online training and classification.

For offline classification, all electrodes were potentially able to be utilized by the classifier. Ten-fold cross-validation was performed, where 90% of the data was used for feature selection and model training and 10% of the data was used for testing. Cross-validated regularization/feature selection [65], using only the training data, was nested within each fold of cross-validation. To test for linear separability of the ECoG high gamma features while taking into account their time-varying nature, we trained and tested different classifiers at fixed time points relative to movement onset.

5.5 JHU/APL Modular Prosthetic Limb

The JHU/APL Modular Prosthetic Limb (MPL) is an advanced upper-body extremity prosthetic and human rehabilitation device, developed with support from the Defense Advanced Research Projects Agency (DARPA) as part of the Revolutionizing Prosthetics Project [66]. The MPL has 17 controllable degrees of freedom (DoF) and 26 articulating DoF in total (Fig. 3), including the ability to independently actuate arm, hand, and finger joints. The MPL is controlled via a custom software interface (VulcanX) that receives movement commands and converts them into low-level commands for driving each joint on the limb [67]. VulcanX is able to interpret three fundamental command types: (1) degree of motion (DOM) commands for driving the position and/or velocity of each joint in the limb, (2) endpoint control (EC) commands for driving the hand and wrist to

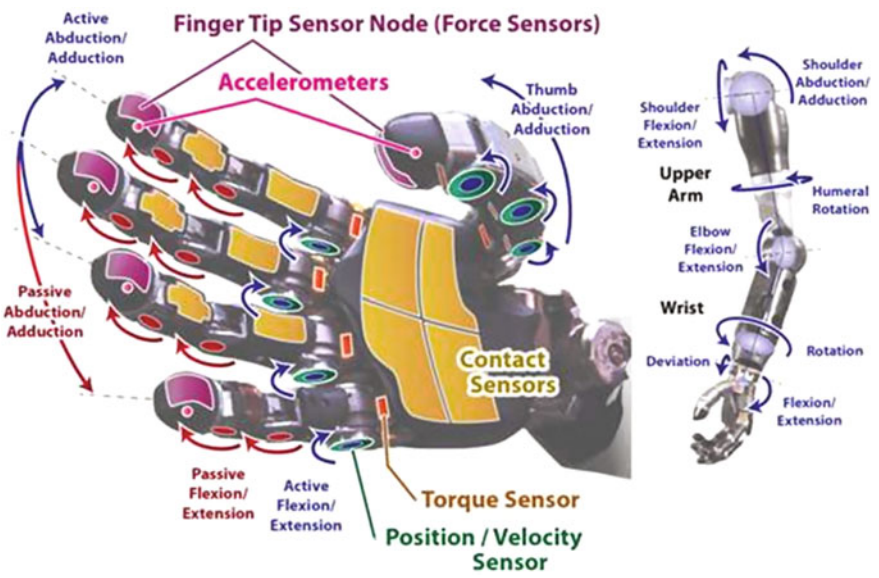

Fig. 3 Degrees of freedom of the JHU/APL MPL. Schematics showing the controllable joints along the MPL arm (*right*) controllable and passive joints of the MPL hand (*left*)

three-dimensional positions and three-dimensional orientations using Jacobian-based inverse kinematics, and (3) reduced order control (ROC) for uni-dimensional control of configurable movements spanning multiple joints (i.e., a movement "synergy"), predominantly used to control grasps [68, 69].

The MPL has been used in a variety of pilot studies by amputees [70, 71] and quadriplegic patients [17, 24, 25]. In MPL studies with amputees, individual finger control has been performed, though it is more common for fingers to be controlled through configurable multi-joint grasp synergies in ROC mode [71]. Cortical control over MPL fingers by quadriplegic individuals generally also relies on one-dimensional grasp ROC commands, although occasionally the user is given control over multiple dimensions of the grasp configuration itself [26].

5.6 *Online Decoding Accuracy*

During the online BMI control task, the decoder detected individual finger movement states and rest states. Whenever the decoder determined movement of a specific finger from the ECoG features, the MPL was instructed to flex the corresponding finger on its hand at a fixed velocity (Fig. 4). When the decoder detected no movement, the MPL fingers were instructed to extend fingers to the rest position. Figure 5 shows the classification accuracies in movement detection and finger

Fig. 4 Online control of individual finger movements. First a cue was presented on the screen highlighting the finger to be moved in *black* (*top*). The patient then flexed the highlighted finger 5 times. During the movement, the decoder classifies which finger is moving from the ECoG features and sends a command to the MPL to flex the same finger (*bottom*)

prediction over time relative to movement onset. Finger movement detection reached 97% accuracy from about 1.6 to 3.1 s after movement onset. Individual finger classification reached a maximum of 81% accuracy within that same time period when predicting from all five fingers. However, while the fourth ("ring") and fifth ("pinky" or "little") fingers were cued separately, the patient predictably had difficulty moving them independently. When combining the classifications of the ring and little fingers into a single class during post hoc analysis, the classification accuracy reached a maximum of 94%. At the onset of peak movement detection, classification accuracy was 76% for five fingers and 88% when the ring and little fingers were combined. Even though the electrodes selected for training and testing

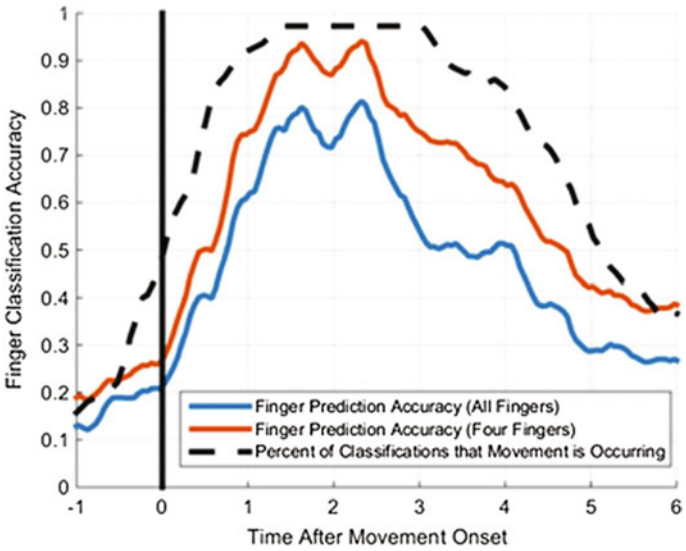

Fig. 5 Classification accuracies over time for movement detection and finger decoding. Predictions were aggregated in 250 ms time bins and then averaged across trials. The *black vertical line* denotes movement onset. The *black dashed* trace shows average percentage of predictions showing movement is occurring within a specific time window. The *blue* and *orange* traces show the average finger classification accuracy within the specific time window among all fingers and four fingers (ring and little fingers combined), respectively. (© IOP Publishing. Reproduced with permission. All rights reserved [3])

the decoder mostly excluded electrodes on the postcentral gyrus, it was found that four out of the five electrodes that had the most finger discriminability also showed significant sensory activation (Fig. 2).

5.7 *Offline Decoding Accuracy*

Electrode selection for the decoder was further optimized during offline analysis in order to account for the somatosensory feedback seen during finger movements. Deafferented patients and paralyzed patients would not exhibit cortical activations corresponding to somatosensory feedback during movements, so it was necessary to also examine the results when eliminating activations in the somatosensory cortex. The time course of activations during the finger tapping task and vibrotactile task were compared to determine the segment of finger movement activation preceding sensory feedback that could be used for decoding. Figure 6 shows the spectral activation during the finger movement task and vibrotactile stimulation in the two electrodes that had the most finger discriminability during online decoding. It can be seen that significant motor-related activation precedes significant

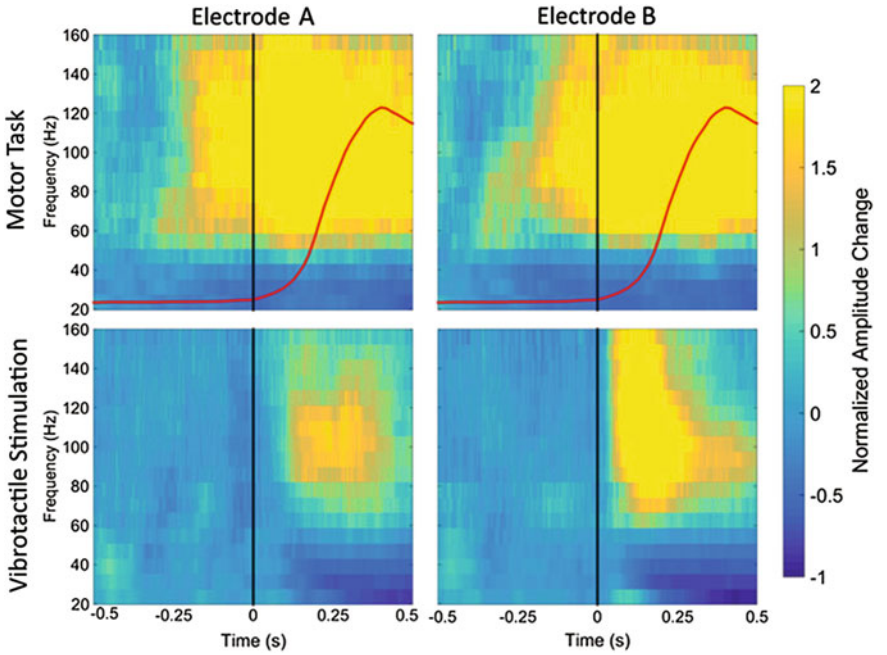

Fig. 6 Spectral activation in two electrodes that contained the most information for BMI control during offline index finger tapping (*top*) and vibrotactile stimulation of index finger (*bottom*). The *solid black line* denotes onset of any hand movement measured by CyberGlove for the motor task, and onset of vibrotactile stimulation for the sensory task. The *red* trace for the motor task denotes the average finger movement trace recorded by CyberGlove sensors on the index finger. Spectral activation significantly exceeded baseline levels 160 and 48 ms before movement onset during the motor task (*top row*), and 48 ms after the onset of vibrotactile stimulation (*bottom row*). (© IOP Publishing. Reproduced with permission. All rights reserved [3])

sensory-related activation, which suggests that there is a window of activation during finger movements that does not involve sensory feedback.

Figure 7 shows the average finger classification accuracy over time for the motor and sensory tasks. The features from the motor task were aligned to the onset of movement recorded from the Cyberglove data, and the features from the sensory task were aligned to the onset of the motor vibration. All features were extracted in a causal manner, meaning the classification at time $t = 0$ only used data samples recorded prior to movement/vibration onset. Early in the tasks (−32 to 224 ms), the decoding accuracy during the finger tapping task was higher than the decoding accuracy during vibrotactile stimulation. Decoding accuracy exceeded chance much earlier for the motor task than for sensory stimulation, reaching 70.7% accuracy at the time when decoding during sensory task exceeded chance. This result suggests that neural activation related only to attempted finger movements could potentially be used to control BMIs by a patient population with deafferentation of sensorimotor cortex.

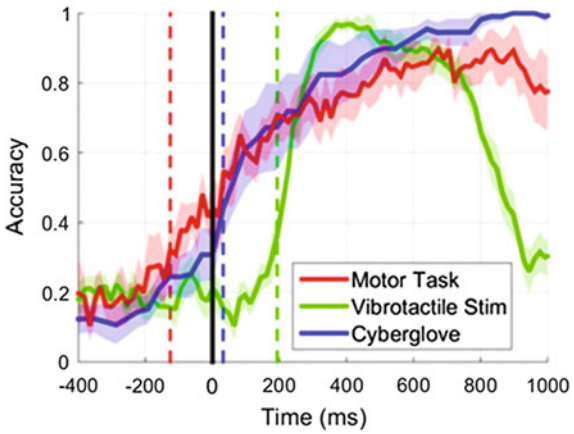

Fig. 7 Finger classification accuracy over time using CyberGlove data and ECoG recordings during the motor and sensory tasks. The *solid black line* denotes onset of any hand movement during the motor task, and onset of vibrotactile stimulation during the sensory task. The *red, green*, and *blue dashed lines* mark when decoding accuracies, using motor task high gamma, vibrotactile stimulation high gamma, and motor task CyberGlove data, exceeded chance levels. Classification accuracy at time t is based on data collected from a 352 ms window prior to and including time t. *Shading* along the *solid* traces marks the 95% confidence interval of the mean. (© IOP Publishing. Reproduced with permission. All rights reserved [3])

6 Discussion

6.1 Impact of Study

Our study showed for the first time that ECoG signals recorded from the sensorimotor cortex in humans can be used for online control of individual finger movements of a dexterous prosthetic arm. When combined with recent studies showing BMI control of arm and hand movements [2, 17, 21, 22, 72], this study points to new possibilities for neural control of prosthetic limbs to execute the finer hand movements used in actions such as ADLs. The decoding model used in this study did not require a long training period or learning a new mapping to control finger movements. Instead, it extracted information from the neural signals normally associated with finger movements, allowing for natural control of the MPL fingers. By analyzing the decoding accuracy of neural activations that precede the timescale of sensory feedback, we found it is likely that a BMI could provide individual finger control even when sensory afferent information is absent, such as is the case in patients with spinal cord injuries.

6.2 Study Limitations

While the results of this study are very convincing, they have only been demonstrated in one patient so far. A larger sample size is needed in order to generalize the conclusion that ECoG signals from the sensorimotor cortex can be used to control individual finger movements in real-time across many people. However, it is difficult to obtain more than a few patients with implanted electrodes in the proper area of the motor cortex, especially since these major surgeries are mostly done as part of clinical treatment. It is also difficult to say how these results can be generalized to volitional control by quadriplegics and amputees, who have almost no sensory or motor responses. One study has provided preliminary evidence that ECoG signals recorded from postcentral gyrus can be used for real-time BMI control [17]. The question is whether the neural activations in these patients during attempted movements can reliably carry enough information to achieve adequate control of upper limb movements using a prosthetic arm. Szameitat et al. found extensive fMRI activation in sensorimotor areas of hemiparetic patients attempting wrist movements [73]. This resembled their cortical activation from imagined movements, and was much more extensive than activation from motor imagery in healthy subjects, which has been used to control BMI in the past [15]. Studies have shown that ECoG and MEA recordings from the sensorimotor cortex of a tetraplegic patient can be used to control 3D movements of a prosthetic arm and hand [17, 21, 23, 24, 26]. However, the overall number of subjects used to demonstrate this remains low.

Analysis in this online finger control study did show significant neural activity in both precentral and postcentral gyri before movement in the finger tapping task, which means neural activations during periods of no movement could potentially include relevant information for motor decoding. While post-movement activity in postcentral gyrus can be attributed to sensory feedback and proprioceptive information, pre-movement activity in this area could arise from an 'efference copy' signal sent from premotor and motor cortices during motor planning [74–78]. If such information is sent to somatosensory cortex before movement onset, it may be possible to leverage the somatotopic organization in S1 to predict finger movements before movement onset, or even without movement execution in the case of patients with deafferentation of S1.

6.3 Future Directions

Further control of complex upper limb movements is necessary for restoring motor function to patients with upper limb paralysis. Combined control of arm, hand, and finger movements would allow patients to perform complex actions relevant to different goals or ADLs. Complete neural control of complex movements would require long-term implantable electrodes and possibly frequent re-training periods. Modeling movements of individual parts of the arm and hand, such as individual

fingers, as components of movement synergies could improve patients' abilities to accomplish functional tasks. Furthermore, a more expansive coverage that includes other cortical areas also involved in motor planning would provide additional control of goal-directed movements, but the network connections involved in planning and executing such movements are still being studied. In the meantime, an alternative may be to develop shared-control BMIs, which use a combination of neural signals and intelligent robots to increase the functionality and usefulness of BMIs. One such instantiation of a semi-autonomous BMI incorporated eye tracking and computer vision with neural signals to initiate reaching and grasping of objects using the MPL [72]. Another study demonstrated shared offline control of 3D endpoint trajectories using neural signals and dynamic movement primitive models of common trajectories [79]. With these systems, neural control would either be used to initiate or modify machine-calculated movement trajectories without relying completely on noisy neural signals for movement execution.

References

1. J. Kubánek, K.J. Miller, J.G. Ojemann, J.R. Wolpaw, G. Schalk, Decoding flexion of individual fingers using electrocorticographic signals in humans. J. Neural Eng. **6**(6), 66001 (2009)
2. C.A. Chestek et al., Hand posture classification using electrocorticography signals in the gamma band over human sensorimotor brain areas. J. Neural Eng. **10**(2), 26002 (2013)
3. G. Hotson et al., Individual finger control of a modular prosthetic limb using high-density electrocorticography in a human subject. J. Neural Eng. **13**(2), 26017 (2016)
4. S.N. Flesher et al., Intracortical microstimulation of human somatosensory cortex. Sci. Transl. Med. aaf8083 (2016)
5. M.J. Morrell, Responsive cortical stimulation for the treatment of medically intractable partial epilepsy. Neurology **77**(13), 1295–1304 (2011)
6. T. Tsubokawa, Y. Katayama, T. Yamamoto, T. Hirayama, S. Koyama, Chronic motor cortex stimulation in patients with thalamic pain. J. Neurosurg. **78**(3), 393–401 (1993)
7. Y. Katayama, C. Fukaya, T. Yamamoto, Poststroke pain control by chronic motor cortex stimulation: neurological characteristics predicting a favorable response. J. Neurosurg. **89**(4), 585–591 (1998)
8. J.-P. Nguyen et al., Treatment of chronic neuropathic pain by motor cortex stimulation: results of a bicentric controlled crossover trial. Brain Stimul. **1**(2), 89–96 (2008)
9. Z.C. Chao, Y. Nagasaka, N. Fujii, Long-term asynchronous decoding of arm motion using electrocorticographic signals in monkeys. Front. Neuroeng. **3**, 3 (2010)
10. N.E. Crone, D.L. Miglioretti, B. Gordon, R.P. Lesser, Functional mapping of human sensorimotor cortex with electrocorticographic spectral analysis. II. Event-related synchronization in the gamma band. Brain **121**(12), 2301–2315 (1998)
11. K.J. Miller, M. den Nijs, P. Shenoy, J.W. Miller, R.P.N. Rao, J.G. Ojemann, Real-time functional brain mapping using electrocorticography. NeuroImage **37**(2), 504–507 (2007)
12. E.C. Leuthardt et al., Electrocorticographic frequency alteration mapping: a clinical technique for mapping the motor cortex. Oper. Neurosurg. **60**, 260–271 (2007)
13. E.C. Leuthardt, G. Schalk, J.R. Wolpaw, J.G. Ojemann, D.W. Moran, A brain–computer interface using electrocorticographic signals in humans. J. Neural Eng. **1**(2), 63 (2004)

14. G. Schalk et al., Two-dimensional movement control using electrocorticographic signals in humans. J. Neural Eng. **5**(1), 75 (2008)
15. E.C. Leuthardt, K.J. Miller, G. Schalk, R.P.N. Rao, J.G. Ojemann, Electrocorticography-based brain computer Interface-the seattle experience. IEEE Trans. Neural Syst. Rehabil. Eng. **14**(2), 194–198 (2006)
16. K.J. Miller, G. Schalk, E.E. Fetz, M. den Nijs, J.G. Ojemann, R.P.N. Rao, Cortical activity during motor execution, motor imagery, and imagery-based online feedback. Proc. Natl. Acad. Sci. **107**(9), 4430–4435 (2010)
17. W. Wang et al., An electrocorticographic brain interface in an individual with tetraplegia. PLoS ONE **8**(2), e55344 (2013)
18. M.G. Bleichner, Z.V. Freudenburg, J.M. Jansma, E.J. Aarnoutse, M.J. Vansteensel, N.F. Ramsey, Give me a sign: decoding four complex hand gestures based on high-density ECoG. Brain Struct. Funct. 1–14 (2014)
19. T. Pistohl, T. Ball, A. Schulze-Bonhage, A. Aertsen, C. Mehring, Prediction of arm movement trajectories from ECoG-recordings in humans. J. Neurosci. Methods **167**(1), 105–114 (2008)
20. T. Pistohl, A. Schulze-Bonhage, A. Aertsen, C. Mehring, T. Ball, Decoding natural grasp types from human ECoG. NeuroImage **59**(1), 248–260 (2012)
21. T. Yanagisawa et al., Real-time control of a prosthetic hand using human electrocorticography signals. J. Neurosurg. **114**(6), 1715–1722 (2011)
22. M.S. Fifer et al., Simultaneous neural control of simple reaching and grasping with the modular prosthetic limb using intracranial EEG. IEEE Trans. Neural Syst. Rehabil. Eng. **22** (3), 695–705 (2014)
23. L.R. Hochberg et al., Reach and grasp by people with tetraplegia using a neurally controlled robotic arm. Nature **485**(7398), 372–375 (2012)
24. J.L. Collinger et al., High-performance neuroprosthetic control by an individual with tetraplegia. The Lancet **381**(9866), 557–564 (2013)
25. T. Aflalo et al., Decoding motor imagery from the posterior parietal cortex of a tetraplegic human. Science **348**(6237), 906–910 (2015)
26. B. Wodlinger, J.E. Downey, E.C. Tyler-Kabara, A.B. Schwartz, M.L. Boninger, J.-L. Collinger, Ten-dimensional anthropomorphic arm control in a human brain–machine interface: difficulties, solutions, and limitations. J. Neural Eng. **12**(1), 16011 (2015)
27. C.E. Bouton et al., Restoring cortical control of functional movement in a human with quadriplegia. Nature **533**(7602), 247–250 (2016)
28. S.B. Hamed, M.H. Schieber, A. Pouget, Decoding M1 neurons during multiple finger movements. J. Neurophysiol. **98**(1), 327–333 (2007)
29. V. Aggarwal et al., Asynchronous decoding of dexterous finger movements using M1 neurons. IEEE Trans. Neural Syst. Rehabil. Eng. **16**(1), 3–14 (2008)
30. S. Acharya, F. Tenore, V. Aggarwal, R. Etienne-Cummings, M.H. Schieber, N.V. Thakor, Decoding individuated finger movements using volume-constrained neuronal ensembles in the M1 hand area. IEEE Trans. Neural Syst. Rehabil. Eng. **16**(1), 15–23 (2008)
31. K. Liao, R. Xiao, J. Gonzalez, L. Ding, Decoding individual finger movements from one hand using human EEG signals. PLoS ONE **9**(1), e85192 (2014)
32. A.Y. Paek, H.A. Agashe, J.L. Contreras-Vidal, Decoding repetitive finger movements with brain activity acquired via non-invasive electroencephalography. Front. Neuroeng. **7** (2014)
33. S. Acharya, M.S. Fifer, H.L. Benz, N.E. Crone, N.V. Thakor, Electrocorticographic amplitude predicts finger positions during slow grasping motions of the hand. J. Neural Eng. **7**(4), 46002 (2010)
34. R. Flamary, A. Rakotomamonjy, Decoding finger movements from ECoG signals using switching linear models. Front. Neurosci. **6** (2012)
35. N. Liang, L. Bougrain, Decoding finger flexion from band-specific ECoG signals in humans. Front. Neurosci. 6 (2012)

36. Y. Nakanishi et al., Decoding fingertip trajectory from electrocorticographic signals in humans. Neurosci. Res. **85**, 20–27 (2014)
37. J. Hammer et al., Predominance of movement speed over direction in neuronal population signals of motor cortex: intracranial EEG data and a simple explanatory model. Cereb. Cortex **26**(6), 2863–2881 (2016)
38. G. Schalk et al., Decoding two-dimensional movement trajectories using electrocorticographic signals in humans. J. Neural Eng. **4**(3), 264 (2007)
39. D.T. Bundy, M. Pahwa, N. Szrama, E.C. Leuthardt, Decoding three-dimensional reaching movements using electrocorticographic signals in humans. J. Neural Eng. **13**(2), 26021 (2016)
40. W. Penfield, E. Boldrey, Somatic motor and sensory representation in the cerebral cortex of man as studied by electrical stimulation. Brain J. Neurol. (1937)
41. P. Hluštík, A. Solodkin, R.P. Gullapalli, D.C. Noll, S.L. Small, Somatotopy in human primary motor and somatosensory hand representations revisited. Cereb. Cortex **11**(4), 312–321 (2001)
42. R.M. Sanchez-Panchuelo, S. Francis, R. Bowtell, D. Schluppeck, Mapping human somatosensory cortex in individual subjects with 7T functional MRI. J. Neurophysiol. **103**(5), 2544–2556 (2010)
43. M.H. Schieber, Constraints on somatotopic organization in the primary motor cortex. J. Neurophysiol. **86**(5), 2125–2143 (2001)
44. J.N. Sanes, J.P. Donoghue, V. Thangaraj, R.R. Edelman, S. Warach, Shared neural substrates controlling hand movements in human motor cortex. Science **268**(5218), 1775–1777 (1995)
45. I. Indovina, J.N. Sanes, On somatotopic representation centers for finger movements in human primary motor cortex and supplementary motor area. NeuroImage **13**(6), 1027–1034 (2001)
46. M.H. Schieber, Somatotopic gradients in the distributed organization of the human primary motor cortex hand area: evidence from small infarcts. Exp. Brain Res. **128**(1–2), 139–148 (1999)
47. C.E. Vargas-Irwin, G. Shakhnarovich, P. Yadollahpour, J.M.K. Mislow, M.J. Black, J.P. Donoghue, Decoding complete reach and grasp actions from local primary motor cortex populations. J. Neurosci. **30**(29), 9659–9669 (2010)
48. M. Saleh, K. Takahashi, Y. Amit, N.G. Hatsopoulos, Encoding of coordinated grasp trajectories in primary motor cortex. J. Neurosci. **30**(50), 17079–17090 (2010)
49. M. Saleh, K. Takahashi, N.G. Hatsopoulos, Encoding of coordinated reach and grasp trajectories in primary motor cortex. J. Neurosci. **32**(4), 1220–1232 (2012)
50. J.C. Kao, P. Nuyujukian, S.I. Ryu, M.M. Churchland, J.P. Cunningham, K.V. Shenoy, Single-trial dynamics of motor cortex and their applications to brain-machine interfaces. Nat. Commun. **6**, 7759 (2015)
51. S.A. Overduin, A. d'Avella, J. Roh, J.M. Carmena, E. Bizzi, Representation of muscle synergies in the primate brain. J. Neurosci. **35**(37), 12615–12624 (2015)
52. A. d'Avella, A. Portone, L. Fernandez, F. Lacquaniti, Control of fast-reaching movements by muscle synergy combinations. J. Neurosci. **26**(30), 7791–7810 (2006)
53. S.A. Overduin, A. d'Avella, J. Roh, E. Bizzi, Modulation of muscle synergy recruitment in primate grasping. J. Neurosci. **28**(4), 880–892 (2008)
54. A. d'Avella, A. Portone, F. Lacquaniti, Superposition and modulation of muscle synergies for reaching in response to a change in target location. J. Neurophysiol. **106**(6), 2796–2812 (2011)
55. C.R. Mason, J.E. Gomez, T.J. Ebner, Hand synergies during reach-to-grasp. J. Neurophysiol. **86**(6), 2896–2910 (2001)
56. P.H. Thakur, A.J. Bastian, S.S. Hsiao, Multidigit movement synergies of the human hand in an unconstrained haptic exploration task. J. Neurosci. **28**(6), 1271–1281 (2008)
57. R. Vinjamuri, M. Sun, C.-C. Chang, H.-N. Lee, R.J. Sclabassi, Z.-H. Mao, Dimensionality reduction in control and coordination of the human hand. IEEE Trans. Biomed. Eng. **57**(2), 284–295 (2010)

58. S.A. Overduin, A. d'Avella, J.M. Carmena, E. Bizzi, Microstimulation activates a handful of muscle synergies. Neuron **76**(6), 1071–1077. (2012)
59. S.A. Overduin, A. d'Avella, J.M. Carmena, E. Bizzi, Muscle synergies evoked by microstimulation are preferentially encoded during behavior. Front. Comput. Neurosci. 8 (2014)
60. M.S. Graziano, C.S. Taylor, T. Moore, Complex movements evoked by microstimulation of precentral cortex. Neuron **34**(5), 841–851 (2002)
61. M. Desmurget et al., Neural representations of ethologically relevant hand/mouth synergies in the human precentral gyrus. Proc. Natl. Acad. Sci. U.S.A. **111**(15), 5718–5722 (2014)
62. M. Mollazadeh, V. Aggarwal, N.V. Thakor, M.H. Schieber, Principal components of hand kinematics and neurophysiological signals in motor cortex during reach to grasp movements. J. Neurophysiol. **112**(8), 1857–1870 (2014)
63. E. Kirsch, G. Rivlis, M.H. Schieber, Primary motor cortex neurons during individuated finger and wrist movements: correlation of spike firing rates with the motion of individual digits versus their principal components. Front. Neurol. **5** (2014)
64. J.S. Duncan, X. Papademetris, J. Yang, M. Jackowski, X. Zeng, L.H. Staib, Geometric strategies for neuroanatomic analysis from MRI. NeuroImage **23**(Supplement 1), S34–S45 (2004)
65. Y. Guo, T. Hastie, R. Tibshirani, Regularized linear discriminant analysis and its application in microarrays. Biostatistics **8**(1), 86–100 (2007)
66. M.S. Johannes, J.D. Bigelow, J.M. Burck, S.D. Harshbarger, M.V. Kozlowski, T. Van Doren, An overview of the developmental process for the modular prosthetic limb. Johns Hopkins APL Tech. Dig. **30**(3), 207–216 (2011)
67. A. Harris, K. Katyal, M. Para, J. Thomas, Revolutionizing prosthetics software technology, in *2011 IEEE International Conference on Systems, Man, and Cybernetics* (2011), pp. 2877–2884
68. M.M. Bridges, M.P. Para, M.J. Mashner, Control system architecture for the modular prosthetic limb. Johns Hopkins APL Tech. Dig. **30**(3) (2011)
69. M.S. Fifer, S. Acharya, H.L. Benz, M. Mollazadeh, N.E. Crone, N.V. Thakor, Towards electrocorticographic control of a dexterous upper limb prosthesis. IEEE Pulse **3**(1), 38–42 (2012)
70. Amputee Makes History with APL's Modular Prosthetic Limb, http://www.jhuapl.edu/newscenter/pressreleases/2014/141216.asp. Accessed 30 Nov 2016
71. APL's Modular Prosthetic Limb Reaches New Levels of Operability, http://www.jhuapl.edu/newscenter/pressreleases/2016/160112.asp. Accessed 30 Nov 2016
72. D.P. McMullen et al., Demonstration of a semi-autonomous hybrid brain–machine Interface using human intracranial EEG, eye tracking, and computer vision to control a robotic upper limb prosthetic. IEEE Trans. Neural Syst. Rehabil. Eng. **22**(4), 784–796 (2014)
73. A.J. Szameitat, S. Shen, A. Conforto, A. Sterr, Cortical activation during executed, imagined, observed, and passive wrist movements in healthy volunteers and stroke patients. NeuroImage **62**(1), 266–280 (2012)
74. R.J. Nelson, Interactions between motor commands and somatic perception in sensorimotor cortex. Curr. Opin. Neurobiol. **6**(6), 801–810 (1996)
75. M.S. Christensen, J. Lundbye-Jensen, S.S. Geertsen, T.H. Petersen, O.B. Paulson, J.B. Nielsen, Premotor cortex modulates somatosensory cortex during voluntary movements without proprioceptive feedback. Nat. Neurosci. **10**(4), 417–419 (2007)
76. T.B. Crapse, M.A. Sommer, Corollary discharge circuits in the primate brain. Curr. Opin. Neurobiol. **18**(6), 552–557 (2008)
77. V. Gritsenko, N.I. Krouchev, J.F. Kalaska, Afferent input, efference copy, signal noise, and biases in perception of joint angle during active versus passive elbow movements. J. Neurophysiol. **98**(3), 1140–1154 (2007)

78. H. Sun et al., Sequential activation of premotor, primary somatosensory and primary motor areas in humans during cued finger movements. Clin. Neurophysiol. Off. J. Int. Fed. Clin. Neurophysiol. (2015)
79. G. Hotson, R.J. Smith, A.G. Rouse, M.H. Schieber, N.V. Thakor, B.A. Wester, High precision neural decoding of complex movement trajectories using recursive Bayesian estimation with dynamic movement primitives. IEEE Robot. Autom. Lett. **1**(2), 676–683 (2016)

Motor Imagery BCI with Auditory Feedback as a Mechanism for Assessment and Communication in Disorders of Consciousness

Damien Coyle, Jacqueline Stow, Karl McCreadie, Nadia Sciacca, Jacinta McElligott and Áine Carroll

Abbreviations

BCI	Brain-computer interface
MCS	Minimally conscious state
CRS-R	Coma Recovery Scale Revised
VS	Vegetative state
EEG	Electroencephalography
SMR	Sensorimotor rhythms
MI	Motor imagery
DoC	Disorders of consciousness
WHIM	Wessex Head Index Measurement

1 Introduction

Patients with disorders of consciousness (DoC) are difficult to assess both because of their unpredictable fluctuation of awareness and the current adopted scales, which have a poor prognostic reliability [1]. Individuals who are in a minimally conscious state (MCS) or vegetative state (VS), or with unresponsive wakefulness syndrome (UWS), may be incapable of providing volitional overt motor responses. This has resulted in a rate of 43% of patients who were diagnosed as having VS being reclassified as MCS after further assessment [2]. The relatively few patients with these disorders who can alter their brain activity in response to stimuli or

D. Coyle (✉) · K. McCreadie · N. Sciacca
Intelligent Systems Research Centre, Faculty of Computing and Engineering, Magee Campus, Ulster University, Northland Road, Derry BT48 7JL, Northern Ireland, UK
e-mail: dh.coyle@ulster.ac.uk

J. Stow · J. McElligott · Á. Carroll
National Rehabilitation Hospital, Rochestown Avenue, Dun Laoghaire, Republic of Ireland

C. Guger et al. (eds.), *Brain-Computer Interface Research*,
SpringerBriefs in Electrical and Computer Engineering,
DOI 10.1007/978-3-319-57132-4_5

commands are potentially capable of providing information about their state and condition through direct measures of brain activity using a brain-computer interface (BCI). Such potential may enable adoption of more efficient devices to detect awareness in these patients and enable them to participate actively in decision making. These methods can include equipment that may be incorporated in rehabilitation programs and daily life.

EEG μ (8–12 Hz) and β (13–30 Hz) bands are altered during sensorimotor processing. Oscillations in these bands are known as sensorimotor rhythms (SMR) [3–5]. Event-related desynchronization and synchronization have been evaluated in cognitive studies and provide distinct EEG pattern differences that form the basis of left or right hand or foot SMR-based BCIs [3–5]. Brain-computer interfaces bypass the normal neuromuscular communication pathways, where the intention of the user is determined from various brain activations measured invasively or noninvasively. Brain responses to external stimuli or voluntary modulation of brain activity may provide intended communication. Brain-computer interfaces have been evaluated in gaming, stroke rehabilitation, and by other people who have limited neuromuscular control because of disease or injury [6–9]. Detection of awareness based on EEG has followed BCI protocols [9–12]. People who have DoC may achieve comprehension and follow instructions to perform motor imageries by assessing the event-related desynchronization and synchronization patterns or distinguishing motor imageries using EEG patterns. Sensorimotor rhythm activations may occur in 19% of subjects who have an MCS or VS, with some patients capable of sustained attention, response selection, working memory, and language comprehension [11]. Real-time SMR feedback in an uncommunicative patient with MCS may affect the awareness detection protocol, as the patient may become aware that the motor imagery (MI) task being performed can affect the position of a sound or visual object presented on a screen and this may be encouraging or provide an impetus to remain attentive [9]. Visual and auditory feedback may allow users of a BCI to see or hear the effects of their MI and enable them to modulate or affect something external to their body without movement [13]. Feedback may motivate patients who have spinal cord injury or stroke subjects and increase performance when learning to control a BCI [14, 15]. Real-time feedback may encourage, motivate, and inform the user of the technology that they may be capable of engaging the BCI by intentionally modulating brain activity.

With the present study, we showed for the first time both real-time feedback of SMR in DoC and the use of auditory SMR feedback. Visual acuity and gaze control of many DoC suffers may be insufficient for gaze dependent BCIs; therefore, the presentation of auditory cues and feedback for sensorimotor BCI protocols may be more appropriate for DoC based BCI applications.

In this chapter, we present a method for auditory feedback of SMR during MI using a BCI framework. We present an overview of results of four patients who have DoC, showing the ability of the systems to detect differences in binary MI related rhythms and how feedback may influence a patient's ability to modulate sensorimotor activity over multiple sessions of training with real-time visual and auditory feedback.

2 Methods

2.1 Participants

The study included 4 subjects based in Ireland: E, a 27-year-old man who was 12 years after treatment for a juvenile posterior fossa astrocytoma and postoperative complications that caused severe brain damage and MCS(Coma Recovery Scale Revised [CRS-R] score, 4); J, a 53-year-old man who was 4 years after anoxic brain injury that caused MCS (CRS-R score, 3); P, a 30-year-old man who was 4 years after severe head trauma that caused MCS; and Z, a 31-year-old woman who was 12 months after a subarachnoid haemorrhage and seizure with possible hypoxic brain injury that caused MCS (Wessex Head Index Measurement [WHIM], 26), (see Table 1) [16–18]. All subjects required full assistance for all activities of daily living. All subjects had an initial EEG-based assessment in a single session. Further BCI training sessions were performed with participants E (19 sessions), J (10 sessions), and P (7 sessions). Initial assessments were performed in the hospital (subjects E and Z), care home (subject P), and family home (subject J). Follow up BCI training was performed in their family homes (subjects E and J) and care home (subject P). Informed consent was given by the families and medical teams of the subjects. Ethical approval was granted by the National Rehabilitation Hospital and the Ulster University Research Ethics Committees. A summary of the patient data is shown in Table 1.

2.2 Study Design

For awareness detection, initial EEG-based assessment involved imagined hand versus toe movement and was performed to activate sensorimotor areas and

Table 1 Study participants E, J, P and Z summary including gender/age, injury, diagnosis, and post injury period

	Participant E	Participant J	Participant P	Participant Z
Gender/Age	Male, 27	Male, 53	Male, 30	Female, 31
Injury	Juvenile posterior Fossa Astrocytoma with complications after post-operative surgery	Anoxic brain injury	Severe head trauma	Subarachnoid haemorrhage and seizure with possible hypoxic brain injury
Diagnosis	MCS, CRS-R scores 4/23.	MCS, CSR-R score 3	MCS	Unclear, possible MCS, WHIM score 26 (since injury)
Post injury period	12 years	4 years	4 years	11 months

modulate brain rhythms during 90 trials for each subject. Within-subject and within-group analyses were performed to determine significant activations.

For BCI performance, within-subject analysis was performed in multiple BCI technology training sessions. The training sessions aimed to improve the capacity of the user to modulate SMR through visual and auditory feedback and to determine whether response reliability could be reached to enable the BCI to be used as a basic communication channel.

2.3 Data Acquisition

The study included an initial assessment and BCI phase 1 and phase 2 training sessions. In the initial assessment and phase 1 trials, 3 bipolar EEG channels were recorded using a mobile EEG device (g.MOBIlab, g.tec Medical Engineering, Schiedlberg, Austria) as previously described [11]. In phase 2, 16 channels over sensorimotor areas were recorded (g.BSamp, g.tec), digitized (cDAQ 9171, National Instruments, Austin, TX, USA), oversampled at 2 kHz, and average subsampled to 125 Hz. Active electrodes were used (g.GAMMAsys, g.tec). Results from only 3 bipolar channels around electrode positions C3, Cz, and C4 are reported for the majority of sessions. Participant J's final two sessions were conducted with a 16 channel g.Nautilus amplifier. The subjects sat in front of a laptop computer in a wheelchair with the head held upright with a head strap, or sat in the upright position in a bed with the head resting on a pillow.

2.4 Initial Assessment Protocol

The first repetition in the session was similar to a previously described protocol, with MI to squeeze the right hand or wiggle the toes performed in 6 blocks of 15 trials/block (3 blocks for hand squeezing, alternating with 3 blocks for toe wiggling) [10]. Consecutive blocks alternated between hand and toe MI. Each block began with visual and auditory task instructions, which were, "Every time you hear a beep and/or see an arrow on the screen, try to imagine that you are squeezing your right hand into a fist and then relaxing it" or the first part followed "…try to imagine that you are wiggling your toes and then relaxing. Concentrate on the way your muscles would feel if you actually were performing this movement. Try to do this as soon as you hear each beep or see the arrow." After 5 s, the instructions were followed by the binaural presentation of 15 beep tones (each tone, 600 Hz for 60 ms; time between tones, 1 to 2 s, time chosen randomly) synchronized with a cue arrow appearing on the screen (Fig. 1). After 15 trials requesting hand squeeze or toe wiggle imagery, the block concluded with an instruction to relax. The subject rested for 1 to 2 min before the start of the next block (Fig. 1). The protocol differed from the previously reported protocol because instructions and cues currently were

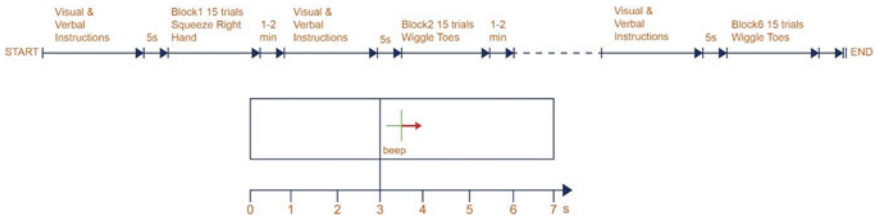

Fig. 1 Initial assessment sessions for subjects with disorders of consciousness. **a** Timing of initial assessment trials. **b** Structure of blocks in initial assessment

presented both aurally and visually [10]. Some participants closed the eyes and may have fallen asleep after the first block. For the remaining rounds a member of the research team observed the subject and provided verbal instructions "imagine squeezing the right hand" (or "imagine wiggling the toes") when the subject appeared to be disengaged or asleep.

2.5 Real-Time Visual Feedback During Initial Repetition

Feedback is necessary to improve sensorimotor learning to control a BCI that is based on SMR [14, 15]. Subjects had fluctuating alertness and wakefulness but frequently closed their eyes. Real-time feedback was provided to gain and maintain the attention of the participant. Feedback presented in the form of a game was used in this instance to engage the participant and to add interest to the often tedious task of MI training.

2.6 Additional Assessment

After the first repetition of 6 rounds, the EEG data were analysed and subject-specific parameters were selected to enable discrimination of the two MI tasks (hand and toes) using EEG. Subject E participated in feedback experiments using a ball-basket model (See Fig. 2). The experiment included 60 trials in which the subject was asked to direct a ball into 1 of 2 green target baskets that were positioned on the left or right at the bottom of the screen. The ball fell continuously for 3 s and could be directed to the left with imagery to wiggle the toes or to the right with imagery to squeeze the right hand. After a brief rest, another feedback experiment was performed with a spaceship that moved on the screen to the left or right using MI to dodge asteroids that fell from the top to bottom of the screen (See Fig. 2) [19]. Only subjects E and J participated in the spaceship experiment. The subjects were given verbal instructions about how to control the feedback; during the initial 4 trials and periodically during each repetition, attentiveness was encouraged by prompting the subject verbally about the correct MI required.

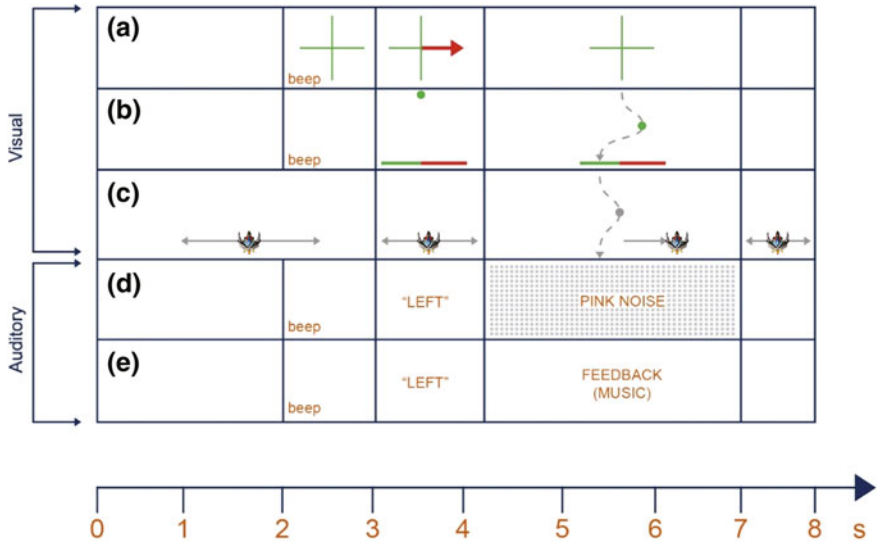

Fig. 2 Trial timing for training sessions with a brain-computer interface. **a** Visual cue training with no feedback. **b** Visual ball and basket feedback. **c** Visual spaceship game training. **d** Auditory feedback with pink noise. **e** Auditory feedback with musical samples

2.7 Follow-up Training Sessions

In follow-up BCI training sessions, subjects were asked to use left or right hand MI to activate sensorimotor areas. Stereo auditory feedback was given as broadband noise (1/frequency or pink noise) or a musical sample. The broadband noise contained cues above and below 1.5 kHz, important in the effective localization of an auditory event. A musical palette included 10 popular musical genres (blues, classical, country, electronic, folk, hip-hop, Irish traditional, jazz, reggae, and rock music). Each genre included an excerpt from a track from each of 3 artists such as Benny Goodman, Charlie Parker, and Miles Davis for jazz music. Auditory feedback was provided with earphones (ER4P, Etymotic Research, Inc., Elk Grove Village, IL, USA). Targets were presented to subjects as a spoken command (left or right), heard in the corresponding ear. Feedback was modulated by continually varying the azimuthal position of the sounds between ±90° using left and right hand movement imagination. Visual feedback was given (subject E only) with the ball-basket and spaceship models. For feedback, the subject was given verbal instruction about how to modulate the feedback signals, and the subject was prompted verbally periodically during visual feedback with the correct MI to perform and ensure awareness of the target during periods of eye shutting or visual acuity degradation. Trial timing was standardized with a cue at 3 s and feedback from 4 to 7 s for all feedback types (See Fig. 2).

Subject E participated in visual and auditory feedback phases. Subjects J and P participated in an auditory feedback phase only. For subject E, the feedback visual phase (visual cues, feedback, and occasional verbal prompts) was performed 6 months after initial assessment. The stereo auditory feedback phase occurred 6 months after the visual feedback phase for subject E, 6 months after initial assessment for subject J, and 8 months after initial assessment for subject P. There were ≤ 8 sessions (1–1.5 h with 2–4 repetitions each; 60 trials/repetition; 8 min/repetition), with 1 to 2 sessions per day (morning and/or evening) in each phase, and each phase was performed during 1 week of intensive sessions.

2.8 Data Analysis

After the initial assessment without feedback, a leave-1-out cross validation was performed on the 6 rounds on each repetition using a BCI signal processing framework that involved the automated selection of subject-specific frequency bands (range, 1–30 Hz) and neural time-series prediction preprocessing using neural networks in conjunction with regularized common spatial patterns. Features were derived from the log-variance of pre-processed or surrogate signals within a sliding window (2 s) and classified using linear discriminant analysis. The operation of the classification step can be simplified as being that of a transform of quantitative input data to qualitative output information [20]. Discriminant analysis and classification are multivariate techniques concerned with separating distinct sets of objects (features or observations) and with allocating new objects (features or observations) to previously defined groups [19, 21–23]. The mean classification accuracy was calculated across the data folds at every sample in the trial to obtain a time course of accuracy across the trial, from imagery onset to completion. Baseline (1000 ms before cue at onset) performance was compared with peak mean classification accuracy. The discrimination accuracy of two baselines before the cued MI period also was assessed. There was no distinction expected in the EEG or correlation with the cue that occurred at 3 s. The two baselines were compared to show that differences between two points of sensorimotor activity with no event-related activation were insignificant, as expected when the subject was not performing MI. These supported the evidence that the observed activations were not obtained by chance. Nonparametric Wilcoxon signed rank test was used to assess the significance of activations. Baseline or chance performance was 50 to 60% for the 2 classes (hand versus toe or left versus right hand movement). During the feedback session, the first repetition in each session used the BCI classifier from the previous day to provide feedback or was a calibration repetition with no feedback; the first repetition each day was used to calibrate a new classifier. In some first repetitions in each session that were earlier in the training phase (i.e., in the first 2–3 sessions), no feedback was given; this enabled the user to focus solely on repeating the imagery to aid in producing a better classifier for the feedback repetitions. In a limited number of cases, if the results of the newly built classifier each day were poor, as a result of poor

data quality due to technical problems or subject inattentiveness/engagement in the task during the first repetition, the classifier from the previous day was used for the complete session on that day. In the initial assessment, the 6 no-feedback rounds were used to set up the classifier. Subsequent repetitions included visual feedback or pink noise followed by musical feedback. Analysis was performed for each repetition because different repetitions involved different feedback types, and the level of awareness or engagement was unknown and may have varied for the subjects who had MCS. Many trials were rejected because the head strap occasionally distorted the electrode cap, the subject wheezed, or teeth grinding occurred; the number of trials per repetition after artefact removal by visual inspection was reported. Statistical significance was defined by $P \leq 0.05$.

3 Results

3.1 Initial Assessment

The time course of mean classification accuracy for each subject in the initial assessment, and a feedback repetition with high mean classification accuracy, showed an increase from approximately 50% at baseline (<3 s) toward a peak in the event-related period (Table 2 and Fig. 3). All subjects had significant differences between baseline mean classification accuracy (2 s) and peak mean classification accuracy ($P \leq 0.05$) in all cases where the differences between peak and baseline (peak-baseline) range were between 15 and 45%. In contrast, the difference between 2 baseline points (1000 and 500 ms before cue) for all subjects was not significant in all subjects and repetitions, and the difference between the 2 baseline accuracies ranged from 1 to 18%. The peak mean classification accuracy for all subjects exceeded the 70% criterion level normally used to determine whether a subject was capable of using a 2 class MI BCI [24]. A group analysis comparing baseline and peak accuracies indicated significant brain activation across all subjects (P 0.001). The time at which peak mean classification accuracy was reached was beyond the cue time (3 s) for all subjects, indicating that it was not affected by the cue stimulus during the feedback repetitions. The stimulus response mechanism is normally present between 0.5 to 1 s immediately after the cue stimulus is presented. Although the peak for subject Z was at 3.8 s, this initial assessment did not have different cues for each class of MI (same auditory tone for toe movement and right hand squeeze), so the stimulus responses mechanism should not influence the accuracy in the initial assessment with no feedback. The frequency bands selected to access differences between sensorimotor activation were 8 to 13 Hz (subject E), 8 to 25 Hz (subject J), 12 to 19 Hz (subject P), and 10 to 14 Hz (subject Z), within the normal ranges for detection of differences in SMR oscillations associated with the MI tasks.

Table 2 Results showing the baseline versus peak comparison for the initial assessment and a feedback run (where baseline is the motor imagery discrimination accuracy 1 s before the cued motor imagery period and peak is the peak discrimination accuracy during the motor imagery period). Baseline versus baseline comparisons are also shown (where baselines one and two are the motor imagery discrimination accuracy 1000 and 500 ms before the cued motor imagery period, respectively). *p*-values indicate significant differences between peak versus baseline ($p < 0.05$) with no difference between baseline one versus baseline two ($p > 0.05$)

		No. trials	Peak time (s)	Peak-baseline (%)	Baseline mCA (%)	Peak mCA (%)	Wilcox. p-value	Baseline @ 2 s	Baseline @ 2.5 s	Wilcox. p-value
E	Assessment	38	7.0	21.1	71.1	92.1	0.023	71.1	63.2	0.179
	Feedback run	40	5.0	45.0	42.5	87.5	0.001	42.5	40.0	0.748
J	Assessment	84	4.1	17.9	53.6	71.4	0.011	53.6	54.8	0.841
	Feedback run	50	5.2	20.0	58.0	78.0	0.033	58.0	64.0	0.405
P	Assessment	54	5.7	18.5	51.9	72.2	0.012	51.9	50.0	0.796
	Feedback run	28	5.4	28.6	46.4	75.0	0.046	46.4	28.6	0.096
Z	Assessment	74	3.8	14.9	62.2	77.0	0.008	62.2	67.6	0.206

Fig. 3 Relation between mean classification accuracy and time for subjects who had disorders of consciousness and training sessions with the brain-computer interface system. Data shown include the initial assessment and peak auditory feedback repetition (*subject P*, feedback in the initial assessment; *subjects E* and *J*, brain-computer interface training; *subject Z*, no feedback repetition participation)

3.2 Brain-Computer Interface Training Sessions

Subjects E, J, and P participated in BCI training (multiple sessions). Subject E was involved in phases of visual and auditory feedback. Subject J and P had partaken mainly in auditory feedback repetitions because auditory feedback was the most suitable for subjects with MCS. The peak mean classification accuracy in each repetition in each session and the baseline mean classification accuracy, number of trials, and peak-baseline showed that participants E, J and P intentionally activated sensorimotor areas in responses to commands, producing significant differences between baseline and peak mean classification accuracy and (in the majority of

repetitions) producing accuracy above the 70% criterion level for two class BCI (See Fig. 4). Many trials were affected by artefacts (subject E, 34%; subject J, 10%; subject P, 2%) and were excluded from the analysis. Labels for the type of feedback (visual: ball, space game, or auditory: pink noise, musical feedback) were noted (See Fig. 4). The plots showed there were SMR activations during feedback with most repetitions showing a statistically significant difference ($P \leq 0.05$) between baseline and peak mean classification accuracy (differences between 2 baselines before cue were not significant in all repetitions except for 1 repetition for subject P [data not shown]). For subject E, the visual and auditory feedback modalities showed similar performance (visual, 80%; auditory, 79% [all repetitions]).

It was important to analyse peak-baseline because of the limited number of artefact-free trials in each repetition. Visual impairment made it unclear whether subjects were aware when the trial was ending using visual feedback, especially for the spaceship game in which the spaceship was on-screen continuously and could be modulated throughout the repetition. In addition to the lack of perceivable visual feedback, visual impairment may have caused reduced baseline versus peak accuracy differences during the visual feedback phase for subject E, but an improvement in accuracy is evident in the auditory feedback phase. Subject J showed consistent activations of sensorimotor areas in all sessions. Subject P was less engaged in the fifth and later than earlier sessions, and a family member noted that he had been physically sick during that period. The results indicated that peak accuracy did not change, but baseline accuracy increased (reason unknown) and caused the detected activation to be insignificant for all repetitions during session 5, 6, and 7 (session 7 was stopped after an initial assessment to determine interest in participating in the session, but the EEG response suggested there was no attempts been made to perform MI). Subject E, who had participated the longest in the study, produced the highest peak performances of all subjects and achieved most results >80% after session 8, suggesting that the subject was improving in performance and sensorimotor learning occurred.

Figure 5 shows topological plots of event related desynchronization/synchronization ERD/S in the most discriminative frequency band for initial assessment (squeeze right hand versus wiggle toes MI) (all subjects) and for a feedback run (hand versus foot MI) for subject E, J and P. For subject E, there is clear discrimination in the μ band during initial assessment, however ERS during right hand MI appears ipsilateral to the movement, which is unusual. In the later feedback session, there is clear ERD in the μ band in the contralateral hemisphere for right hand movement with slight ERS in the ipsilateral hemisphere. There is slight ERD observable in contralateral hemisphere for left hand movement.

Subject J exhibits clear ERS in higher μ and lower β band contralateral to right hand movement and in central midline for foot movement. ERS in these bands in indicative of activation in regions of the motor cortex that is consistent with other able-bodied studies involving these MI types. During a feedback run, subject J shows clear ERD across μ and lower to central β bands during left hand MI in contralateral motor areas and ERS in these bands in the ipsilateral hemisphere during right arm movement. These findings are again consistent with able-bodied

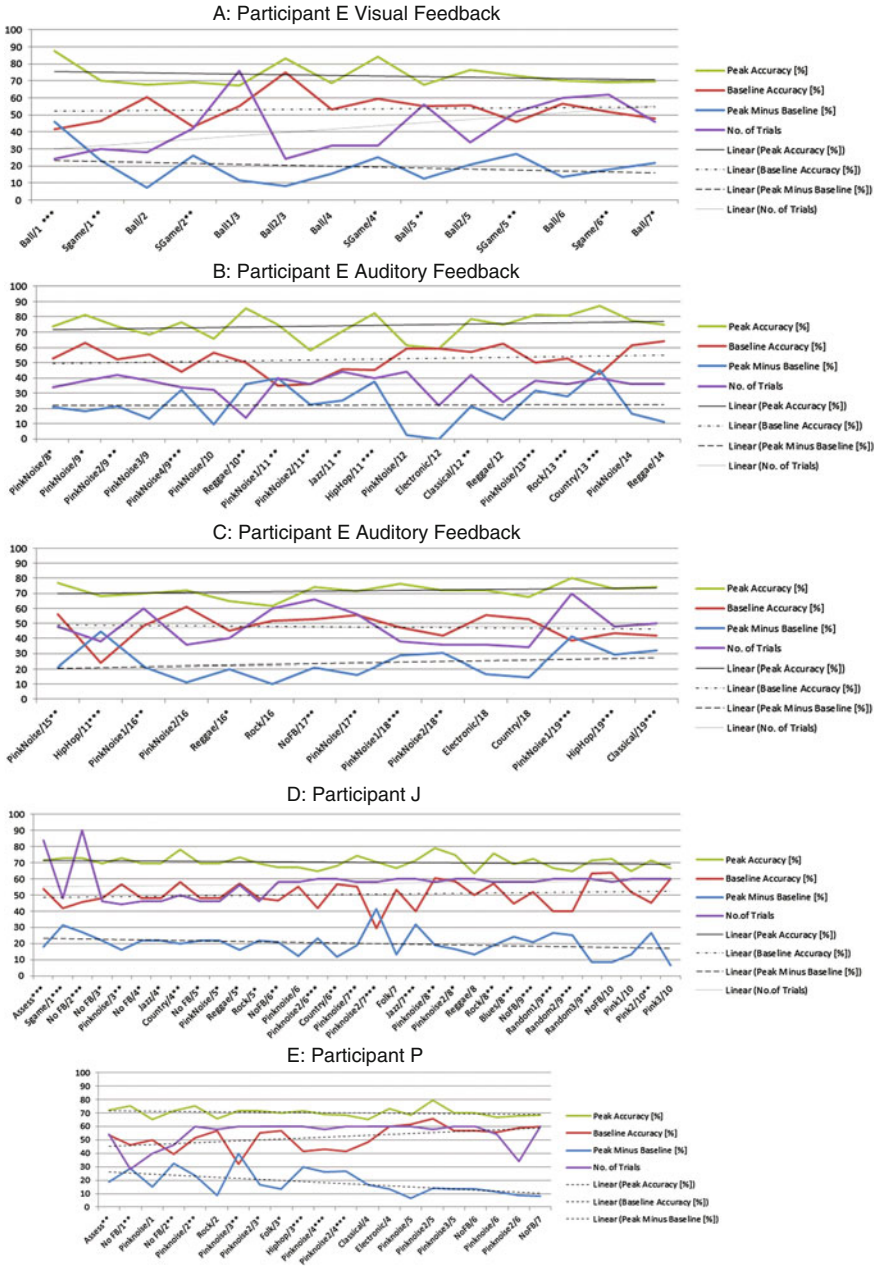

Fig. 4 Relation between baseline and peak mean classification accuracy, peak-baseline accuracy, number of trials and repetitions in subjects with disorders of consciousness and training sessions with the Brain-Computer Interface system. Data include peak, baseline (1000 ms before cue), baseline-peak mean classification accuracy from leave-1-out cross validation, number of trials in each repetition after artifact rejection, and type of feedback presented in each repetition (***$P \leq 0.005$; **$P \leq 0.05$; *$P \leq 0.1$). **a** *Subject E* results from visual feedback sessions; **b** *Subject E* results from auditory feedback sessions; **c** *Subject E* results from auditory feedback sessions (last phase); **d** *Subject J* all sessions; **e** *Subject P* all sessions

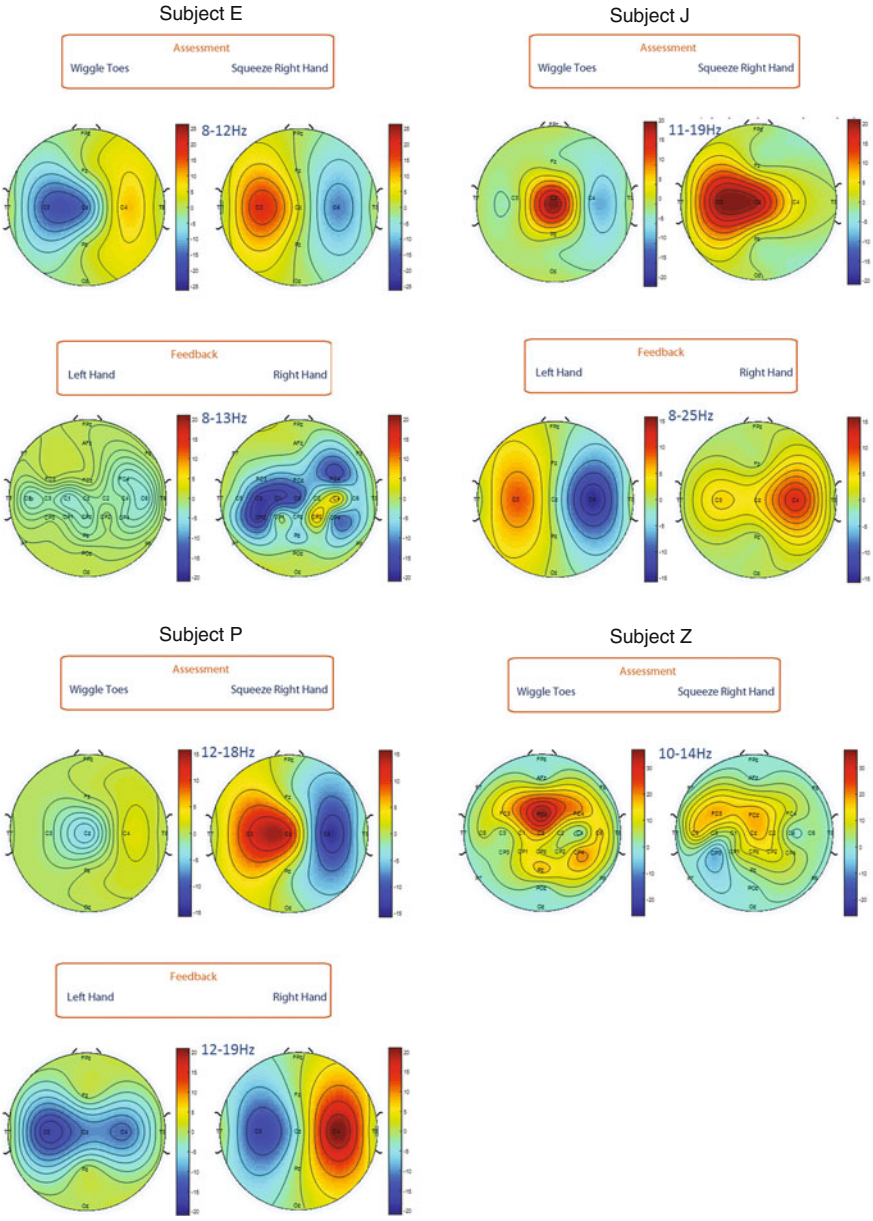

Fig. 5 Topoplots showing event-related desynchronization and synchronization in the most discriminative frequency band for initial assessment (squeeze *right* hand versus wiggle toes motor imagery) (all subjects) and for a feedback run (hand versus foot motor imagery) for *subject E*, *J* and *P*

results and provide clear indication of normal cortical activation in the MCS. Participant P has midline ERD upper μ/lower β during wiggle toes which is normal, with ipsilateral ERD and contralateral ERS in these bands during squeeze hand imagery in the initial assessment which is unusual. However, during later feedback runs, the subject shows upper μ/lower β ERD in the contralateral hemisphere and ipsilateral ERS during right hand MI. Participant J shows contralateral ERD and ERS in the upper μ band in the contralateral hemisphere during initial assessment of squeeze right hand imagery and midline ERS during wiggle toe, which is consistent with expected spatial activation and somewhat consistent with anticipated spectral changes during these MI tasks.

4 Discussion

The evidence obtained from the initial assessment suggests that these subjects who had MCS were aware of themselves and the environment. BCIs use self-directed neurophysiological processes such as the activation of the sensorimotor cortex during MI or attempted motor execution. The results observed in the initial assessment involving a cue, with instructions presented visually and verbally, suggest that subjects had the capacity for sustained attention, response selection, working memory, language comprehension, and visual and/or auditory acuity. The initial assessment results suggest that EEG-based BCI may complement current awareness assessment tests to gain a more detailed understanding of the level of awareness in patients who have a DoC. Attaining information using BCI also may clarify initial diagnosis by complementing existing assessments that involve overt motor responses. The present BCI setup required only 3 EEG channels, mobile data acquisition equipment, and automated analysis and feedback software. Therefore, a bedside assessment may easily be performed in <1 h by a patient's medical team. The EEG recording equipment is decreasing in cost, and medical teams may be easily trained to perform these assessments. After the initial assessment, subjects seemed to realize that they could modulate feedback, and they seemed to increase their attentiveness and level of arousal, which was evident in their demeanour. The realization of the possibility of affecting a visual object or sound external to the body without movement, especially after being unable to do so (for 12 years in subject E), may improve a person's psychological well-being. The subjects were more alert during audio than visual feedback, and audio trial cues were clearer with the musical palette apparently aiding alertness. This was noted anecdotally by researchers and family members of the subjects. The within-subject and between-subject differences in performance during the musical and broadband (pink) noise feedback were insignificant. Therefore, although pink noise is easier to localize than music that includes multiple instruments and vocals, the variety of sounds in the musical feedback did not adversely affect performance. However, the presentation of pink noise may be less appealing than music. The peak performances during auditory feedback for subjects E and J were obtained with musical

feedback, which suggests that musical feedback may help increase performance with SMR BCI control. The awareness assessment, MCS baseline versus peak difference, for subjects E and J suggested that their awareness was beyond the MCS and above the 70% accuracy criterion for the discrimination of 2-class MI BCI. The present results confirm the feasibility of using musical stereo audio feedback in SMR BCIs, especially for patients who have visual impairment or DoC, and it may be possible to use sound spatialisation techniques and 3-dimensional sound to improve this experience [25].

The study aimed to assess whether BCIs could provide a communication channel for subjects who have DoC. The results showed that all subjects could be trained to operate a BCI. However, to ensure reliability of the response, the aim is to continue the study in an attempt to train subjects to perform consistently at >85% accuracy prior to introducing a binary ("yes or no") response question system for MCS subjects. The consistent activation of motor areas observed suggests that sensorimotor learning in multiple sessions with auditory feedback may enable communication for users who have DoC. However, 15 to 30% of BCI users may not achieve the criterion level of control (70% accuracy) [26]. In addition, mean EEG amplitude, even in the best trained subjects, may vary over time and between sessions, and consistent performance may be difficult to attain [27]. Therefore, expectations about outcomes with BCI training programs may be guarded [28].

Subjects may become disengaged, as was the case with subject P, and not all repetitions may show significant activations. The experimenter consistently attempted to maintain dialogue and provide encouragement to all subjects and engage family members and/or carers in an interactive discussion to ensure maintenance of subject willingness to improve at using a BCI. At the end of the sessions, it was not possible to detect a consistently reliable single-trial response in all subjects, but it was possible to determine willingness to participate by assessing the data during the repetition or trials. For example, in session 7 for subject P, after no clear observation of activations during sessions 5 and 6, it was decided to ask the subject to perform the MI during the first repetition only, if he wished to continue with the session; when activation was not observed, the session was terminated. Patients who have minimally conscious state may have fluctuations in awareness. The BCI training results may not show activations when subjects are less engaged or aware, and the BCI session may help assess fluctuations in awareness.

4.1 Study Limitations

Limitations in the present study included the limited number of subjects, and there are a limited number of studies that have reported SMR and BCI-based assessment in DoC patients [10, 12]. Family members and care teams for all subjects consented to participate in further BCI training sessions, and we aim to recruit additional subjects for future study. It was difficult to use a consistent format for experiments and obtain useful data because of the new technology available for this study

population, resources required, challenges in recording EEG from nonresponsive individuals, and fluctuations in subject awareness. Study subjects were recruited at different stages of the research during the evolution of the BCI training research protocol, based on experiences gained in working with subjects who had DoC. Although the initial assessment was consistent for all 4 subjects, the sequence of BCI training sessions for subjects E, J, and P had subtle differences. Subject E participated in a visual feedback phase before the auditory feedback phase began; subject J and P began BCI training with audio after brief initial visual feedback. In addition, the variation in the type of audio feedback (pink noise or music) limited the identification of the best type of audio feedback. A variety of feedback during training may help attentiveness and interest but may affect the subject's ability to learn from the feedback. In another study of able-bodied individuals, there was no difference in performance when presenting visual and auditory feedback or when presenting different types of audio [16]. Future study may determine the best feedback presentation methods and timing to adapt the BCI classifier [29]. The present study may enable a more consistent approach in future studies that evaluates the effects of audio feedback on BCI performance in DoC and classifier adaptation or calibration.

Another study limitation was the small number of sessions for each subject. Training durations from months to years have been reported for different patient groups, e.g., a tetraplegic patient learned to control a hand orthosis after 62 sessions [30]. In comparison, the results produced by subjects in the present study are promising and consistent with performance of able-bodied subject investigations with similar protocols and number of sessions [16]. Motor imagery strategy may be changed to maximize performance, one approach may not be optimal for all subjects, and modulating sensorimotor cortical rhythms may require motor learning, time, and persistent effort [2]. In the present study, we did not assess the most appropriate MI for each individual or a larger number of electrodes to assess the brain areas that were most activated during MI, and this may be addressed in future studies.

5 Conclusions

In patients who have MCS, the true level of awareness may not be known because the patient may be unable to provide overt motor responses. The present EEG-based assessment showed that subjects attempted to activate sensorimotor areas, and this suggests that these subjects had awareness and cognitive ability. Therefore, diagnosis of these patients may be improved with an EEG-based assessment, and individuals who have DoC may have the capacity to learn how to modulate brain activity and communicate using BCI. Further research may increase the reliability of EEG-based BCI and reduce training times to enable a binary response (yes or no) to questions and enable communication for patients who cannot communicate with gestures such as an eye gaze or thumb movement.

Moreover, a number of testimonies from family members suggests that, as the results of this research provided better evidence of awareness in the patients, this has had an impact on care and treatment plans. These testimonies also indicate that there may be therapeutic values and stimulation gained by patients as they attempt to activate cognitive process during MI and whilst listening or observing feedback based on their efforts. Subjects therefore might benefit from prolonged use of BCI for stimulation and brain engagement as well as communication. With the auditory online real-time feedback setup, evaluated with DoC in research studies preceding this chapter for the first time [10, 13], MI BCIs are broadened to those with visual impairments who may not be capable of seeing targets and feedback presented visually. This is particularly important for DoC based applications of MI BCI, as visual acuity and gaze control capacity is often unknown as the eyes closed condition is prevalent in DoC.

It is recommended that online real-time feedback be provided in studies which involve MI paradigms and DoC patients. In future work, we aim to evaluate SMR BCI in a larger cohort as an assessment tool for use in diagnostic settings and for establishing communication with unresponsive patients. The therapeutic benefits of prolonged training of intentional control by brain activity through motor imagery and stimulation provided by the feedback during the process of learning to modulate SMR will also be investigated.

Acknowledgements This work is partly funded by the UK Engineering and Physical Sciences Research Council and a Royal Academy of Engineering/The Leverhulme Trust Senior Research Fellowship.

References

1. J.N. Mak, J.R. Wolpaw, Clinical applications of brain-computer interfaces: current state and future prospects. IEEE Rev. Biomed. Eng. **2**, 187–199 (2009)
2. A.M. Owen, M.R. Coleman, M. Boly, M.H. Davis, S. Laureys, J.D. Pickard, Detecting awareness in the vegetative state. Science **313**(5792), 1402 (2006)
3. G. Pfurtscheller, C. Neuper, A. Schlögl, K. Lugger, Separability of EEG signals recorded during right and left motor imagery using adaptive autoregressive parameters. IEEE Trans. Rehabil. Eng. **6**(3), 316–325 (1998)
4. G. Pfurtscheller, EEG event-related desynchronization (ERD) and event-related synchronization (ERS), in *Electroencephalography, Basic Principles, Clinical Application and Related Fields*, 4th edn., ed. by E. Niedermeyer, F.L. da Silva (Williams and Wilkins, Baltimore, MD, 1999), pp. 958–967
5. D. Coyle, G. Prasad, T.M. McGinnity, A time-frequency approach to feature extraction for a brain-computer interface with a comparative analysis of performance measures. EURASIP J. Adv. Signal Process. **2005**(19), 3141–3151 (2005)
6. D. Marshall, D. Coyle, S. Wilson, M. Callaghan, Games, gameplay, and BCI: the state of the art. IEEE Trans. Comput. Intell. AI Games **5**(2), 82–99 (2013)
7. G. Prasad, P. Herman, D. Coyle, S. McDonough, J. Crosbie, Applying a brain-computer interface to support motor imagery practice in people with stroke for upper limb recovery: a feasibility study. J. Neuroeng. Rehabil. **7**(1), 60 (2010)

8. D. Coyle, A. Satti, J. Stow, K. Mccreadie, A. Carroll, J. Mcelligott, Operating a Brain Computer Interface : Able Bodied vs. Physically Impaired Performance, in *Proceedings of the Recent Advances in Assistive Technology & Engineering Conference* (2011)
9. D. Coyle, A. Carroll, J. Stow, A. McCann, A. Ally, J. McElligott, Enabling Control in the Minimally Conscious State in a Single Session with a Three Channel BCI, in *1st Integer Decoder Workshop*, no. April (2012), pp. 1–4
10. D. Coyle, Á. Carroll, J. Stow, K. McCreadie, J. McElligott, Visual and stereo audio sensorimotor rhythm feedback in the minimally conscious state, in *Proceedings of the Fifth International Brain-Computer Interface Meeting 2013* (2013), pp. 38–39
11. D. Cruse, S. Chennu, D. Fernández-Espejo, W.L. Payne, G.B. Young, A.M. Owen, Detecting awareness in the vegetative state: electroencephalographic evidence for attempted movements to command. PLoS ONE **7**(11), e49933 (2012)
12. D. Cruse, S. Chennu, C. Chatelle, T. Bekinschtein, D. Fernández-Espejo, J.D. Pickard, S. Laureys, A.M. Owen, Bedside detection of awareness in the vegetative state: a cohort study. Lancet **378**(9809), 2088–2094 (2011)
13. D. Coyle, J. Stow, K. McCreadie, J. McElligott, Á. Carroll, Sensorimotor modulation assessment and brain-computer interface training in disorders of consciousness. Arch. Phys. Med. Rehabil. **96**(3), S62–S70 (2015)
14. J.R. Wolpaw, H. Ramoser, D.J. McFarland, G. Pfurtscheller, EEG-based communication: improved accuracy by response verification. IEEE Trans. Rehabil. Eng. **6**(3), 326–333 (1998)
15. A. Barbero, M. Grosse-Wentrup, Biased feedback in brain-computer interfaces. J. Neuroeng. Rehabil. **7**, 34 (2010)
16. J.T. Giacino, K. Kalmar, J. Whyte, The JFK Coma Recovery Scale-Revised: Measurement characteristics and diagnostic utility. Arch. Phys. Med. Rehabil. **85**(12), 2020–2029 (2004)
17. A. Shiel, S.A. Horn, B.A. Wilson, M.J. Watson, M.J. Campbell, D.L. McLellan, The Wessex Head Injury Matrix (WHIM) main scale: a preliminary report on a scale to assess and monitor patient recovery after severe head injury. Clin. Rehabil. **14**(4), 408–416 (2000)
18. F.C. Wilson, V. Elder, E. McCrudden, S. Caldwell, Neuropsychological rehabilitation : an international analysis of Wessex Head Injury Matrix (WHIM) scores in consecutive vegetative and minimally conscious state patients. Neuropsychol. Rehabil. **19** February 2012, 754–760 (2009)
19. D. Coyle, J. Garcia, A.R. Satti, T.M. Mcginnity, EEG-based Continuous Control of a Game using a 3 Channel Motor Imagery BCI, in *IEEE Symposium Series on Computational Intelligence* (2011), pp. 88–94
20. C.T. Leondes, in *Image Processing and Pattern Recognition* (Academic Press, 1998)
21. D. Coyle, Neural network based auto association and time-series prediction for biosignal processing in brain-computer interfaces. IEEE Comput. Intell. Mag. **4**(4), 47–59 (2009)
22. D. Coyle, G. Prasad, T.M. McGinnity, A time-series prediction approach for feature extraction in a brain-computer interface. IEEE Trans. Neural Syst. Rehabil. Eng. **13**(4), 461–467 (2005)
23. F. Lotte, C. Guan, Regularizing common spatial patterns to improve BCI designs: unified theory and new algorithms. IEEE Trans. Biomed. Eng. **58**(2), 355–362 (2011)
24. A. Kübler, F. Nijboer, J. Mellinger, T.M. Vaughan, H. Pawelzik, G. Schalk, D.J. McFarland, N. Birbaumer, J.R. Wolpaw, Patients with ALS can use sensorimotor rhythms to operate a brain-computer interface. Neurology **64**(10), 1775–1777 (2005)
25. K.A. Mccreadie, D.H. Coyle, G. Prasad, Motor imagery BCI feedback presented as a 3D VBAP auditory asteroids game, in *Proceedings of the Fifth International Brain-Computer Interface Meeting 2013* (2013), no. c, pp. 319–320
26. C. Vidaurre, B. Blankertz, Towards a cure for BCI illiteracy. Brain Topogr. **23**(2), 194–198 (2010)
27. D.J. Mcfarland, W.A. Sarnacki, J.R. Wolpaw, Should the parameters of a BCI translation algorithm be continually adapted? J. Neurosci. Methods **199**(1), 103–107 (2011)
28. Nuffield Council on Bioethics Report, in *Novel Neurotechnologies : Intervening in the Brain* (2013)

29. K.A. McCreadie, D.H. Coyle, G. Prasad, Sensorimotor learning with stereo auditory feedback for a brain-computer interface. Med. Biol. Eng. Comput. **51**(3), 285–293 (2013)
30. G. Pfurtscheller, C. Guger, G. Müller, G. Krausz, C. Neuper, Brain oscillations control hand orthosis in a tetraplegic. Neurosci. Lett. **292**(3), 211–214 (2000)

Brain-Computer Interface Controlling Cyborg: A Functional Brain-to-Brain Interface Between Human and Cockroach

Guangye Li and Dingguo Zhang

Abstract A kind of cyborg was developed by surgically linking a portable microstimulator with the nerves of antennas of a live cockroach. Through applying specific micro electrical stimulation, the cyborg could be remotely controlled to make left and right turns. The motion intention could be retrieved from the human brain via brain-computer interface (BCI). Steady-state visual evoked potential (SSVEP) based-electroencephalography (EEG), as a robust BCI, was used to translate human intention. By merging the technologies of cyborg and BCI, it was possible to guide a live cockroach with human brain. Experiments with different paradigms were designed and conducted to verify the performance of the proposed system. The experimental results showed that the average success rates of both human BCI and cyborg reactions in a single decision were over 85%. The cyborg could be steered successfully via the human brain to complete walking along pre-set tracks with a 20% success rate.

Keywords Brain-computer interface · Electroencephalography · Steady-state visual evoked potential · Cyborg navigation · Vockroach

1 Introduction

A cyborg is an organism with both biological and electronic parts. A variety of cyborgs or biobots were developed in recent years, such as rats, moths, cockroaches, and beetles [1–5]. Among these achievements, researchers had already been able to steer the animals or insects manually with the help of a computer or remote controller. Unlike previous work, we want to move one step forward by achieving the target of navigating a cyborg with human intention directly. To build a system that enables real-time control of a cyborg with human brain, at least two

G. Li · D. Zhang (✉)
Robotics Institute, School of Mechanical Engineering,
Shanghai Jiao Tong University, Shanghai, China
e-mail: dgzhang@sjtu.edu.cn

C. Guger et al. (eds.), *Brain-Computer Interface Research*,
SpringerBriefs in Electrical and Computer Engineering,
DOI 10.1007/978-3-319-57132-4_6

parts need to be set up. One part is a subsystem used to realize the functional control of a cyborg, and the other one is a subsystem used to translate the human brain signals. Fortunately, it's possible to realize such two key parts with current technologies.

Neural electrical stimulation was widely used when developing cyborgs based on the increasing understanding of flight dynamics and the neurophysiology of animals or insects [6]. We aim at developing a kind of cyborg based on the cockroach, due to its robust performance and easy implementability. The cockroach antennas used for navigation during walking are important sensory organs that can generate multiple sensations (such as tactile, thermal, humidity and olfactory) [7]. When sending specific micro-electrical pulse trains through the antenna nerve, stimulation information will activate the descending mechanosensory interneurons (DMIs) (interneurons with the largest caliber axons descending to thoracic levels from the brain) and subsequently activate the thoracic motor centers, then evasive behaviors such as turning will be elicited [8–10]. Therefore, a neural interface used to control the walking direction of a cockroach with a micro electrical stimulator needed be developed in this work.

Brain-computer interfaces (BCIs) can help people communicate with the external world through measuring and translating brain activities without involving muscular movements or peripheral nervous system [11]. In this study, we choose the steady-state visual evoked potential (SSVEP) based BCI to recognize the human intention because SSVEP has high signal-to-noise ratio (SNR) and information transfer rate (ITR) and is currently safe, reliable, versatile and robust in the available BCIs including invasive and non-invasive BCIs [12–15].

Based on the SSVEP-based BCI and neural stimulation technology, we build up an all-chain wireless system that enables controlling the walking directions of a cockroach with human brain directly.

2 Methodology

BCI Implementation. The framework of the developed system is shown in Fig. 1. A three-state SSVEP-based BCI was used to decode the controller's control intention. Three flashing square blocks represented the stimulation source of SSVEP [15, 16], which were located separately in the upper middle, lower left and lower right on a PC screen. The flickering frequency of each block was set as 12.5, 8.33, 6.818 Hz, denoting the rest, left-turn and right-turn control commands respectively. The human subject (controller) sat in front of the LCD screen of PC to manage direction control, wearing a portable EEG capture device (EPOC, Emotiv System Inc.) (Fig. 2a). Because the SSVEP mainly appears in the visual cortex, EEG signals from four channels (locations PO3, PO4, O1, O2 according to the international extended 10/20 system, with two CMS/DRL reference electrodes placed on C5/C6) were used for analysis. All electrode impedances were kept below 10 kΩ, and the sampling frequency was 128 Hz. A notch filter at 50 and

60 Hz was applied to process the EEG signals and the band pass is set to 0.16–43 Hz.

Cyborg Implementation. A cyborg cockroach acting as a receiver was developed after simple surgical process by the experimenters (Fig. 2b). The live Madagascar hissing cockroaches (Gromphadorhina portentosa) were adopted to make the cyborgs, since they are strong and large (about 50–80 mm) and have a slow walking speed. We surgically installed a microstimulator (Roboroach, v1.1b, Backyard Brains Inc. US) in the cockroach by inserting three tiny silver needles (left, right, ground electrode, 0.06 mm bare/0.08 mm coated) into the cockroach antennae (left, right) and the first segment of the thorax separately. The electrical stimulation pattern for the cyborg was a monopole square pulse with 1.5 V, 50 Hz, 50% duty cycle, and 500-ms pulse width. This configuration could generate a modest and proper reaction of the cyborgs, and therefore guaranteed the good online control performance.

Online Communication. Two custom software tools were written for the system. One was the SSVEP program, which included data acquisition, online analysis, and graphic user interface. The other software tool was used to realize the real-time communication between the SSVEP program and the microstimulator placed on the back of the cyborg.

Video Capture. We utilized a wireless video capture module in the SSVEP program to visually obtain the real-time response of the cyborg, and projected it to the LCD screen for the human subject (Fig. 4). Therefore, a closed-loop control system was established as shown in Fig. 1.

Experimental Paradigm. Three cyborg cockroaches were made, and three healthy human subjects were recruited. In each experiment, a cockroach was placed at a distance of about 1.5 m from the host computer. The human controller took

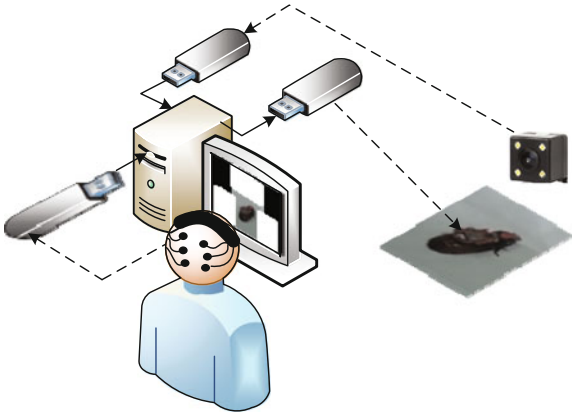

Fig. 1 System framework. Four modules are included in the system: (1) the EEG acquisition module is used to obtain the brain signals from the human; (2) the host computer runs the SSVEP program and acts as an integrated platform; (3) data travels to the cyborg cockroach and its USB-based adapter; and (4) the wireless video capture module is used to transfer the real-time images of the cyborg to the LCD screen of PC for the human

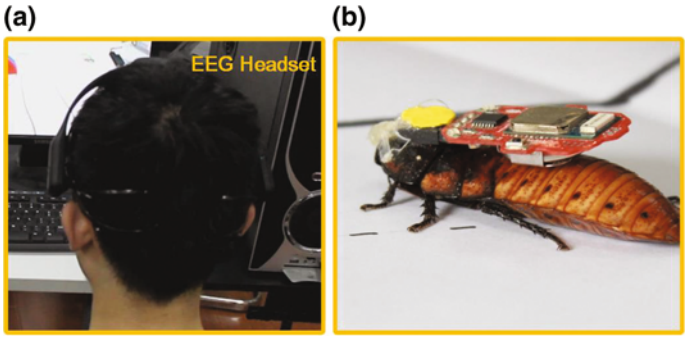

Fig. 2 Experimental setup. **a** A subject (controller) wearing a portable BCI device performed the experiment to acquire the SSVEP signals. **b** A cyborg cockroach (receiver) was made successfully after surgery

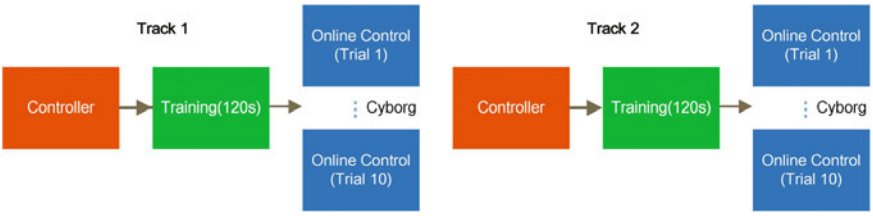

Fig. 3 Experimental paradigm. Controllers manage online control of different cyborgs with two different tracks (S-shape track and obstacle-avoidance track)

online control of the cyborg to complete walking along the presetting tracks after the cyborg started to move forward from the start point of the track with a certain speed range (1.5–5.5 cm/s). Ten online-control trials were conducted for each subject and cyborg (Fig. 3). Before online control, each subject completed a 120-s training run first to optimize the classifier of SSVEP. A 120-s rest was given between two consecutive trials to minimize the effects of fatigue from both the humans and insects. In addition, experiments for control groups were also conducted in this study. Three cyborgs walked along the designed track freely without control from any human subject for ten trials separately in control groups. Two kinds of tracks were designed and tested for the system in the experiments: S-shape and obstacle-avoidance tracks.

The first track used in the online control experiments was an S-shape track (135 mm (W) * 750 mm (L)) (Fig. 4a). Completing walking along the S-shape track without going outside of the boundary was counted as a successful trial in the online control experiment.

The other one was an obstacle-avoiding track (270 mm (W) * 750 mm (L)) (Fig. 4b). Controllers performed the online control of the cyborg to finish walking along the track from one side to the other side without crossing obstacles (red dots)

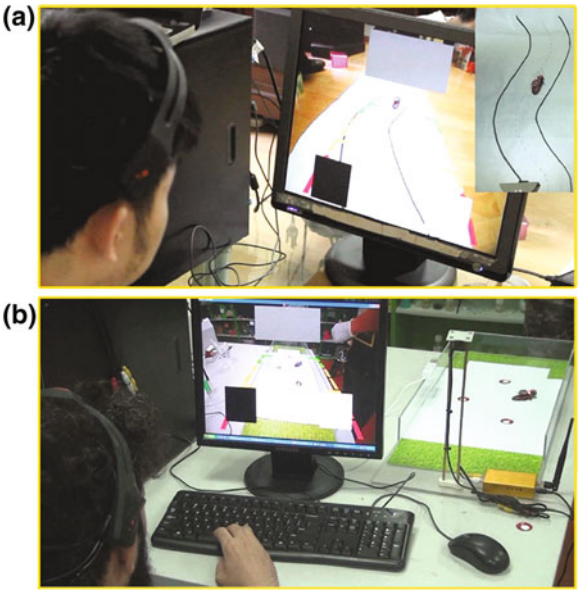

Fig. 4 Online control experiment. **a** One subject controlled a cyborg to walk along the S-shape track with brain signals. **b** One subject controlled a cyborg to walk along the obstacle-avoiding track with brain signals

on the sheet. Walking through the entire obstacle-avoiding track without touching any obstacles was counted as a successful trial.

Besides the above single-control experiments, we also conducted a double-control experiment to primarily explore the possibility of applying the designed system to further entertainment in daily life (Fig. 5). In this experiment, two human subjects each took control of a cyborg to complete walking along the S-shape track (the same size as in single-control paradigm) in the form of competition. Two cyborgs started moving forward in the same time, and between the two controllers, the one who navigated the cyborg to walk inside the track and reach the finish line first won the trial. Ten trials in total were completed in this experimental paradigm.

3 Results

During the online control experiments, the cyborgs could produce quick responses to the applied invasive neural stimulation, and the time measured from sending a command from SSVEP to the completion of the cyborg's reaction was about 772 ms in the present system. The cyborgs showed accurate response to the applied stimulation in most cases as well, and the mean response accuracy to the control commands reached 89.5 ± 15%. On the human side, average classification accuracy of SSVEP across three subjects in training sessions reached 86.0 ± 10.4%, indicating that both the BCI and neural stimulation subsystems in this study have the possibility to be used in an online control system.

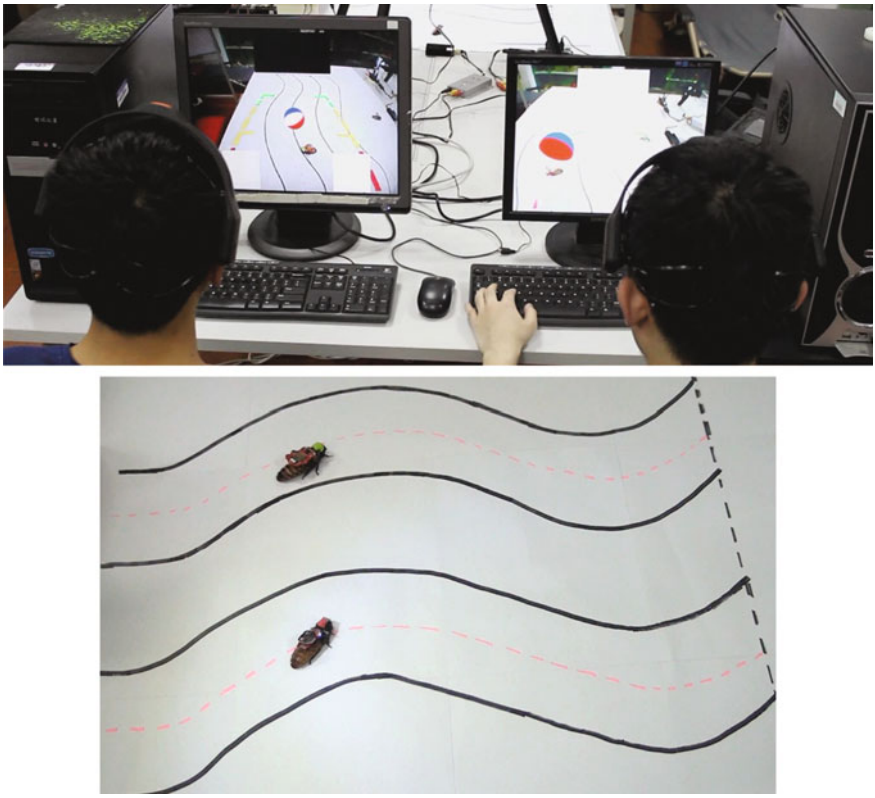

Fig. 5 Double-control experiment. In this contest, two human subjects navigated two cyborgs to walk along the two S-shape tracks, respectively. The competition aimed to show which one was the first to reach the finish line

The experimental results showed that all subjects could navigate all cyborgs to accomplish walking along both the different two tracks. The mean success rate for the online experiments achieved with this system was 20% for the S-shape track. Although not especially high, it was significantly higher than the value achieved in the control groups (0%) ($t = 3.464$, $P = 0.0085$). When using the obstacle-avoiding track, the success rate of online control could reach 40% (Fig. 4b). A demonstration video of a successful navigation of S-shape track is available through the link (https://www.youtube.com/watch?v=k5t6WkTkJkA).

An entertainment contest (double-control experiment) was also conducted, in which two persons competed to control two cockroaches, respectively. In this interesting paradigm, the success rate of navigation for each subject was the same as that in the single-control experiment (~20%). If both subjects were required to completely and successfully navigate in the same trial, this formidable task was still

possible, but the average success rate was very low (~5%). Generally using the cyborgs that were more sensitive to the micro-stimulation would be more likely to win the contest.

4 Discussion

We presented a feasible method to navigate a cyborg with human brain in this study. The human subjects could successfully steer cockroaches to make desired turns with an SSVEP-based BCI and micro invasive neural stimulation. Using only 4 channels on the scalp of visual cortex with a portable EEG device, the SSVEP achieved high classification accuracy. However, misclassification appeared frequently in the SSVEP during the shifting period from one intention to another intention. Therefore, developing a program to detect transitions of the EEG signal to different frequencies before classification in further studies may help the SSVEP achieve more accurate classification and can be used in the asynchronous BCIs as well.

The performance of the online control varied among subjects and cyborgs. The biological factors of human and cockroaches affected the success rate of the present system, which actually cannot be easily solved by current technologies. Latif et al. [17] tried to steer a cockroach manually to walk along an S-shape line and finally achieved a 10% success rate. However, navigating a cyborg successfully with human brain signals in this study is much more challenging, which requires continuously high level of accuracy from both sides of "controller" (human) and "receiver" (cyborg), and calls for constantly quick response from both human intention recognition and cyborg reaction as well.

From another point of view, some other factors related to the online control task may influence the control performance as well, such as constraint level of the tracks used, BCI skills and experience from the human and so on. The result shows that the success rate of online navigation increases from 20 to 40% when switching the S-shape track to the obstacle-avoiding track that allows more freedom of control. It demonstrates well that the task and experimental paradigm can also affect the success rate.

All these factors account for the success rate, which is not high enough even though both the "controller" and the "receiver" have a relatively high accuracy of information translation for a single decision. The double-control experiment is very interesting, but this protocol, which requires two human subjects to control two cyborgs to hit the finish line in sequence, is a rather high standard in current BCI applications. It is more complicated than the single-control experiments, and we will go on exploring this issue in future study. To some extent, the performance of online control with current system is reasonable and instructive.

At present, we are developing a new type of wireless microstimulator with multiple stimulation channels and modes, which can technically contribute to the improvement of the control performance as well.

This work has realized the idea on utilizing the brain signals to steer a cyborg continuously for the first time. The idea may be used for detection in complex and dangerous environments in far future. Most importantly, this study also succeeds in building up an embryonic virtual brain-to-brain interface (BBI) to functionally transfer information from one brain to another [18–20]. With nogoing efforts from researchers, we believe that more modalities of both BCI and cyborg technologies will be developed and used in a variety of ways in the future.

Acknowledgements We wish to acknowledge the human and cockroach subjects from our laboratory, both past and present. In particular, we thank Jinming Zhang for assisting us in the experiments and preparing some of the figures.

References

1. A. Bozkurt, R. Gilmour, D. Stern, A. Lal, MEMS based bioelectronic neuromuscular interfaces for insect cyborg flight control (IEEE, 2008), pp. 160–163
2. H. Sato, C. Berry, Y. Peeri, E. Baghoomian, B. Casey et al., Remote radio control of insect flight. Frontiers in integrative neuroscience **3**, 24 (2008)
3. H. Sato, C.W. Berry, B.E. Casey, G. Lavella, Y. Yao et al., A cyborg beetle: insect flight control through an implantable, tetherless microsystem (IEEE, 2008), pp. 164–167
4. H. Sato, Y. Peeri, E. Baghoomian, C. Berry, M. Maharbiz, Radio-controlled cyborg beetles: a radio-frequency system for insect neural flight control (IEEE, 2009), pp. 216–219
5. S.K. Talwar, S. Xu, E.S. Hawley, S.A. Weiss, K.A. Moxon et al., Behavioural neuroscience: rat navigation guided by remote control. Nature **417**, 37–38 (2002)
6. E.S. Krames, P.H. Peckham, A. Rezai, F. Aboelsaad, chapter 1—What is neuromodulation? in *Neuromodulation*, ed. by E.S.K.H.P.R. Rezai (San Diego, Academic Press, 2009), pp. 3–8
7. J. Okada, Cockroach antennae. Scholarpedia **4**, 6842 (2009)
8. C. Comer, Y. Baba, Active touch in orthopteroid insects: behaviours, multisensory substrates and evolution. Philos. Trans. Royal Soc. B: Biol. Sci. **366**, 3006–3015 (2011)
9. C. Comer, L. Parks, M. Halvorsen, A. Breese-Terteling, The antennal system and cockroach evasive behavior. II. Stimulus identification and localization are separable antennal functions. J. Comp. Physiol. A. **189**, 97–103 (2003)
10. S. Ye, C.M. Comer, Correspondence of escape-turning behavior with activity of descending mechanosensory interneurons in the cockroach, Periplaneta americana. J. Neurosci. **16**, 5844–5853 (1996)
11. J.R. Wolpaw, N. Birbaumer, D.J. McFarland, G. Pfurtscheller, T.M. Vaughan, Brain–computer interfaces for communication and control. Clin. Neurophysiol. **113**, 767–791 (2002)
12. B. Graimann, B. Allison, G. Pfurtscheller, *Brain–computer interfaces: A gentle introduction* (Springer, Brain-Computer Interfaces, 2010), pp. 1–27
13. J.J. Shih, D.J. Krusienski, J.R. Wolpaw, in *Brain-Computer Interfaces in Medicine* (Elsevier, 2012), pp. 268–279
14. B.Z. Allison, E.W. Wolpaw, J.R. Wolpaw, Brain–computer interface systems: progress and prospects. Expert Rev. Med. Devices **4**, 463–474 (2007)
15. G. Bin, X. Gao, Z. Yan, B. Hong, S. Gao, An online multi-channel SSVEP-based brain–computer interface using a canonical correlation analysis method. J. Neural Eng. **6**, 046002 (2009)
16. X. Gao, D. Xu, M. Cheng, S. Gao, A BCI-based environmental controller for the motion-disabled. IEEE Trans. Neural Syst. Rehabil. Eng. **11**, 137–140 (2003)
17. T. Latif, A. Bozkurt, Line following terrestrial insect biobots (2011), pp. 972–975

18. M. Pais-Vieira, M. Lebedev, C. Kunicki, J. Wang, M. Nicolelis, A brain-to-brain interface for real-time sharing of sensorimotor information. Sci. Rep. **3**, 1319 (2012)
19. R.P. Rao, A. Stocco, M. Bryan, D. Sarma, T.M. Youngquist et al., A direct brain-to-brain interface in humans. PLoS ONE **9**, e111332 (2014)
20. S.-S. Yoo, H. Kim, E. Filandrianos, S.J. Taghados, S. Park, Non-invasive brain-to-brain interface (BBI): establishing functional links between two brains. PLoS ONE **8**, e60410 (2013)

Recovery of Brain Function by Neuroprostheses: A Challenge for Neuroscience and Technology

Roni Hogri, Simeon A. Bamford, Paolo Del Giudice and Matti Mintz

In a series of studies, we demonstrated a brain-computer interface (BCI) system in which a disabled cerebellar network in rat's brain was replaced by a biomimetic synthetic model that reliably recovered the motor learning function of the cerebellar network [34, 21]. While we proved feasibility by managing some neuroscientific and methodological challenges, this project was critically suggestive of the grave challenges expected on the way to reach a level of a clinically relevant neuroprosthesis. In this chapter we briefly describe the cerebellar neuroprosthesis and discuss some of the generic neuroscientific and technological challenges on the way to developing fully functional neuroprostheses.

Paolo Del Giudice and Matti Mintz authors contributed equally to this work.

R. Hogri
Department of Neurophysiology, Center for Brain Research,
Medical University of Vienna, Vienna, Austria

S.A. Bamford · P.D. Giudice
Complex Systems Modeling Group, Istituto Superiore di Sanita, Rome, Italy

P.D. Giudice
Istituto Nazionale di Fisica Nucleare, Sezione di Roma, Rome, Italy

M. Mintz (✉)
Psychobiology Research Unit, School of Psychological Sciences
and Sagol School of Neuroscience, Tel Aviv University, Tel Aviv, Israel
e-mail: mintz@tauex.tau.ac.il

C. Guger et al. (eds.), *Brain-Computer Interface Research*,
SpringerBriefs in Electrical and Computer Engineering,
DOI 10.1007/978-3-319-57132-4_7

1 The Cerebellar Neuroprosthesis

The cerebellum is well-known for its critical role in the learning and execution of precisely-timed motor commands, and deficits in cerebellar function may lead to severe impairments in coordination, balance, and procedural memory, to name a few [38]. One of the most commonly used tasks for assessing cerebellar learning and motor control in both humans and animals is the eyeblink conditioning task [1, 26, 41, 47]. In this task, the subject is presented with 2 consecutive stimuli, which are separated by a fixed short interval—a benign conditioned stimulus (CS, e.g., a tone), followed by an unconditioned stimulus (US, e.g., an aversive airpuff directed at the cornea) which elicits a reflexive blink—the unconditioned response (UR). Following repeated CS-US pairing, the subject acquires a conditioned response (CR)—a blink elicited by the CS. In the well trained subject, the timing of CRs is stabilized such that the eyelid is fully closed at the time of incoming aversive US, thus protecting the organism's cornea. However, if the CS is then presented repeatedly without being followed by the US, the CR is eventually extinguished, and the CS ceases to elicit an eyeblink-CR.

Our goal was to test the feasibility of replacing the cerebellar circuitry necessary for the acquisition and extinction of eyeblink CRs with a closed-loop neuroprosthesis that would include the basic components of the anatomy and physiology of the biological system (Fig. 1). As a test preparation, we chose anesthetized rats in which motor responses are absent, and cerebellar learning is not normally evident. Recording electrodes were implanted in the brainstem precerebellar nuclei through which the CS and US signals are conveyed to the cerebellar cortical Purkinje cells, via the parallel fibers and climbing fibers, respectively. The raw neurophysiological

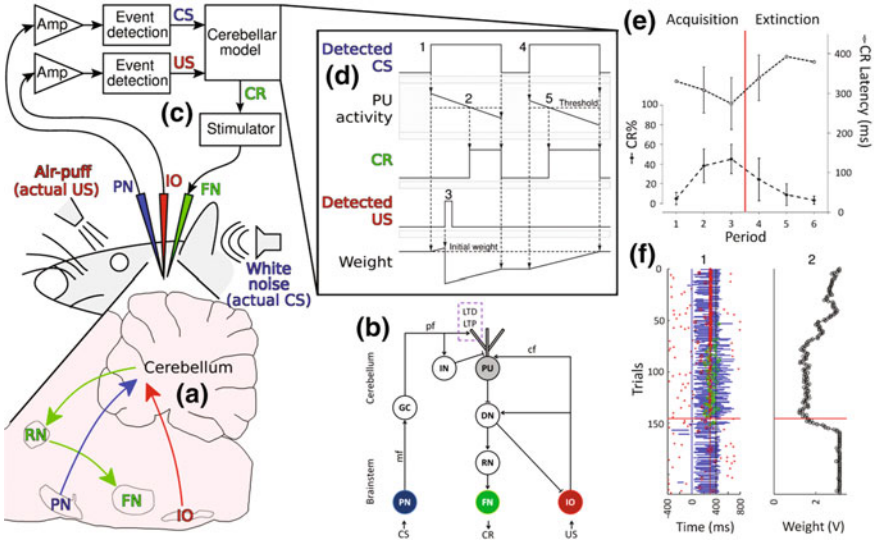

◀**Fig. 1** Overview of cerebellar neuroprostheses. **a**–**d** General system overview. **a** Brainstem-cerebellum input and output pathways underlying eyeblink conditioning: The pontine nucleus (PN) and inferior olive (IO) relay CS and US to the cerebellum, respectively. CRs are relayed from the cerebellum, via the red nucleus (RN) to the motor facial nucleus (FN) which elicits a blink. **b** Neural circuitry schematics. *Arrows* and *bars* represent excitatory and inhibitory synapses, respectively. GC, granule cells; PU, Purkinje cell; IN, inhibitory interneurons; DN, deep cerebellar nuclei. Convergence of CS and US signals on a PU causes long term depression (LTD) at the GC-PU excitatory synapse (*dashed rectangle*); if only the CS signal arrives at the PU there is long term potentiation (LTP). PUs regularly inhibit DN neurons, and DN disinhibition elicits a CR via the FN and also inhibits the IO, thus suppressing the US signal and promoting LTP. **c** Brain-machine interface. Electrodes recorded CS- and US-evoked neuronal activity, which was then relayed to a cerebellar model implemented in software or hardware. When the model produced an output (representing DN activation), this caused the activation of a stimulating electrode in the FN, eliciting a blink. **d** Illustration of the cerebellar model through two example trials. CS detection (*1*) triggered a decaying PU response (*2*), the initial level of which was proportional to the weight of the synthetic synapse. LTP and LTD were represented as voltage increase and decrease, respectively. Detected CS events caused LTP, unless a US event was concomitantly detected (*3*), in which case LTD occurred. In the second trial (*4*), the CR preceded US onset (*5*); this prevented US detection, resulting in LTP. **e**–**f** Results of a series of experiments in which the cerebellar model was implemented in an autonomous VLSI chip. **e** Progression of learning across 3 rats interconnected with the VLSI chip (mean ± SEM) during 3 periods of acquisition and extinction (each period is 1/3 of the trials in each block). CR rate increased during acquisition and decreased during extinction, and was negatively correlated with CR onset latency ($r = -0.75$, $P = 0.01$). Points without error bars indicate data from a single brain-chip hybrid, as other hybrids had no CRs during these periods and were not included in calculating the correlation of CR rate and latency. **f** Trial-by-trial data for one hybrid. *Vertical blue*, *red* and *black lines* indicate CS onset (time 0), US onset (300 ms), and co-termination of both stimuli (400 ms), respectively. Acquisition (*top*) and extinction (*bottom*) blocks are separated by a *red horizontal line*. *1* Stimuli detections and produced CRs. *Horizontal blue* is detected CS; *red circles* are concomitant US detections; US detections that did not coincide with CSs (*red dots*) did not induce plasticity; *green* is evoked CRs. *2* The weight (analog voltage) of the synthetic GC-PU synapse dropped gradually during acquisition, and stabilized from around trial 80 onwards; in the extinction block, it *rose* back to its maximum value within 15 trials

signals recorded from the precerebellar nuclei were then fed into a VLSI chip, which extracted the relevant sensory CS and US signals and conveyed them to the artificial cerebellar model (Fig. 1c). Stimulating electrodes, conveying the motor signal from the output of the cerebellar model, were implanted in the brainstem final motor output pathway by which the muscles involved in producing eyeblink-CRs are controlled (Fig. 1a, b).

2 Reduction of the Cerebellar Network to a Computationally Workable Model

Given the modest aims of a feasibility study, modeling of the cerebellar network was constrained to include only components that are essential for conditioning and extinction of eyeblink-CRs. Included were components that control the amount of

paired CS-US trials required to reach the asymptotic plateau of the learning curve and those that progressively shorten the delay and finally stabilize the timing of the eyeblink-CRs to coincide with the incoming US. Defining such minimal functionality of the model was instrumental in setting the inclusion/exclusion criteria for the many components of the cerebellar network. In practical terms, it helped prune the vast available data to enable biomimetic bottom-up modeling of cerebellar anatomy and top-down modeling of cerebellar physiology. The excitatory parallel fibers-Purkinje synapse was modeled as a site of LTD-plasticity in response to paired CS-US trials and LTP-plasticity in response to CS-alone trials [23, 29, 36]. Since parallel fiber activation also excites interneurons which inhibit Purkinje cells [13], the incoming CS signal had both excitatory and inhibitory effects on the modeled Purkinje cell. Thus, progress of LTD along paired CS-US trials was translated to progressive shortening of the Purkinje excitatory response to the CS, followed by a pause in Purkinje cell firing (Fig. 1d). The synaptic connection between mossy fibers and cerebellar deep nuclei (DN) neurons was excluded from the model, reasoning that plasticity in these synapses is insufficient for achieving precisely-timed motor responses—a task that depends on the cerebellar cortex [27]. Since DN activity is controlled by inhibitory drive from Purkinje cells, DN response to CSs was conceptualized as a mirror-pattern of the Purkinje cell response, i.e., paired CS-US trials resulted in progressive shortening of DN inhibitory response followed by excitation, activating the motor pathways and eliciting an eyeblink-CR [19, 35, 44]. Therefore, the DN was not explicitly modeled; instead, the weight of the parallel fiber-Purkinje synapse at the time of CS detection determined the occurrence and latency of the electrical stimulation of the motor pathway, thus generating the eyeblink-CR. Communicated through the DN-IO GABAergic pathway, DN excitation also triggers inhibitory gating of the IO. When the DN excitation adaptively precedes the US onset, this gating prevents the US signal from arriving to Purkinje cells through climbing fibers [5, 24, 37]. Since, in this scenario, the Purkinje cell only receives the CS signal but not the subsequent US signal in a paired CS-US trial, the parallel fiber-Purkinje synapse undergoes LTP instead of LTD. To model this phenomenon, the neuronal signals from the precerebellar IO nucleus were blocked from entering the cerebellar neuroprosthesis during the electrical stimulation of motor pathways.

The S/N ratio of the CS signal is enhanced by filter-like operation of the cortical granule cells [2]. This mechanism was excluded from the model, since it would require recording separate mossy fiber inputs from many single granule cells, which would be implausible in vivo using current technology. Instead, detection of the CS was achieved through a detection algorithm applying signal processing engineering principles. The variety of inhibitory interneurons was not explicitly modeled, mostly since their contribution to cerebellar learning is currently not well understood. Moreover, available data suggest that their role is auxiliary to the primary processes already included in our system; for example, if parallel fiber-Purkinje LTD is compromised, LTP at parallel fiber-interneuron synapses can compensate for it [13]. Our constrained model demonstrated the learning curve typical of mammalian subjects and stabilization of eyeblink-CR latency corresponding to the

timing of the expected US onset, as well as extinction of CRs following repeated CS-alone presentations (Fig. 1e, f). *Reduction of the model to its most essential components required detailed analysis of the components contribution to the final function of the entire cerebellar network. The implication is that biomimetic modeling is only a viable option for brain networks for which a fairly detailed knowledge of the anatomy and physiology is available.*

3 Successive Stages of the Neuroprosthesis Testing

Development of the neuroprosthesis was intimately guided by the applicative aim of project, which was set as recovering of a lost cerebellar learning function. This dictated the necessity to test the functionality of the brain-machine hybrid in a realistic biological context. Development of the neuroprosthesis triggered what we believe, a generic process of testing of its functionality, which boiled down to embedding the model in gradually more ecologically realist context. In the following we describe the successive stages of neuroprosthesis testing.

In the 1st stage, a graphical computational cerebellar model was run with digital signals serving as the CS and US inputs and CR and UR outputs [42]. Learning along repeated paired CS-US trials was evaluated at the circuit level as progression of LTD at the CS-conveying parallel fiber-Purkinje synapse, CR acquisition and adaptive shortening of the CRs delay. Adaptive CR timing was achieved by the DN output inhibiting the US signal at the IO level, which resulted in LTP—thus antagonizing the LTD—at the parallel fiber-Purkinje synapse. Tuning the parameters of LTD/LTP ratio and delay to IO inhibition produced learning curves compatible with those of either animals or human subjects.

In the 2nd stage, the cerebellar model was interfaced with a mobile micro-robot [20]. The CS input was a predefined distance of the robot from a vertically striped surrounding wall acquired by the robot's camera, calculated on-line as spatial-frequency of the strips. The US input was the robot's collision with the wall, acquired by the robot's short-range infra-red sensors. The robot was equipped with an "innate" (i.e., hard wired) unconditioned US → UR reflex expressed as a U-turn in response to the US-collision with a wall. Learning along free 'exploration' of the arena was evaluated as gradual acquisition of collision avoidance, i.e., U-turn just ahead of the wall. Model parameters had to be re-tuned to accommodate for the delays and variance in CS and US detection and CR execution imposed by the angle of the robot's approach to the wall, physical peculiarities of the agent and the environment, and computational delays. The robustness of the model was demonstrated by its ability to support learning in spite of the aforementioned inter-trial variances. The fully tuned model was subsequently embedded in a VLSI chip, interfaced with the robot. This served to demonstrate that the chip's limited computational power could nevertheless support real-time learning and adaptive behavior by an autonomous agent moving in a realistic environment. *Achieving*

these milestones was essential in demonstrating the potential usefulness of the model as a neuroprosthetic device.

In the 3rd stage, the model was returned to a software state and was interfaced with the cerebellum of anaesthetized rats [18, 34]. Inputs to the model were signals of auditory-CS and periorbital-US extracted from recordings in the pre-cerebellar brainstem nuclei. The output of the model was an electrical train injected into a post-cerebellar brainstem motor nucleus triggering eyeblink-CR. Learning along paired CS-US trials was evaluated as acquisition of eyeblink-CRs and the correspondence of CR timing with the onset of periorbital-US in the final acquisition trials. One of the main challenges in this stage was the algorithmic detection of the CS and US events to be fed into the cerebellar model. A central dilemma was determining the type of neuronal signals that should be fed into the neuroprosthesis in future studies. Some BCI studies have improved detection of sensory events by simultaneously recording single-unit activity from multiple neurons in brain structures such as the primate hippocampus [15] or neocortex [14, 22]. Such recordings have obvious advantages in terms of algorithmic detection of sensory-related events as compared to multiple-unit recordings without single-unit separation. However, simultaneous recording of single-unit activity from a large number of neurons in the brainstem precerebellar nuclei in vivo is technically challenging, and to the best of our knowledge has never been reported. While it would have been feasible to record single-unit activity from a small number of neurons in our preparation, neurons in the precerebellar nuclei are not sensory neurons per se, in the sense that they show considerable spontaneous activity, thus hindering attempts of real-time event detection from single neuron firing (Fig. 2). Perhaps more importantly, single-unit recordings currently suffer from low reliability and yield over chronic recordings lasting months or years [11], and thus make an unlikely candidate for clinically-relevant neuroprostheses. Given all of the above, we chose to avoid single-unit recordings altogether, and utilized multi-unit recordings instead. While multi-unit recordings hold a promise for better reliability over chronic recordings, they have so far attracted limited attempts to develop algorithmic tools for real-time signal processing [25]. Therefore, throughout this and later stages of the project we developed our own algorithms for event detection from multi-unit recordings. These algorithms required subject-specific optimization, not unlike the tuning of deep-brain stimulation parameters in human patients [4]. In particular, the prevalence of type 1 (false alarm) versus type 2 (misdetection) detection errors varied across subjects and required re-tuning of detection parameters as well as the LTD/LTP ratio at the synthetic parallel fiber-Purkinje neuron synapse.

In the 4th stage, the model and the CS and US event detection algorithms were embedded in a VLSI chip [3], which was interfaced with the brainstem of an anesthetized rat, as described above [21]. To date, this version served as our final feasibility test of recovered motor learning in the hybrid. The implementation involved a dedicated chip that was designed and implemented to support the multiple real-time tasks of providing a front-end towards the recorded neural signals, performing the needed signal processing, emulating the relevant synaptic

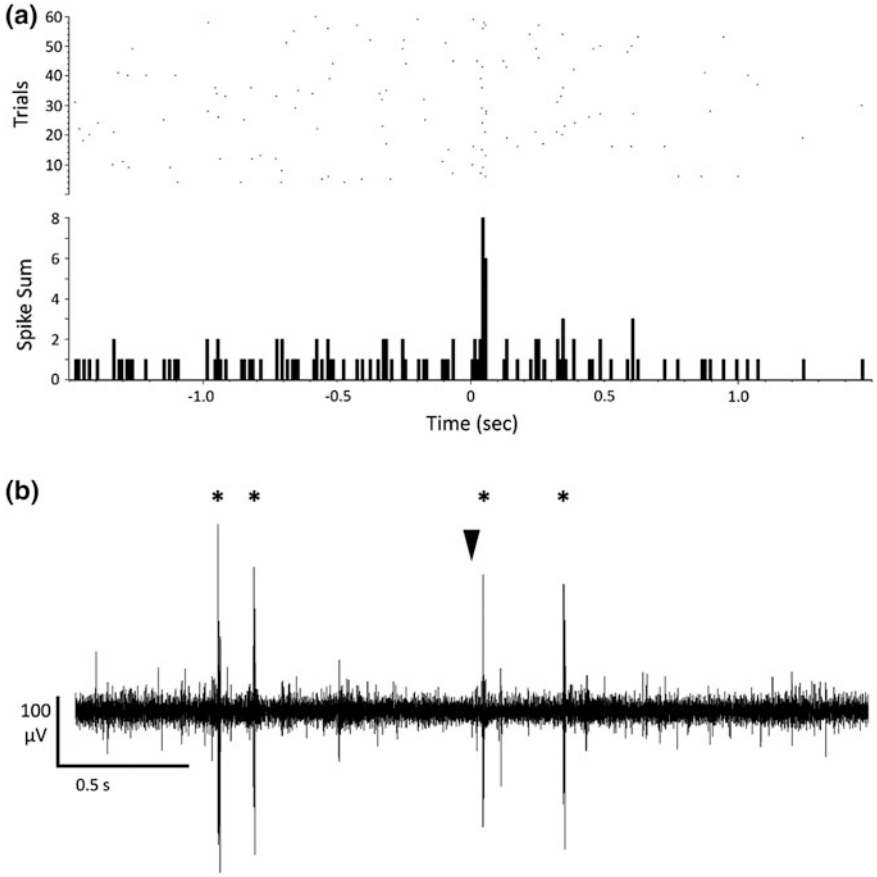

Fig. 2 Peri-stimulus complex spikes recorded from a single cerebellar Purkinje cell, representing the activity of a single IO neuron. **a** It is clear from the raster (*top*) and the peri-stimulus time histogram (*bottom*) that, on average, this IO neuron preferably fired 40–60 ms following the onset of a periorbital airpuff (Time 0). However, it is also clear from the raster that an algorithm blind to the experimental conditions would not have been able to distinguish between spontaneous and airpuff-evoked events of this single neuron as they occur in real time. **b** Raw data showing complex spikes (marked with *asterisks*) before and after airpuff onset (marked by *arrowhead*). Sensory-evoked complex spikes were indistinguishable from spontaneous firing in amplitude, frequency, or waveform

plasticity (LTD/LTP at the parallel fibers—Purkinje cell junction), and generating the trigger signal for motor-neuron stimulation under the appropriate conditions, as learning proceeds. The chosen design approach was to create a field-programmable mixed-signal array (FPMA) circuitry, where 'mixed' refers to the coexistence of digital and analog components (Fig. 3). Importantly, the innovative route we followed was not based on the simultaneous presence of digital (field-programmable gate array, FPGA) components and analog ones, with converters managing the

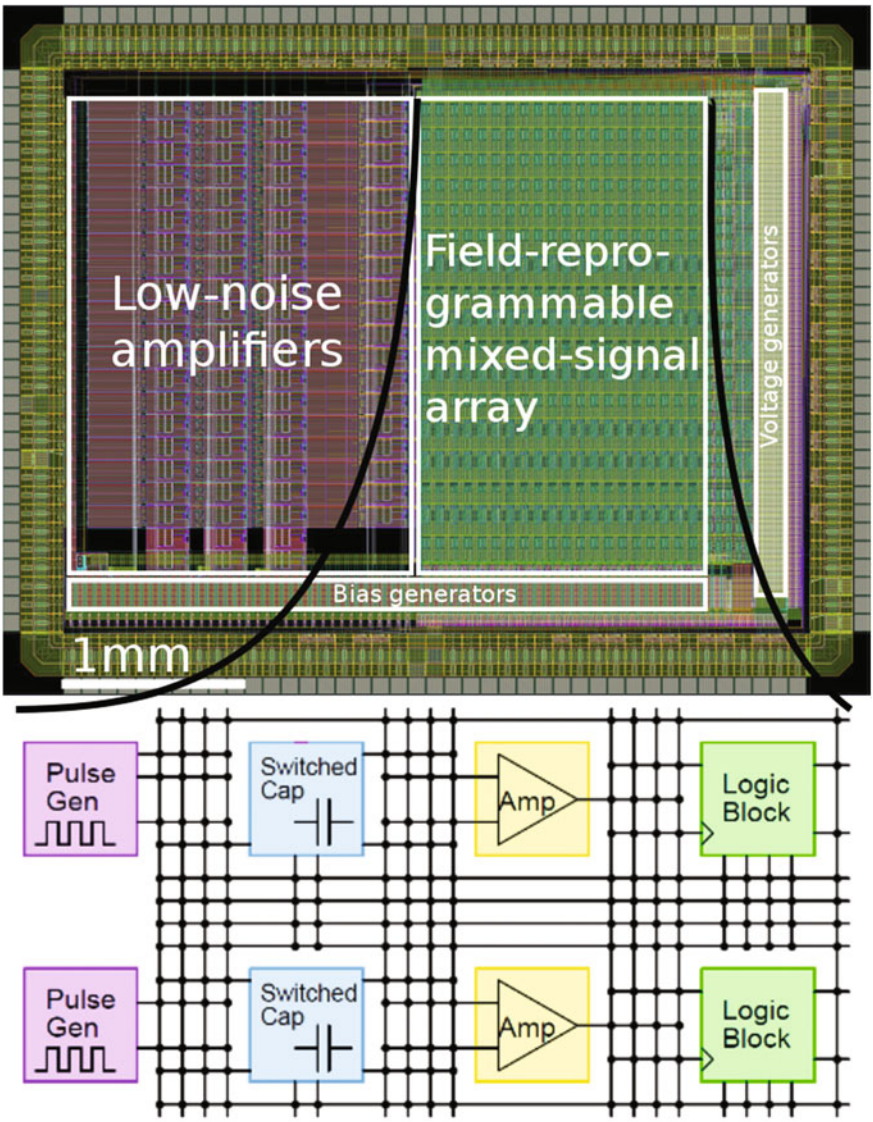

Fig. 3 The layout of the chip (*above*). The figurative zoom of the field programmable mixed-signal array (*below*) shows that there are 4 types of components that can be connected in any configuration using a surrounding matrix of programmable switches. The low noise amplifiers were not used in the work reported here

communication between them. Rather it was based on obtaining a controllable and stable 'intimate mixing', by which analog and digital signals share the same routing and currents are controlled in order to make this possible. Four primitives are implemented in the FPMA: pulse generators, configurable switched capacitors,

operational transconductance amplifiers and configurable logic blocks (Fig. 3); the chip hosts 500 elements of the above kinds. The chip was fabricated using the process AMS 0.35um with 4 metal layers and it was 3.8 × 4.8 mm in size. After initial band-pass filtering (300–3000 Hz), the signal processing section of the reconfigurable array provided a chain composed of: weighted sum of input signals, full-wave rectification, band-pass filtering (1–10 Hz for PN; 5–40 Hz for IO), and a hysteretic threshold, to allow for event detection; the outcome of the latter drove the plasticity model of the cerebellar synapse, hosted in another section of the FPMA.

In summary, construction of functional cerebellar neuroprosthesis was enabled by its tuning and testing in gradually more realistic developmental environment. The challenge for the future is to test the neuroprosthesis in a freely moving, autonomous animal.

4 What Function Is Recovered by the Neuroprostheses?

Multiple brain systems, including the cerebellum, are capable of learning that includes acquisition and consolidation of new responses and eventually execution of both new and old responses. The biomimetic cerebellar model enabled the hybrid to learn and execute new responses; however, it had no means of executing old responses, learned and subsequently lost by the deactivation of the biological cerebellum. Others have demonstrated neuroprostheses that could execute previously learned responses [6]. Their strategy included interfacing with the input and output of a hippocampal microcircuitry (areas CA3 and CA1, respectively) in intact naïve rats using extensive electrode arrays, and recording the activity at the two sites along a behavioral task. This enabled construction of the neuroprosthesis as an algorithm that translates the pattern of recorded input activity into the appropriate pattern of electrical stimulation of the output. After deactivation of the biological hippocampus, the hybrid was able to execute the old learned responses under the task conditions. This input/output model preserves the old memories but has no means of learning new responses. *It seems that the function of such input/output model is complementary to the function of our biomimetic model, and neuroprostheses combining the two models would be in position to fully substitute a biological learning network.*

Another advantage of the input/output approach is that it can be readily adapted to other neuronal systems. Indeed, similar algorithms have been used to target the hippocampus of rodents and the prefrontal cortex of primates [6, 14]. Due to its biomimetic infrastructure, our prosthesis would not have been suitable for the replacement of neuronal circuits outside of the cerebellum. However, it is worth noting that the basic circuitry embedded in our system holds true for all cerebellar modules [9]. Consequently, similar systems to the one we have developed could be used to recover other cerebellar functions. For example, cerebellar degeneration has been reported to cause balance, ataxia and coordination deficits in elderly patients, and essential tremor is a severe motor dysfunction common to this population

following cerebellar dysfunction [17]. One can envision that an approach similar to ours could be used in the treatment of such conditions, in which some of the cerebellar tissue can no longer be recovered.

Learning networks are extensively studied in the cerebellum, hippocampus, amygdala and the basal ganglia. The accumulated knowledge seems ripe to support the construction of biomimetic models aiming at learning of new responses. These models may in turn be amalgamated with the input/output models responsible for the preservation of old memories. Such amalgamated architecture is interesting in a sense that the newly learned responses in the layer of the learning model will have eventually to migrate to the storage layer of input/output model. The migration process is reminiscent of migration of memories from the hippocampus to the neocortex [32], or migration of learned sequences from the basal ganglia to the cerebellum, or vice versa [12]. *In summary, a neuroprosthesis supporting a full recovery of a learning function will require some generic consideration of strategies to combine the two functionally different types of models, those that preserve old memories and those that acquire novel memories.*

5 How Close to the Damaged Area Can the Neuroprosthesis Be Interfaced

Some publications aiming at replacement of a damaged brain circuit, including our own publications, seem to prematurely imply a translational relevance. We alluded to the possibility of replacing a damaged cerebellar microcircuit by a biomimetic neuroprosthesis. In practice, the cerebellar microcircuit together with the rest of the brain was anaesthetized rather than physically damaged [18, 21, 34]. Similarly, attempts to replace the hippocampus or the prefrontal cortex circuitry involved injections of drugs such as cocaine and MK-801 rather than organic damage [6, 14]. These acute pharmacological interventions clearly distorted the neuronal activity of the to-be-replaced brain sites but they imposed no structural effects characteristic of organic damage. Preservation of the anatomical structure is indeed essential for interfacing the neuroprosthesis with the inputs and outputs of the to-be-replaced brain structure. In retrospect, pharmacological preparations seem to miss the essence of structural damage to the brain in clinical cases. Indeed, localized structural damage is likely to induce up- and down-stream trans-synaptic plasticity and degeneration. For example, cerebellar cortical damage depletes Purkinje neurons, leading to retrograde degeneration of the afferent IO neurons and their climbing fibers [45, 46]. This would exclude the IO as an interface site for detection of the US signal in the cerebellar model, as practiced by us. Similarly, structural damage to the hippocampus results in retrograde and anterograde degeneration would make obsolete the array of recording and stimulating electrodes implanted at proximal input and output sites of the hippocampus, as suggested by Theodor Berger's group. A related concern is that organic damage tends also to affect the

activity at the upstream structures through distortion of the feedback loops, which are a pervasive feature of neuronal networks.

Clearly, deciding on the location of the interface requires some generic considerations. First, one may consider avoiding the trans-synaptic effects of the lesion by distancing the interface up- and down-stream from the damaged brain area. In the case of our cerebellar neuroprosthesis, instead of recording the input airpuff-US signal at the IO, which suffers from retrograde degeneration after cortical damage, one may interface the brainstem trigeminal nucleus (e.g., [21] or even the somatosensory cerebral cortex. However, brain networks typically have a converging input pattern, and therefore distancing the interface up-stream inevitably reduces the relevance of the captured information for a reliable functioning of a biomimetic model, and may increase the computational challenge. Similarly, brain networks typically have a diverging output pattern, and therefore distancing the interface down-stream may reproduce only limited components of the composite response generated by the brain network. A somehow cumbersome solution may involve interfacing multiple up- and down-stream distant sites. Second, after distancing the interfaces from the site of damage, one may decide to extend the biomimetic model to also include the nuclei and pathways that underwent secondary degeneration after the primary damage. *Clearly, these and other prospective solutions require extensive testing of potential sites of neuroprosthesis interface in subjects with organic brain damage, and probably a custom-design based on the condition of each individual patient.*

6 Interaction of the Model with the Rest of the Brain

Sites of interface should also be analyzed in the context of inter-network communication. Brain networks typically communicate with several other networks, and thus participate in multiple functions. The efficiency of a neuroprosthesis should therefore be judged on the basis of recovery of multiple functions. We observe that the site of neuroprosthesis interface determines de facto the prospects of the model's interaction with other biological networks, thus constraining the range of recovered functions. In our cerebellar neuroprosthesis, the model's output drove motoneurons in the facial nucleus, two synapses downstream from the cerebellar output DN neurons and one synapse upstream of the eyelid musculature. Stimulation at this site served to show that the model was successful in acquiring and executing of correctly-timed discrete motor eyeblink-CRs; a cerebellar learning function to which many studies have been devoted over several decades. However, positioning the interface at the final-motor-pathway is functionally equivalent to peripheral stimulation proximal to the eyes musculature, while excluding the effects of cerebellar output on multiple brain networks, mostly through the red nucleus [31]. This implies that distancing the output interface from the site of damage constrains the range of functions that can be recovered by the model. These considerations suggest that a true integration of the model with brain networks requires

interfacing the output as close as possible to the damaged network. Since this would not be typically possible, we reiterate to the alternative strategy as discussed in the previous section, to interface the output along several of the diverging outputs of the damaged network.

On the input side, converging information coming from the cerebrum drives the activity of the precerebellar nuclei. In the PN, convergence of multiple sensory modalities and non-sensory afferents such as from the limbic system has been reported by us and others [33, 39]. Similarly, the IO has been shown to receive afferents from cerebral and brainstem areas involved in sensory, motor and emotional processing [1, 7, 8, 10, 43]. While an obvious feature of normal brain processing, such convergence on the precerebellar nuclei does increase the biological "noise", thus hindering detection of the sensory-evoked events relevant for correct learning by the model, heavily experienced in our cerebellar neuroprostheses. In an attempt to improve the detection of sensory events, one is tempted to move the input interface up-the-stream from the damaged network, for example in sensory nuclei. While improving the detection, this move will exclude the modulatory effects of other networks on the sensory inputs to the cerebellum. For example, amygdala afferents seem to enhance the auditory signals arriving in the brainstem PN, in functional terms increasing the signals' relevance, and consequently enhancing eyeblink conditioning even to weak signals, both in terms of acceleration of conditioning and the final asymptotic level [39, 40]. In summary, these considerations imply that a true integration of the model with other networks requires interfacing the inputs and outputs of the neuroprosthesis close to the damaged network. *Since this would not be always possible, we are again left with the alternative strategy discussed in the previous section, to interface the inputs and outputs along several of the converging and diverging nuclei, respectively.*

7 Does Development of Neuroprostheses Advance Neuroscience?

Clearly, the fact that we were able to reproduce a cerebellar function does not indicate that we have faithfully replicated cerebellar biology. Indeed, the caveats concerning our attempts at constructing a cerebellar neuroprosthesis have been thoroughly discussed here and in previous reports [21]. By comparison, the MIMO systems advanced by Berger and collaborators did not aim at replicating explicit neuronal elements, but rather relied on non-linear general purpose system identification techniques [6]. Nevertheless, when approaching such a challenge as constructing a functional neuroprosthesis, one must consider the nature of the neural context in which one must operate, and this invariably leads to questions and hypotheses about the generic nature of the system to be recovered.

One open generic question considers the rate of motor conditioning. What are the mechanisms playing a role in the slow acquisition of the motor eyeblink-CRs,

for example in comparison to the one trial acquisition of the emotional fear-CRs [30]? And on top of this basic slowness, in our hands the rate of eyeblink-CRs acquisition greatly varies across the mammalian species (count of trials to a reliable conditioning varies from hundreds in rats—about one hundred in rabbits and a few of tens in Psychology students), in spite of the apparently similar architecture of the cerebellar network. Planning, composing and testing of the cerebellar model gave us good opportunity to tackle the above questions.

When attempting to decipher the auditory-CS signal from the precerebellar-PN, several features of the system contributing to slow and variable rate of acquisition became apparent. First, we faced a challenge in algorithmic detection of the PN response (measured as a multiple unit activity) to the auditory-CS. We found that detection was compromised by the response variability, which was largely contributed by the noisy background activity, probably generated by the multiple sensory and non-sensory inputs converging on single PN neurons. This brought us to realize that that the noisy PN background likely reflects a similar computational challenge for the biological cerebellum. Applying the auditory-CS selectively on a low-amplitude PN background increased the S/N ratio of the PN response to the auditory-CS and significantly accelerated the acquisition of the eyeblink-CRs [40]. It is conceivable that the species differences in learning rates are also affected by the level of noise in cerebellar inputs—perhaps humans have a better control of the "filtration" system than rodents, allowing greater fidelity in signals relayed to the cerebellum. Here we suggest that learning based on coincidence of events, as is the case with classical conditioning, is prone to being slowed down by poor detection of event-related signals passing through input nuclei with noisy background activity.

We also observed that the rate of acquisition in the model could be up- or down-regulated by changing the weight of the parallel fibers-Purkinje synapse. For example, acquisition could be accelerated by increasing the LTD step upon application of paired CS-US trials and by decreasing the LTP step upon the application of CS-alone trials, and thus increasing the LTP/LTD ratio (data not shown). Thus, by maneuvering the LTD and LTP parameters we could reproduce the entire range of acquisition rates from rodents to human subjects. However, we observed that accelerating the acquisition often came with a price in the form of a non-adaptive timing of the eyeblink-CRs. Closer inquiry revealed that increasing the LTD step at the parallel fibers-PU synapse could shorten the delay to the conditioned-CR too drastically, such that this response emerged—and therefore, ended—too early ahead of the periorbital-US, thus losing its adaptive value of protecting the eye from the noxious US. Here we suggest that learning aimed at acquisition of well-timed responses is prone to be slowed-down by the necessity to change the synaptic plasticity in small steps, which implies many conditioning trials. *In conclusion, we observe that development of neuroprostheses, which is largely based on amalgamation and reductive application of known neurophysiological data, can nevertheless lead to comprehensive inquiry into neuroscientific questions.*

8 A Closing Note

As a closing note we briefly elaborate, in a more general perspective, on the logical status of model-based neuroprostheses like the one we have described. The neuroscientific endeavor can be largely seen as an effort to 'reverse engineer' the brain, by which careful experimental analysis of the nervous system generates hypotheses on the dynamic and organizational principles underlying observed function. Contrary to reverse engineering of man-made artifacts, in the case of the brain, our lack of prior knowledge about design principles and relevant scales of organization complicates matters (see the discussion in [28]).

In this perspective, the 'understanding by building' approach of neuromorphic engineering can be of heuristic value. The scope of its inquiry is, in its most general sense: what does it take for a complex system composed of neuron-like elements to express perceptual and cognitive abilities in interaction with a natural environment? However, neuromorphic systems maintain a separation between the artificial system (its sensors, its 'cognitive' network, and its actuators) and the nervous system whose function it is meant to emulate.

In a way, closed-loop model-based neuro-prostheses may create a bridge between the outcome of reverse-engineering (a model capturing putative principles at work) and the neuromorphic approach, to create synthetic equivalents of nervous systems. In principle, a neuromorphic device acting as an 'equal partner' in real-time with the nervous system would allow to best abstract a meaningful 'conceptual nervous system' [16]. The work summarized here is clearly a tiny step in this direction, but we believe the approach holds great promise.

Acknowledgements The research involving the cerebellar neuroprosthesis received funding from the European Community's Seventh Framework Program (FP7) under grant agreement #216809 to P.D.G. and M.M.; the Converging Technologies (ISF) research grant #1709/07, and ISF grant #390/12 to M.M.; and the Dan David Prize Scholarship and the Michael Myslobodsky Foundation to R.H.

References

1. R. Ackerley, J. Pardoe, R. Apps R, A novel site of synaptic relay for climbing fibre pathways relaying signals from the motor cortex to the cerebellar cortical C1 zone. J Physiol. **576,** 503–518 (2006)
2. A. Arenz, E.F. Bracey, T.W. Margrie, Sensory representations in cerebellar granule cells. Curr. Opin. Neurobiol. **19**(4), 445–451 (2009)
3. S.A. Bamford, R. Hogri, A. Giovannucci, A.H. Taub, I. Herreros, P.F.M.J. Verschure, M. Mintz, P. Del Giudice, A VLSI field-programmable mixed-signal array to perform neural signal processing and neural modeling in a prosthetic system. IEEE Trans. Neural Syst. Rehabil. Eng. **20**, 455–467 (2012)
4. A.L. Benabid, S. Chabardes, J. Mitrofanis, P. Pollak, Deep brain stimulation of the subthalamic nucleus for the treatment of Parkinson's disease. Lancet Neurol. **8**(1), 67–81 (2009)

5. F. Bengtsson, D.A. Jirenhed, P. Svensson, G. Hesslow, Extinction of conditioned blink responses by cerebello-olivary pathway stimulation. NeuroReport **18**, 1479–1482 (2007)
6. T.W. Berger, R.E. Hampson, D. Song, A. Goonawardena, V.Z. Marmarelis, S.A. Deadwyler, A cortical neural prosthesis for restoring and enhancing memory. J. Neural Eng. **8**, 046017 (2011)
7. I.E. Brown, J.M. Bower, The influence of somatosensory cortex on climbing fiber responses in the lateral hemispheres of the rat cerebellum after peripheral tactile stimulation. J. Neurosci. **22**, 6819–6829 (2002)
8. J.T. Brown, V. Chan-Palay, S.L. Palay, A study of afferent input to the inferior olivary complex in the rat by retrograde axonal transport of horseradish peroxidase. J. Comp. Neurol. **176**, 1–22 (1977)
9. N.L. Cerminara, H. Aoki, M. Loft, I. Sugihara, R. Apps, Structural basis of cerebellar microcircuits in the rat. J. Neurosci. **33**(42), 16427–16442 (2013)
10. N.L. Cerminara, S. Koutsikou, B.M. Lumb, R. Apps, The periaqueductal grey modulates sensory input to the cerebellum: a role in coping behaviour? Eur. J. Neurosci. **29**, 2197–2206 (2009)
11. A.S. Dickey, A. Suminski, Y. Amit, N.G. Hatsopoulos, Single-unit stability using chronically implanted multielectrode arrays. J. Neurophysiol. **102**(2), 1331–1339 (2009)
12. J. Doyon, P. Bellec, R. Amsel, V. Penhune, O. Monchi, J. Carrier, S. Lehéricy, H. Benali, Contributions of the basal ganglia and functionally related brain structures to motor learning. Behav. Brain Res. **199**(1), 61–75 (2009)
13. Z. Gao, B.J. van Beugen, C.I. De Zeeuw, Distributed synergistic plasticity and cerebellar learning. Nat. Rev. Neurosci. **13**, 619–635 (2012)
14. R.E. Hampson, G.A. Gerhardt, V. Marmarelis, D. Song, I. Opris, L. Santos, T.W. Berger, S.A. Deadwyler, Facilitation and restoration of cognitive function in primate prefrontal cortex by a neuroprosthesis that utilizes minicolumn-specific neural firing. J. Neural Eng. **9**, 056012 (2012)
15. R.E. Hampson, D. Song, I. Opris, L.M. Santos, D.C. Shin, G.A. Gerhardt, V.Z. Marmarelis, T.W. Berger, S.A. Deadwyler, Facilitation of memory encoding in primate hippocampus by a neuroprosthesis that promotes task-specific neural firing. J. Neural Eng. **10**(6), 066013 (2013)
16. D.O. Hebb, Drives and the CNS (conceptual nervous system). Psychol. Rev. **62**(4), 243 (1955)
17. R.C. Helmich, I. Toni, G. Deuschl, B.R. Bloem, The pathophysiology of essential tremor and Parkinson's tremor. Curr. Neurol. Neurosci. Rep. **13**(9), 1–10 (2013)
18. I. Herreros, A. Giovannucci, A.H. Taub, R. Hogri, A. Magal, S. Bamford, R. Prueckl, P.F. Verschure, A cerebellar neuroprosthetic system: computational architecture and in vivo test. Front Bioeng. Biotechnol. **2**, 14 (2014)
19. G. Hesslow, Correspondence between climbing fibre input and motor output in eyeblink-related areas in cat cerebellar cortex. J. Physiol. **476**, 229–244 (1994)
20. C. Hofstötter, M. Mintz, P.F.M.J. Verschure, The cerebellum in action: a simulation and robotics study. Eur. J. Neurosci. **16**, 1361–1376 (2002)
21. R. Hogri, S.A. Bamford, A.H. Taub, A. Magal, P. Del Giudice, M. Mintz, A neuro-inspired model-based closed-loop neuroprosthesis for the substitution of a cerebellar learning function in anesthetized rats. Sci. Rep. **5**, 8451 (2015)
22. P.J. Ifft, S. Shokur, Z. Li, M.A. Lebedev, M.A. Nicolelis, A brain-machine interface enables bimanual arm movements in monkeys. Sci. Transl. Med. **5**, 210ra154 (2013)
23. M. Ito, M. Kano, Long-lasting depression of parallel fiber-purkinje cell transmission induced by conjunctive stimulation of parallel fibers and climbing fibers in the cerebellar cortex. Neurosci. Lett. **33**, 253–258 (1982)
24. J.J. Kim, D.J. Krupa, R.F. Thompson, Inhibitory cerebello-olivary projections and blocking effect in classical conditioning. Science **279**, 570–573 (1998)

25. T.D. Kozai, Z. Du, Z.V. Gugel, M.A. Smith, S.M. Chase, L.M. Bodily, E.M. Caparosa, R.M. Friedlander, X.T. Cui, Comprehensive chronic laminar single-unit, multi-unit, and local field potential recording performance with planar single shank electrode arrays. J. Neurosci. Methods **242**, 15–40 (2015)
26. D.G. Lavond, J.J. Kim, R.F. Thompson, Mammalian brain substrates of aversive classical conditioning. Ann. Rev. Psychol. **44**, 317–342 (1993)
27. D.G. Lavond, Role of the nuclei in eyeblink conditioning. Ann. NY Acad. Sci. **978**, 93–105 (2002)
28. S. Marom, R. Meir, E. Braun, A. Gal, E. Kermany, D. Eytan, On the precarious path of reverse neuro-engineering. Front Comput. Neurosci. **4**(3), 5 (2009)
29. A. Mathy, S.S.N. Ho, J.T. Davie, I.C. Duguid, B.A. Clark, M. Hausser, Encoding of oscillations by axonal bursts in inferior olive neurons. Neuron **62**, 388–399 (2009)
30. J.F. Medina, J.C. Repa, M.D. Mauk, J.E. LeDoux, Parallels between cerebellum- and amygdala-dependent conditioning. Nat. Rev. Neurosci. **3**, 122–131 (2002)
31. D. Milardi, A. Cacciola, G. Cutroneo, S. Marino, M. Irrera, G. Cacciola, G. Santoro, P. Ciolli, G. Anastasi, R.S. Calabrò, A. Quartarone, Red nucleus connectivity as revealed by constrained spherical deconvolution tractography. Neurosci. Lett. **626**, 68–73 (2016)
32. M. Moscovitch, R. Cabeza, G. Winocur, L. Nadel, Episodic memory and beyond: the hippocampus and neocortex in transformation. Ann. Rev. Psychol. **67**, 105–134 (2016)
33. R.F. Potter, D.G. Ruegg, M. Wiesendanger, Responses of neurones of the pontine nuclei to stimulation of the sensorimotor, visual and auditory cortex of rats. Brain Res. Bull. **3**, 15–19 (1978)
34. R. Prueckl, A.H. Taub, I. Herreros, R. Hogri, A. Magal, S.A. Bamford, A. Giovannucci, R.O. Almog, Y. Shacham-Diamand, P.F. Verschure, M. Mintz, Behavioral rehabilitation of the eye closure reflex in senescent rats using a real-time biosignal acquisition system, in *2011 Annual International Conference of the IEEE Engineering in Medicine and Biology Society* (IEEE, 2011), pp. 4211–4214
35. R.F. Rogers, G.B. Britton, J.E. Steinmetz, Learning-related interpositus activity is conserved across species as studied during eyeblink conditioning in the rat. Brain Res. **905**, 171–177 (2001)
36. P.A. Salin, R.G. Malenka, A. Roger, Cyclic AMP mediates a presynaptic form of LTP at cerebellar parallel fiber synapses. Neuron **16**, 79–803 (1996)
37. L.L. Sears, J.E. Steinmetz, Dorsal accessory inferior olive activity diminishes during acquisition of the rabbit classically conditioned eyelid response. Brain Res. **545**, 114–122 (1991)
38. C.J. Stoodley, J.D. Schmahmann, Evidence for topographic organization in the cerebellum of motor control versus cognitive and affective processing. Cortex **46**, 831–844 (2010)
39. A.H. Taub, M. Mintz, Amygdala conditioning modulates sensory input to the cerebellum. Neurobiol. Learn. Mem. **94**, 521–529 (2010)
40. A.H. Taub, E. Segalis, M. Marcus-Kalish, M. Mintz, Acceleration of cerebellar conditioning through improved detection of its sensory input. BCI **1**, 5–16 (2014)
41. R.F. Thompson, J.E. Steinmetz, The role of the cerebellum in classical conditioning of discrete behavioral responses. Neuroscience **162**, 732–755 (2009)
42. P.F. Verschure, M. Mintz, A real-time model of the cerebellar circuitry underlying classical conditioning: a combined simulation and robotics study. Neurocomputing **38**, 1019–1024 (2001)
43. T.C. Watson, M.W. Jones, R. Apps, Electrophysiological mapping of novel prefrontal–cerebellar pathways. Front Integr. Neurosci. **3**, 18 (2009)
44. L. Witter, C.B. Canto, T.M. Hoogland, J.R. De Gruijl, C.I. De Zeeuw, Strength and timing of motor responses mediated by rebound firing in the cerebellar nuclei after purkinje cell activation. Front Neural Circuits **7**, 133 (2013)

45. C.H. Yeo, M.J. Hardiman, M. Glickstein, Discrete lesions of the cerebellar cortex abolish the classically conditioned nictitating membrane response of the rabbit. Behav. Brain Res. **13**(3), 261–266 (1984)
46. C.H. Yeo, M.J. Hardiman, M. Glickstein, Classical conditioning of the nictitating membrane response of the rabbit. II. Lesions of the cerebellar cortex. Exp. Brain Res. **60**, 99–113 (1985)
47. C.H. Yeo, G. Hesslow, Cerebellum and conditioned reflexes. Trends Cogn. Sci. **2**, 322–330 (1998)

BCI-Based Facilitation of Cortical Activity Associated to Gait Onset After Single Event Multi-level Surgery in Cerebral Palsy

J. Ignacio Serrano, M.D. del Castillo, C. Bayón, O. Ramírez, S. Lerma Lara, I. Martínez-Caballero and E. Rocon

Abstract Motor rehabilitation strategies by means of neuro-modulation paradigms, taking advantage of the motor predictive characteristics of the electroencephalographic signal, are currently subject to extensive research. Such rehabilitation strategies follow a top-down approach in which targeted neurophysiological changes in the central nervous system are expected to induce functional improvement. However, such approach presents a set of specific limitations and barriers in cerebral palsy patients, given that they typically do not have a normal gait and have suffered abnormal brain development. These limitations get even more critical when Single-Event Multilevel Surgery (SEMLS) is performed. After that procedure, surgery patients must re-learn the gait patterns according to a new biomechanical structure. This chapter presents a neuro-modulation paradigm to enhance the re-education of gait functionality immediately following SEMLS in cerebral palsy patients. The experiments were developed and tested with real patients.

Keywords Neuromodulation · Virtual reality · Cerebral palsy · Gait neurorehabilitation · Single-event multilevel surgery

J. Ignacio Serrano (✉) · M.D. del Castillo · C. Bayón · O. Ramírez · E. Rocon
Neural and Cognitive Engineering Group, Centro de Automática y Robótica, Spanish National Research Council (CSIC), 28500 Arganda del Rey, Spain
e-mail: jignacio.serrano@csic.es

S. Lerma Lara
Gait Analysis Laboratory, Hospital Infantil Universitario Niño Jesús, 28009 Madrid, Spain

I. Martínez-Caballero
Children Orthopedics Service, Hospital Infantil Universitario Niño Jesús, 28009 Madrid, Spain

C. Guger et al. (eds.), *Brain-Computer Interface Research*,
SpringerBriefs in Electrical and Computer Engineering,
DOI 10.1007/978-3-319-57132-4_8

1 Introduction

Cerebral palsy (CP) is a disorder of posture and movement due to a defect or lesion in the immature brain. It is estimated that 17 million people worldwide are affected [1]. In many cases, the development of secondary musculoskeletal pathology contributes to loss of function, gait impairments, fatigue, activity limitations, and participation restriction. In fact, one out of three CP patients is unable to walk. For those patients, orthopaedic surgery is considered one of the best treatments for significant musculoskeletal problems, and thereby minimizing the subsequent impairments and activity limitations. One of the main techniques is multilevel orthopaedic surgery, which focuses on correcting all deformities and to improve gait. It is often referred to as Single-Event Multilevel Surgery (SEMLS) when is performed in a patient without previous surgeries. SEMLS refers to the procedure encompassing several orthopaedic surgeries in one intervention, affecting two or more levels of the lower limbs (knee and ankle, for instance). It differs from other multilevel approaches in that SEMLS is based on the biomechanical principles previously obtained by 3D gait analysis [2]. Currently, SEMLS is indicated up to 70% of CP children under 14 years old. SEMLS has shown benefits in the treatment of musculoskeletal problems of children with CP by reducing the effort and the appearance of walking, improving Gross Motor Function Measure (GMFM) [3], kinematic parameters, gait speed, and Gillette Gait Index score [4]. After this procedure, a period up to 2 years is often required to get a functional plateau level, although there is a lack of published recommendations about the more efficient post-surgical rehabilitation program. New strategies are needed to help to promote, maintain, and rehabilitate the functional capacity, and thereby diminish the dedication and assistance required and the economic demands that this condition represents for the patient, caregivers and society.

Most therapies for rehabilitation after surgery are peripherally driven and are based on motor control reorganization triggered by peripheral physical therapy. However, CP affects primarily brain structures. This suggests that both the Peripheral Nervous System (PNS) and the Central Nervous System (CNS) should to be integrated in a physical and cognitive rehabilitation therapy. This is exactly the approach proposed in this chapter. It is important to highlight the plasticity of the target patients of this study: young children present increased brain plasticity compared to an adult, and are more likely to exhibit a change in motor patterns following an intervention.

Consequently, a BCI system is proposed here in two phases: the first one as re-education of gait-related cortical activity (post-surgery intervention in bed or wheelchair); the second one as active control of the rehabilitation therapy on the robotic platform. Therefore, the first month post-surgery, when the patient is immobilized, is the most appropriate period to prepare the brain for the new gait patterns later promoted with the robotic physical rehabilitation process.

2 Neuro-Modulation in Cerebral Palsy Patients—BCI Perspective

One possible application of BCI that has garnered significant research interest during the last decade is its use to restore motor function by inducing activity-dependent brain plasticity for brain motor re-learning [5]. According to this approach, known as top-down [6], BCIs use brain activity to promote central motor control by operating on the peripheral nervous system in order to recover motor function for people with severe motor disabilities. The objective of these BCI therapeutic applications differs from the BCI applications for communication and device control, since the former application attempts to maximize motor planning ability damaged by disease or trauma by performing tasks related to motor execution or motor imagery.

In any case, there is scarce scientific work about the potential use of BCIs by CP patients independent of the type of application and objective. The complexity associated with the experimental design, given the great amount of symptoms that vary from patient to patient as a consequence of the different brain areas affected, necessitates analysing and meeting individual specific conditions and requirements to identify brain activity evoked by external stimuli or subject to the patient's control. Therefore, the existent works are rather exploratory studies that intend to lay the foundations for developing potential uses of BCI in CP individuals.

In [7], a case study to train a severe paralyzed CP patient by an EEG-based BCI for verbal communication is presented. The patient could produce two distinct EEG patterns by controlling frequency features of sensorimotor rhythms during movement imagery.

The proposal for using ECoG techniques to record brain signals in speech cortex shows an efficient way, with a good spatial and signal-to-noise resolution, to build BCIs for spastic CP patients presenting the motor cortex damaged [8]. The resulting processed signal, representing the intent of the patient, could control different types of computerized devices, including rehabilitation systems. Both studies belong to the BCI paradigm for communication or device control.

A well-known work dealing with a larger population of CP patients, to investigate their ability to gain control of two online BCIs that assist them with their communication needs, is described in [9]. Fourteen individuals with different types of CP were engaged in this experiment by using two different electroencephalographic phenomena, one based on endogenous sensorimotor rhythms (SMR) and the other one based on potentials evoked by exogenous visual stimuli (SSVEP). Both BCIs involve different cognitive processes and cortical areas. SSVEP-based BCI involves attending to oscillatory stimuli that increases in magnitude the activity recorded in the occipital cortex at the corresponding frequency. SMR-based BCI implies carrying out different mental tasks as mental arithmetic or motor imagery of some part of the body. The results of this work show that not all approaches work for every user, although the SMR-based BCI is better commanded by a larger

number of users, and that there is no statistical relation between degree of impairment and the ability to control a BCI.

In healthy people, SMR-based BCIs implicate motor cortex areas that exhibit rhythms whose amplitudes typically change with the movement, the stimulation or sensation and also during motor imagery [10]. Since these rhythms are associated with cortical areas most directly connected to the brain's normal motor output channels, they could be a potential tool for BCI neuro-rehabilitation.

However, the possible motor-cortical lesions in CP patients can alter the neural mechanisms underpinning actual motor execution and motor imagery. In an EEG-based brain mapping study [11], with four healthy children and four children with CP, children with CP showed asymmetrical and global topographical maps regarding SMR rhythms changes when they perform motor imagery tasks compared to healthy children. Another study [12] also focuses on understanding the neural processing underlying BCI control using motor imagery in fourteen CP individuals and twelve healthy individuals, and found significantly lower SMR modulation and connectivity strengths between cerebral areas in CP patients. Although motor imagery training seems to be a promising method to improve motor control in CP, its efficacy needs to be proved by empirical testing.

Summarizing, building a BCI for neuro-rehabilitation purposes in CP patients requires analysing and determining cortical activity and brain areas with neuroplastic potential in a tailored manner, given the congenital damage in their brains. This damage impairs motor planning ability that affects motor execution and motor imagery tasks. Another key aspect to assess lies in the nature of the motor imagery tasks to be proposed, since this population presents impaired sensorimotor integration leading to decreased body awareness. So, promoting body awareness in CP patients when they perform motor imagery tasks by a suited experimental design and paradigm is critical to produce a kinaesthetic image of the motor action and to obtain viable electrophysiological activity. Other crucial issues to take into account are the familiarity of the motor tasks and the imagery instructions in order to encourage the motor imagery capacity in CP.

3 Particular Drawbacks for BCI-Based Motor Neuro-Rehabilitation in Cerebral Palsy Patients Following SEMLS

Due to the very early brain damage and functional limitations, CP patients exhibit abnormal brain development [13]. This causes abnormal brain activity that in turn hinders the decoding of useful information from that activity. In order for a BCI to be effective in motor rehabilitation, motor-related activity should be potentiated by a coherent proprioceptive feedback. Given that BCIs should be non-invasive and easy to wear for the sake of applicability, the most suitable way of measuring the brain activity is Electroencephalography (EEG).

In this sense, there are three main types of disability concerning motor function in CP patients that also alter EEG motor-related brain activity, thus making BCI application more complicated:

- Spasticity. It is the most common dysfunction. It arises from motor cortex damage making muscles appear stiff and tight. Since it implies motor cortex damage, the brain activity in that area is also abnormal and difficult to use for BCI. Besides, the constant muscle activation produces proprioceptive feedback, which is reflexed in activation of somatosensory areas of the cortex that are really close to motor areas. Moreover, the strength of the muscle contraction may cause artefacts that introduce noise in the EEG cortical signals.
- Ataxia. It arises from cerebellar damage. It implies the loss of muscle control, producing shaky movements. It affects balance and sense positioning in space. Although the damage focuses on the cerebellum, the projections to the motor cortex areas also alter the normal cortical activity. Besides, shaky movements and random motor unit discharges represent a complex artefact for EEG-based BCIs.
- Dyskinesia. It arises from basal ganglia damage. It is characterized by involuntary movements. Like in ataxia, damage to the basal ganglia induces abnormal cortical activity through the cortical-striatum loops. The involuntary movements introduce both external and internal artefacts into the EEG motor-related activity.

Apart from the problems introduced by the above mentioned dysfunctions, there are other concerns coming from abnormal development. In terms of the affected limbs, motor pathologies affecting CP patients can be divided into four groups:

- Monoplegia. One limb, either upper or lower, is affected by a motor dysfunction.
- Hemiplegia. This is the most common type, together with diplegia. It affects one side of the body (arm and leg).
- Diplegia. Both legs are affected. The upper limbs may be affected to a lesser extent.
- Quadriplegia. Both upper and lower limbs are affected. The muscles of the trunk, face and mouth are often also affected.

For BCI applicability purposes, monoplegia is the least affecting condition, since the function of the damaged cortical areas is usually assumed by surrounding areas in the motor cortex. However, hemiplegia often implies a cortical reorganization into the contralesional hemisphere [14]. That is, the function of both sides of the body is assumed by the same hemisphere. This makes the decoding of the target side and limb from EEG activity especially hard. This same effect is dramatically augmented in diplegia and quadriplegia, where the reorganization of motor control is unpredictably carried out in other non-motor areas. Consequently, motor function shares cortical areas with a variety of cognitive functions, which in turn makes EEG decoding and neuro-modulation extremely complex.

In addition, CP patients following SEMLS present a particular problem. They have to re-learn walking (either normal or aided), since their structural biomechanics has changed. Given that those patients have never walked before or have not walked normally, their learned brain motor patterns are unusual. Therefore, they are difficult to detect in order to be promoted and guided later on by neuro-modulation to adapt to their new physical capacities.

The difficulty of CP patients for kinaesthetic motor imagery, given their brain damage, abnormal development and poor embodiment, is the ultimate drawback for BCI-based neuro-rehabilitaton. This problem makes the BCI training paradigm hard to accomplish.

4 BCI-Based Gait Rehabilitation for CP Patients Following SEMLS. A Top-Down Approach

The rehabilitation is a therapeutic process that aims to develop the maximum physical, psychological and social potential of the patient [15]. Although 70% of CP patients will manage to partially recover the gait function during development [13], most patients will improve their gait function by SEMLS.

Although the origin of neurologic disabilities is located centrally, conventional therapies have traditionally focused on providing sensory feedback and performing real movements in the affected limbs of the patients. In this sense, they have been based in a bottom-up approach, i.e. the rehabilitation focuses on the peripheral function, which is in turn expected to induce central neurophysiological changes. Nevertheless, the principal mechanisms implicated in the motor recovery of CP patients involve enhanced activity of the motor areas (wherever they were placed) induced by active motor training [16]. While peripheral stimulation has not proven to be a locally specific way of promoting plastic changes, an induced coherent activation of sensory feedback circuits and structures in the primary motor cortex is expected to reinforce cortico-muscular connections according to Hebbian learning principles, and thus support functional recovery [17]. Taking into account that the connection between the sensorimotor cortex and peripheral muscles in CP patients has been altered, such rehabilitation strategy appears to be a logical step to reinforce the cortico-muscular descending pathways to regain gait control.

This implies switching to a top-down rehabilitation strategy, in which the mechanisms that are targeted for modification through rehabilitation are the new central structures of the nervous system in charge of the movement generation. According to this concept, the peripheral rehabilitation is carried out in synchrony with the activity of the functionally associated structures of the brain, or rather triggered by it. The coupling promotes a cause-effect action from intention to execution of movement, thus increasing the associative facilitation of efferent pathways. Indeed, experimental paradigms using Paired Associative Stimulation (PAS, i.e. the application of timely associated electrical stimuli in cortical and

muscular regions) have proven to be an effective way to strengthen the cortico-muscular connections [18].

The sensory feedback may induce plasticity underlying the restoration of normal motor control. The basis of these approaches is that activity-dependent CNS plasticity can induce changes at synaptic, neuronal and circuits levels in cortical and subcortical structures of the brain and so produce a more normal motor control [19].

As said before, most CP patients would benefit from SEMLS. However, the ultimate improvement is reached around 36 months after surgery, following an intensive rehabilitation program [20]. Moreover, the improvement is monotonous during that post-surgery period, except the time range between 12 and 18 months after surgery, where there is a monotonous decrease of the Gait Deviation Index (GDI). After that, the improvement resumes [21]. In this sense, the rehabilitation suggests two points for improvement: Increasing the maximum level of functional recovery and reducing the time to reach that maximum by avoiding the recession period in between. For this purpose, the inclusion of the neuro-rehabilitation of motor activity points to a plausible solution. Since CP patients following SEMLS are in bed during the first 3–4 weeks, the neuro-rehabilitation should begin right after surgery to start modulating brain activity before physical gait rehabilitation. Thus, the brain preparation for the novel upcoming biomechanical feelings of patients is hypothesized as a catalyst for a more efficient and effective physiotherapy.

5 A Virtual Reality-Based BCI Intervention for the Neuro-Rehabilitation of Cortical Motor Patterns Related to Gait in CP Patients Following SEMLS

Three CP children, 11, 13 and 15 years old, respectively, were recruited for the study of this novel intervention. They all had a SEMLS operation. All patients presented no cognitive deficit. The children started the first session of the post-surgery BCI intervention few days after surgery. During the all sessions throughout the intervention, the patients were comfortably seated on a reclining pallet with an inclination of 50° (patients were still unable to control their neck muscles). They wore an EEG scalp and virtual reality glasses (Oculus Rift) as shown in Fig. 1.

EEG signals were recorded from AFz, F3, F1, Fz, F2, F4, FC5, FC3, FC1, FCz, FC2, FC4, FC6, C5, C3, C1, Cz, C2, C4, C6, CP5, CP3, CP1, CPz, CP2, CP4, CP6, P3, P1, Pz and P2 (according to the international 10–20 system) using active Ag/AgCl electrodes (Acticap, Brain Products GmbH, Germany). The FCz channel was used as a reference. AFz was used as ground. The signal was amplified (BrainVision actiCHamp, Brain Products GmbH, Germany) and sampled at 250 Hz. The power values (Power Spectral Density, PSD) were estimated in overlapping segments of 1.5 s and for frequencies between 2–30 Hz in steps of

Fig. 1 BCI-based sessions setup during post-surgery immobilization

1 Hz. Welch's method was used to this end (Hamming windows of 1 s, 50% overlapping).

The virtual reality glasses were used to show the patients the experimental environment in first person view. These glasses cover the total of the human vision range, providing an absolutely immersive feeling and, therefore enabling realistic visual feedback able elicit coherent brain activity. This way, the problem of lack of body awareness or difficulty was reduced. The virtual environment consisted of a fantasy world designed with Unreal Development Kit (UDK), an open-source 3D graphic and game engine. It is projected in stereoscopic mode to the glasses for a more realistic experience. Each session corresponds to a walk (in first person) through a defined path around the world. Along the path, there are different obstacles (gates, stones, trees …). Each time the patient gets close to an obstacle, the walk stops. Then the obstacle disappears and the walk slowly resumes. Each obstacle then constitutes a trial. There are 22 different obstacles along each path. In the first two sessions, the walk is automatic, i.e. it is not controlled by the BCI, although the patients are not informed about this issue (sham condition). Patients always though that they were controlling the walk. This is done because the BCI will not likely perform acceptably in the first two sessions, which might disappoint and discourage the children. Therefore, the automatic walks were used as training trials for further BCI control. In the automatic walk, a trial was designed as depicted in Fig. 2.

Patients were instructed to relax when they faced an obstacle and the walk stopped, if they wanted to make it disappear. After that, they were instructed to kinaesthetically imagine they started walking if they wanted to resume the walk. From these automatic sessions, the pair (channel, 1 Hz—frequency band) with the most pronounced and longest average desynchronization (PSD decay) during the

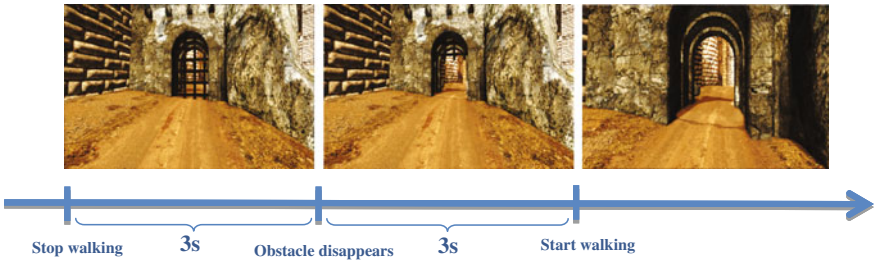

Fig. 2 Description of a trial along the virtual reality automatic sessions

"obstacle disappearing" and "start walking" periods, with respect to the resting periods, was selected. Each session was performed two weeks after the preceding session. Online BCI recording and processing was implemented using BCI2000. A driver was developed to connect BCI2000 and UDK engine.

After the two initial automatic sessions, the best average pairs channel/frequency was extracted for each participant. Given the average time-frequency matrix for each channel, the pair channel/frequency bin with the minimum median value during the 3 s of the obstacle disappearing period, and the first 3 s of the start walking period, was selected. Results for each patient are shown in Fig. 3.

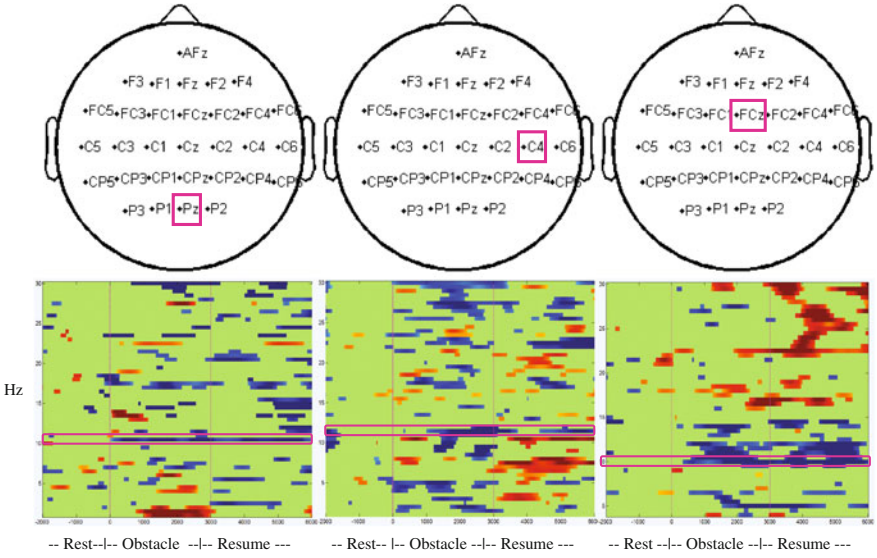

Fig. 3 Average time-frequency graphs showing the most desynchronized pair channel/frequency-bin (*pink box*) during automatic sessions for the three CP patients ($p < 0.05$, with respect to "rest" period; *blue* lower PSD; *red* higher PSD)

The frequency bins selected for gait onset are in the range of *alpha* band or *mu* rhythms (7–12 Hz), the typical frequency of motor preparation. However, the selected channels are diverse and arranges by relevance according to the cortical reorganization described above. Patient 3, with the lowest level of disability, shows a wide desynchronization of *mu* rhythms over the legs area (according to the somatotopic cortical map) of premotor cortex (FCz). However, the two other patients show cortical reorganization of gait onset preparation into other parts of the brain, with a more specialized frequency band.

The patients performed two BCI-controlled sessions along paths different from the automatic sessions. In the BCI-controlled sessions, an obstacle does not disappear until the selected pair (channel, frequency band) reaches the learned power associated with rest and maintains this level for one second (not consecutive) in windows of 2 s. Analogously, once the obstacle disappears, the walk is not re-started until the power value reaches the learned desynchronization for 1 s. The three patients were able to overcome all obstacles and complete the paths.

6 Current State and Future Perspectives

A BCI-based training of cortical activity related to gait has been proposed as a post-SEMLS intervention of CP patients. This intervention prepares the brain during the immobilization period for further physical rehabilitation, thus actively involving the patient in it. The intervention also potentiates the associative facilitation of efferent pathways from cortex to muscles, which in turn benefits the physical rehabilitation. The BCI-guided therapy also boosts the cause-effect feeling of the motor control of the patients, and consequently contributes to increase their sense of agency, in motion terms. Despite the brain damage and heterogeneity, CP patients were able to control the BCI with atypical cortical areas reassigned for gait execution.

Immersive virtual reality has proven to be an effective tool to overcome the problems affecting EEG-based BCI, caused by brain damage, abnormal development, cortical reorganization, new biomechanical structure, impossibility of kinaesthetic imaging of gait and cognitive deficit.

So far, BCI-based neuro-modulation strategies for CP rehabilitation have been able to prove a number of relevant questions in the field. The possibility of developing BCI technology that can be controlled by the cortical waves of patients with cortical lesions has been demonstrated. In addition, recent studies have advanced in the ways to achieve reliable estimations of motor-related cortical states with time precision, which further boosts these neuro-modulation applications. Taken together, these advances represent a strong background for subsequent studies in the near future, in which larger CP populations will need to be recruited in clinical validation studies to further understand the interplay between the BCI reached performance in each person, the attainable neurophysiological changes induced (especially those associated with cortico-muscular facilitation) and the

functional improvement of the patients as a result of different rehabilitation intensities with these technologies. To achieve these goals, further developments in EEG acquisition systems and processing algorithms will need to be carried out so that the technology can be easily transferred to the clinical practice. Additionally, further improvement of placebo-controlled conditions must be achieved to fully quantify the relevance of BCI technology in CP rehabilitation.

Finally, the feasibility of using BCI based on residual or new cortical motor rhythms in CP patients opens the door to the application of neuro-robots for gait rehabilitation or re-education [22], which turns out a promising approach [23].

References

1. I. Novak, M. Hines, S. Goldsmith, R. Barclay, Clinical prognostic messages from a systematic review on cerebral palsy. Pediatrics. **130**(5), e1285–1312 (2012)
2. J.L. McGinley, F. Dobson, R. Ganeshalingam, B.J. Shore, E. Rutz, H.K. Graham, Single-event multilevel surgery for children with cerebral palsy: a systematic review. Dev. Med. Child Neurol. **54**(2), 117–128 (2012)
3. R. Palisano, P. Rosenbaum, S. Walter, D. Russell, E. Wood, B. Galuppi, Development and validation of a gross motor function classification system for children with cerebral palsy. Dev. Med. Child Neurol. **39**, 214–223 (1997)
4. T.A. Wren, K.P. Do, R. Hara, F.J. Dorey, R.M. Kay, N.Y. Otsuka, Gillete Gait Index as a gait analysis summary measure: comparison with qualitative visual assessments of overall gait. J. Pediatr. Orthop. **27**(7), 765–768 (2007)
5. I. Daly, J.R. Wolpaw, Brain-computer interfaces in neurological rehabilitation. Lancet Neurol. **7**, 1032–1043 (2008)
6. J.M. Belda-Lois, S. Mena-del Horno, I. Bermejo-Bosh, J.C. Moreno, J.L. Pons, D. Farina, M. Iosa, M. Molinari, F. Tamburella, A. Ramos, A. Caria, T. Solis-Escalante, C. Brunner, M. Rea, Rehabilitation of gait after stroke: a review towards a top-down approach. J. of Neuroeng. Rehabil. **8**, 66 (2011)
7. C. Neuper, G.R. Müller, A. Kübler, N. Birbaumer, G. Pfurtscheller, Clinical application of an EEG-based brain–computer interface: a case study in a patient with severe motor impairment. Clin. Neurophysiol. **114**, 399–409 (2003)
8. M.J. Mir, Electrocorticography (ECoG) based brain computer interface for cerebral palsy patients. Final Paper BME 5030 Electronic Bioinstrumentation, Department of Biomedical Engineering, Cornell University, New York, USA (2009)
9. I. Daly, M. Billinger, J. Laparra-Hernández, F. Aloise, M.L. García, J. Faller, R. Scherer, G. Müller-Putz, On the control of brain-computer interfaces by users with cerebral palsy. Clin. Neurophysiol. **124**, 1787–1797 (2013)
10. G. Pfurtscheller, C. Guger, G. Müller, G. Krausz, C. Neuper, Brain oscillations control hand orthosis in a tetraplegic. Neurosci. Lett. **292**(3), 211–214 (2000)
11. Y.K. Shin, D.R. Lee, H.J. Hwang, S.H. You, A novel EEG-based brain mapping to determine cortical activation patterns in normal children and children with cerebral palsy during motor imagery tasks. NeuroRehabilitation **31**, 349–355 (2012)
12. I. Daly, J. Faller, R. Scherer, C.M. Sweenwy-Reed, S.J. Nasuto, M. Billinger, G.R. Müller-Putz, Exploration of the neural correlates of cerebral palsy for sensorimotor BCI control. Front. Neuroeng. **7**, 20 (2014)
13. I. Novak, Evidence-based diagnosis, health care, and rehabilitation for children with cerebral palsy. J. Child Neurol. **29**(8), 1141–1156 (2014)

14. L.J. Carr, L.M. Harrison, A.L. Evans, J.A. Stephens, Patterns of central motor reorganization in hemiplegic cerebral palsy. Brain **116**, 1223–1247 (1993)
15. World Health Organization (WHO). World report on disability (2011)
16. M.T. Robert, R. Guberek, H. Sveistrup, M.F. Levin, Motor learning in children with hemiplegic cerebral palsy and the role of sensation in short-term motor training of goal-directed reaching. Dev. Med. Child Neurol. **55**, 1121–1128 (2013)
17. P. Yger, M. Gilson, Models of metaplasticity: a review of concepts. Front. Comput. Neurosci. **9**(138) (2015)
18. V. López-Alonso, B. Cheeran, M. Fernández-Del-Olmo, Relationship between non-invasive brain stimulation-induced plasticity and capacity for motor learning. Brain Stimul. **8**(6), 1209–1219 (2015)
19. G.R. Mileva, I.J. Kozak, J.E. Lewis, Short-term synaptic plasticity across topographic maps in electrosensory system. Neuroscience **318**, 1–11 (2016)
20. K. Lehtonen, H. Mäenpää, A. Piirainen, Does single-event multilevel surgery enhance physical functioning in the real-life environment in children and adolescents with cerebral palsy (CP)?: patient perceptions five years after surgery. Gait Posture **41**(2), 448–453 (2015)
21. S. Lerma Lara, I. Martínez-Caballero, A. Ramírez-Barragán, Cambios en el Gait Deviation Index (GDI) tras cirujía multinivel en niños con parálisis cerebral. Proceedings of the XX Annual Congress of the Spanish Society of Pediatric Orthopedics (2015)
22. C. Bayón, R. Raya, S. Lerma-Lara, O. Ramírez, J.I. Serrano, E. Rocon, Robotic therapies for children with cerebral palsy: a systematic review. Transl. Biomed. (Accepted) (2016a)
23. C. Bayón, O. Ramírez, F. Mollá, J.I. Serrano, M.D. del Castillo, J.M. Belda-Lois, R. Poveda, R. raya, T. Martín-Lorenzo, I. Martínez-Caballero, S. Lerma-Lara, C. Cifuentes, A. Frizera, E. Rocon, Conceptualization, design and evaluation of a robotic platform for gait rehabilitation in patients with cerebral palsy: CPWalker. IEEE Trans. Neural syst. Rehabil. Eng. (Accepted) (2016b)

Estimation of Intracranial P300 Speller Sites with Magnetoencephalography (MEG)—Perspectives for Non-invasive Navigation of Subdural Grid Implantation

M. Korostenskaja, C. Kapeller, P.C. Chen, R. Prueckl, R. Ortner, K.H. Lee, T. Kleineschay, C. Guger, J. Baumgartner and E. Castillo

Abstract Brain-Computer Interfaces (BCIs) are powerful tools for enabling communication between people and the surrounding world by directly utilizing brain activity and avoiding motor pathways. Before moving into invasive implantation of BCIs, a key issue must be resolved—localization of the areas for implantation, which might vary depending on the chosen BCI type as well as on the individual person's characteristics. In this study, we aimed to evaluate the possibility of non-invasive navigation of subdural electrode implantation for P300 speller BCI by using magnetoencephalogaphy (MEG). The accuracy of subdural P300 speller performance based on the sites identified with MEG was comparable with the performance based on the sites identified from subdural electrode grids—80% and 90% averaged accuracy, respectively. Our study demonstrates the feasibility of using MEG as a non-invasive tool for navigating electrode implantation required for high accuracy invasive P300 speller control.

Keywords Brain computer interface (BCI) · Electrocorticography (ECoG) · Magnetoencephalography (MEG) · P300 response · P300 speller

M. Korostenskaja (✉) · P.C. Chen
Milena's Functional Brain Mapping and Brain Computer Interface Lab,
Florida Hospital for Children, Orlando, FL, USA
e-mail: milena.korostenskaja@gmail.com

M. Korostenskaja · T. Kleineschay · E. Castillo
MEG Center, Florida Hospital for Children, Orlando, FL, USA

M. Korostenskaja · P.C. Chen · K.H. Lee · T. Kleineschay · J. Baumgartner · E. Castillo
Florida Epilepsy Center, Florida Hospital, Orlando, FL, USA

M. Korostenskaja
Dr. K's Research and Teaching Innovations, Winter Springs, FL, USA

C. Kapeller · R. Prueckl · R. Ortner · C. Guger
g.tec Medical Engineering GmbH, Graz, Austria

C. Guger et al. (eds.), *Brain-Computer Interface Research*,
SpringerBriefs in Electrical and Computer Engineering,
DOI 10.1007/978-3-319-57132-4_9

1 Introduction

Brain-Computer Interfaces (BCIs) have a strong potential to significantly contribute towards improving quality of life in people with motor system-related disabilities. Indeed, BCIs may provide these people with the much needed possibility of communication by utilizing activity from the central nervous system and bypassing compromised motor pathways. There is evidence to suggest that, for severely disabled patients (such as those with advanced stages of amyotrophic lateral sclerosis—ALS, locked-in syndrome, tetraplegia or severe impairments after stroke), the surgically-implanted intracranial BCIs might be more efficient than scalp-based BCIs [1, 2]. However, before the chronic BCI implantation can be considered as a viable option for these patients, an important issue needs to be addressed—localization of intracranial electrode implantation sites, which might vary depending on the BCI approach used, as well as on each individual person's characteristics.

In our previous studies [2, 3], we have concluded that specific approaches must be developed to identify and extract the data of interest that is necessary to achieve desired performance of chronically implanted BCIs. Among several suggested approaches, the most promising approach for future work with BCIs has been the use of non-invasive technology, such as magnetoencephalography (MEG) [3]. The MEG allows recording of neuromagnetic brain activity with precise temporal resolution. Moreover, when combined with the structural information about the brain, derived from magnetic resonance imaging (MRI), the MEG also provides excellent spatial resolution. It is routinely used for mapping of functionally significant cortical brain areas, such as motor, auditory, visual, and language during pre-surgical evaluation of patients with pharmacoresistant epilepsy [4]. Therefore, it can potentially be utilized for identifying the cortex involved in generation of signals for targeted BCI use.

The aim of our current study was to evaluate feasibility of non-invasive navigation for subdural electrode selection with MEG needed for high accuracy performance of P300 speller.

2 Methods

The study was performed in a 17-year-old right-handed female patient with intractable epilepsy, undergoing evaluation for epilepsy surgery. Two main approaches were utilized to select channels to test invasive P300 speller performance: (1) Protocol #1 (*MEG-based*) used MEG source localization to navigate the choice of P300 speller sites; and (2) A comparison Protocol #2 (*ECoG-based*) utilized statistical ECoG signal analysis.

2.1 MEG-Based Approach

2.1.1 Non-invasive Localization of P300 Generators with MEG

During this test, visual evoked fields were recorded in response to two letter stimuli (O and X) that were presented in an "odd-ball" paradigm manner, with 76% of NON-TARGET (letter "O") and 24% of TARGET stimuli (letter "X") (Fig. 1a). Altogether, 76 frequent and 24 deviant stimuli were presented. Both target and non-target stimuli had durations of 100 ms. The inter-trial interval (ITI) was randomized between 2000 and 3000 ms. The patient was instructed to keep her eyes on the fixation point in the middle of the screen and count all infrequent stimuli that appeared. The MEG signal was subjected to SPSS filtering and averaging off-line. The sources of P300 speller was localized by using equivalent current dipole (ECD) approach. Main sources responsible for P300 generation have been localized in the right central and parieto-occipital areas, as well as left frontal areas.

2.1.2 Merging Information from Subdural Electrode Location and MEG Results

After the patient was implanted with subdural electrodes, the 3-D-rendered map of the patient's cortical surface was created, co-registered and overlaid on subdural electrodes. The localized P300 ECDs were overlaid with the 3-D-rendered cortical and grid map (Fig. 2). Eight electrodes in close proximity with localized P300 sources were selected for on-line P300 speller testing protocol. The P300 responses recorded from sites selected with the MEG-based approach and ECoG electrodes during P300 speller performance are presented in Fig. 3a.

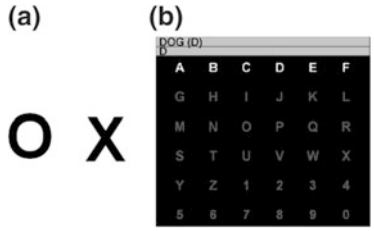

Fig. 1 Stimuli used in the study. **a** Example of TARGET ('O') and NON-TARGET ('X') stimuli presented in odd-ball paradigm for localization of P300 response with MEG; **b** Example of the letter and symbol matrix for the P300 speller used for screening and P300 on-line experiment

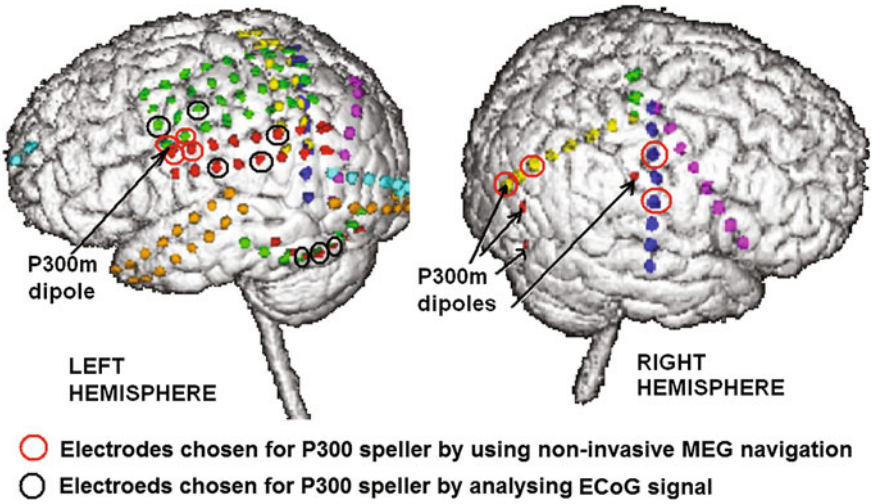

Fig. 2 3D-rendered cortical surface of patient's brain with overlaid subdural grids, P300 dipoles localized with MEG, as well as locations of 8 electrodes selected by using MEG and 8 electrodes selected based on ECoG data. Note that the asymmetric bilateral electrode placement is based entirely on the clinical decision required for successful completion of the pre-surgical patient's evaluation. During the non-invasive phase of pre-surgical evaluation for epilepsy surgery, the patient exhibited ictal activities originating from left hemisphere. However, possible right hemisphere involvement was not completely ruled out. Therefore, the overall completeness of the evaluation could have been biased without adding any additional right hemisphere grids during the second (invasive) phase of pre-surgical evaluation

2.2 ECoG-Based Approach

2.2.1 Screening of All Grid Electrodes

P300 responses were recorded from 158 electrodes implanted for the purpose of evaluation for epilepsy surgery during presentation of a P300 speller grid with flashing letters of the alphabet and symbols (Fig. 1b). The patient was instructed to concentrate on 5 consecutively presented letters comprising the word. Two words were presented. Each letter was highlighted in 15 columns and 15 rows. Neural activity from the subdural grids was recorded with a g.USBamp, g.tec, Austria (sampling frequency 256 Hz).

2.2.2 Selection of the Best 8 Responses Among All 158 Electrodes by Using EcoG-Based Approach

P300 responses were analyzed in a following manner: A Butterworth filter (4th order, 0.1–30 Hz) was applied and data was triggered into TARGET and

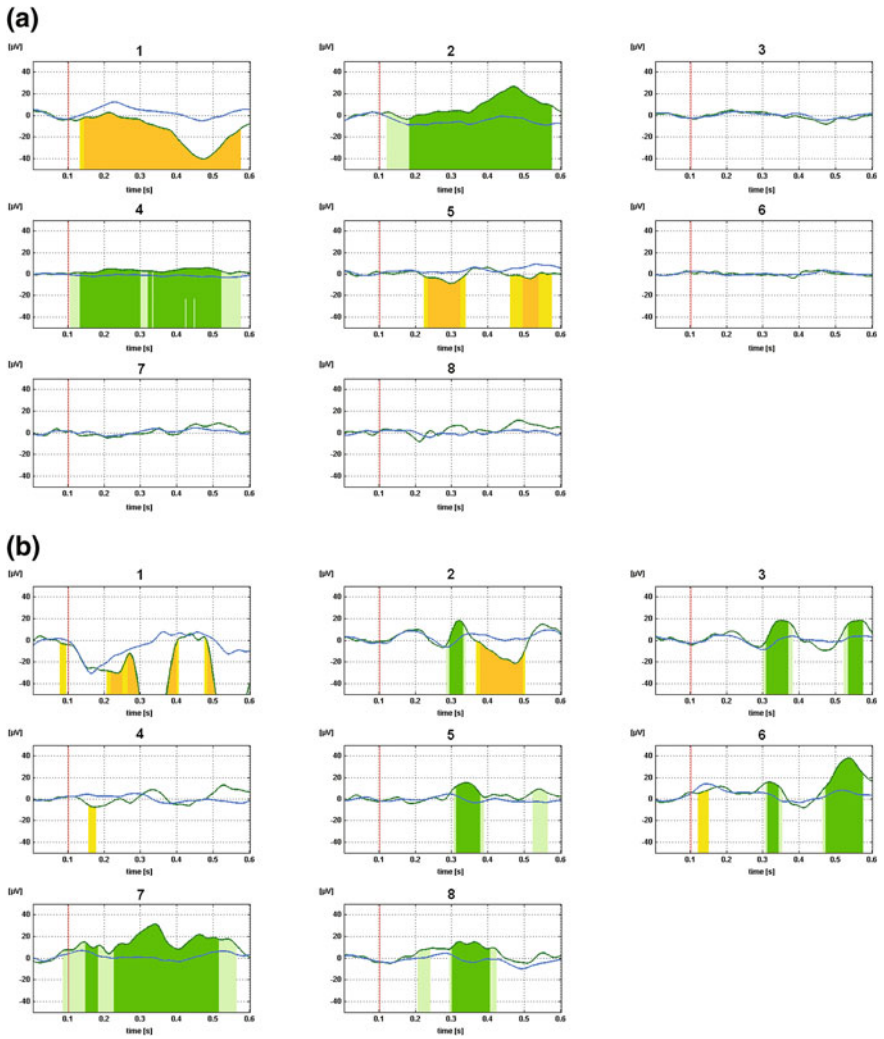

Fig. 3 Significance plots for P300 speller electrode locations for P300 speller BCI selected by: **a** MEG-based source localization approach; and **b** ECoG-based subdural electrodes selection approach. The response to the TARGET stimuli is presented in *blue*, and the response to NON-TARGET stimuli is presented in *green*. The figures contain the significance values of TARGET versus NON-TARGET ($p < 0.05$): The *yellow plots* indicate a significant negative difference; *green plots* indicate a significant positive difference. The variation of the color represents the level of significance (*light green* and *light yellow*: $p < 0.05$; *dark green* and *dark yellow*: $p < 0.01$)

NON-TARGET trials. Trials with artifacts were visually identified and removed. A Kruskal-Wallis test was used to test if TARGET and NON-TARGET samples originated from the same distribution, and led to a p-value for each sample and

channel. The best channels were selected according to the longest period of significant difference ($p < 0.05$) between TARGET and NON-TARGET trials. The eight most significant differences were found in channels 59, 82, 94, 118, 120, 60, 61, 92 (channels 1–8 respectively on Fig. 3b). These channels were located in left frontal, front-central, central and temporo-parietal regions.

3 On-Line Testing

For online classification of the P300 speller results obtained from 8 grid electrodes selected by using MEG-based approach (Fig. 3a) and 8 grid electrodes by using ECoG-based approach (Fig. 3b), a linear classifier was computed based on a temporal feature vector from each of eight selected channels within a linear discriminant analysis (LDA). The features were extracted from the raw data, which was acquired with a sampling rate of 256 Hz. In the first pre-processing step, the raw data was 58–62 Hz notch filtered and 0.1–30 Hz band-pass filtered. After triggering the data into 800 ms trials and down-sampling by factor 12, the baseline corrected trials of all channels were combined to one feature vector containing 120 samples.

4 Results

The accuracy of the subdural P300 speller was compared for 8 electrodes identified with MEG (Protocol #1) and for 8 electrodes identified with ECoG data analysis (Protocol #2) after creating a classifier with 10 letter phrases. The accuracy of the

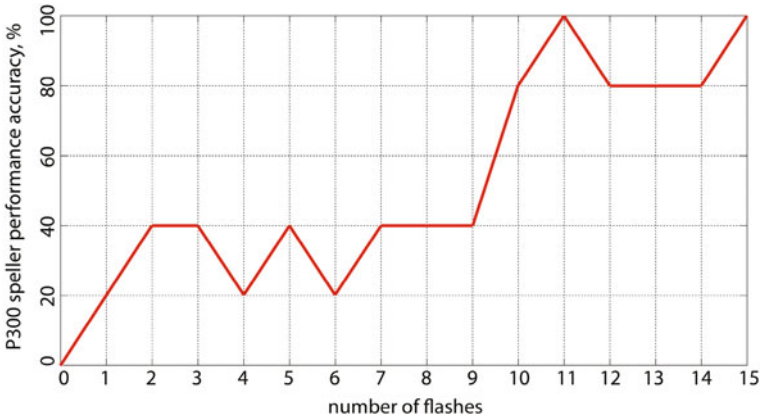

Fig. 4 The accuracy of the 8 selected channels after the ECoG screening using a classifier computed from 150 TARGET and 150 NONTARGET trials, and then tested on 5 characters

subdural P300 speller for MEG-identified sites was 80%, whereas for ECoG-identified sites, accuracy reached 90%. Figure 4 demonstrates the accuracy of the 8 selected channels after the ECoG screening using a classifier computed from 150 TARGET and 150 NONTARGET trials, and then tested on 5 characters. Our data suggest that MEG has a potential to serve as a non-invasive tool for navigating electrode implantation of P300 speller-based BCI.

5 Discussion and Future Perspectives

BCI technology enables communication between its users and the surrounding world by bypassing any muscle activity and utilizing direct brain signal instead (for review, see [5]). The surgically-implanted invasive BCIs (based on the ECoG signal recording) can be more advantageous when compared to non-invasive ones (based on the recordings of EEG signals) [6]. The implantable BCIs might be particularly beneficial for severely disabled patients, such as those with advanced stages of neuromuscular disorders, for example, ALS [7], locked-in syndrome [8], tetraplegia [1] and others. Patients with these severe disabilities report increased willingness to use chronically implanted BCIs [9, 10]. For instance, a telephone survey of people with ALS conveyed by Huggins and colleagues [9] has demonstrated that 72% of survey participants were willing to obtain a BCI by undergoing outpatient surgery and 41% by undergoing surgery with a short hospital stay.

Some of the reasons for patients' interest in obtaining an implantable BCI is a function of convenience and the possibility of uninterrupted access to this technology. For instance, there is no need to reapply electrodes if chronically implanted BCIs are used. Current technological advancements in the development of implantable devices, such as their flexibility due to silicon nanoribbon material [11, 12], their wireless power supply transmitted by using radiofrequencies [13], and a number of other innovative features, make it possible to forecast that implantable BCIs may become a part of people's life in the not too distant future. Importantly, the feasibility of small surgical implantations with microelectrodes has been recently demonstrated [14–16], showing promise for minimally-invasive BCI surgeries [17]. Importantly, such chronic in vivo BCI implantation would allow uninterrupted 24/7 connection between the brain and the external environment for people in need.

Recent reports show that the quality of the signal, as well as ability of pattern recognition and classification in home-based non-invasive BCIs systems with patient-users, both suffer significantly when compared to the same systems used in a controlled laboratory environment [18]. Utilization of invasive BCIs at patients' homes would contribute to the improvement of the recorded brain signal quality and, as a consequence, would lead to better BCI performance in home-based settings. Notably, invasive recordings, such as ECoG, offer higher signal-to-noise ratio than EEG [for review, see 19]. For example, Ball, Kern [20] has demonstrated that the ECoG signal recorded from subdural electrodes had a signal quality twenty to

one hundred times higher than that of EEG signal recorded with scalp electrodes. In addition, the ECoG signal offers vastly superior spatial resolution and is much less susceptible to artifacts [for more information, see review by 21]. Spatial resolution of ECoG recording can be further improved by using microelectrodes. For example, high resolution ECoG (HR-ECoG) recorded with the help of microelectrodes can have 400 times higher resolution than the conventional ECoG [22]. This is of particular importance when aiming at identification of language-related brain areas/classification of spoken words [23, 24], representing a potential use for future language-related BCI systems.

However, the question about the areas of implantation for chronic BCI devices still remains open. Minimal invasiveness dictates precise a priori knowledge of implantation sites and targeted areas of implantation during the surgery. These areas may vary dependent on the targeted BCI type, as well as on each person's individual anatomical and physiological brain characteristics. Indeed, Speier, Fried [6] demonstrated that the location of evoked responses may affect BCI performance, specifically P300 speller bit rate. In our previous study [2], we concluded that specific approaches must be developed to identify and extract the data of interest from ECoG signal recordings in order to achieve desired BCI performance. Among several proposed approaches, the most promising for future work with BCIs, in our opinion, the use of MEG [25, 26]. Although it is feasible to use MEG for BCI purposes [27], it cannot be applied for BCI control directly in everyday settings, because of its current need for a massive shielding from the external electromagnetic activity. However, it can be extremely helpful in estimating the sources of evoked responses used for BCI control. As a consequence, the MEG represents an excellent candidate for guiding desired electrode implantation intended for chronic BCI use.

The "P300 speller" paradigm is the most frequently utilized approach that allows subjects to spell words or phrases by direct brain-controlled selection from material presented on a computer screen [28]. In our current study, we have demonstrated that it is feasible to use MEG for non-invasive determination of intracranial P300 speller recoding sites. We have achieved, on average, 80% P300 speller performance accuracy with MEG-identified electrode sites. Further studies should aim at improving MEG-navigated selection sites to achieve greater BCI performance accuracy. This can be accomplished by tuning various aspects of P300 response localization, including the selection of the P300 response range, it components (P3a and P3b), as well as the selection of P300 response source localization algorithm (e.g., distributed model versus single equivalent current dipole model).

Interestingly, in our current study, the P300 generation sites derived with MEG differed from those derived from ECoG electrodes. For example, whereas MEG-derived P300 sources were localized in both right and left hemispheres (specifically, right central and parieto-occipital areas as well as left frontal areas), the main ECoG-derived P300 response generation sites were found in the left hemisphere only (specifically, in the left frontal, fronto-central, central and temporo-parietal regions). Moreover, while both approaches have identified concordant regions generating P300 responses within the left frontal lobe, the

ECoG-based approach has demonstrated additional P300 responses in the left temporo-parietal region that have not been identified with MEG. The diversity of P300 generation sites identified in our study is not surprising. Indeed, multiple studies have demonstrated P300 generation in widespread areas of the frontal [29, 30], temporal [31, 32] and parietal [33] cortices, including temporo-parietal junction [34], as well as parieto-occipital cortex [35]. Therefore, all P300 generation sites identified with both MEG and ECoG in our study are consistent with previously described sites of P300 generation. The reason for only partial overlap between MEG- and ECoG-identified P300 sites in our study can be explained by different approaches utilized for P300 source/response detection, respectively. Future studies should address the issue of differences in these approaches. Finally, the approaches leading to localization of the P300 generation sites that provide with the highest P300 speller performance accuracy need to be isolated and utilized.

In summary, in our current study, the MEG proved to be a reliable navigation tool for selection of ECoG-based P300 speller sites. Several locations from different brain regions responsible for P300 generation have been selected with MEG to drive ECoG-based P300 speller BCI with reliable performance accuracy. In order to achieve future goal of using minimally invasive chronic BCIs, it is important to identify single P300 generation sites that provide the maximum BCI performance accuracy. An improvement of P300 response source localization approaches with MEG is required to achieve higher ECoG-based P300 speller accuracy. Future studies aiming at attaining these goals are underway.

Acknowledgements Authors want to express their gratitude to Dr. Brendan Allison for his valuable editorial suggestions.

References

1. W. Wang et al., An electrocorticographic brain interface in an individual with tetraplegia. PLoS ONE **8**(2), e55344 (2013)
2. M. Korostenskaja et al., Non-invasive versus invasive brain-computer interfaces. Abstracts from the Fifth International Brain-Computer Interface Meeting 2013 (Asilomar Conference Center, Pacific Grove, CA, USA, 2013)
3. M. Korostenskaja et al., Improving ECoG-based P300 speller accuracy. Proceedings of the 6th International Brain-Computer Interface Conference 2014, vol. 088, (2014) p. 1–4
4. E. Pataraia et al., Magnetoencephalography in presurgical epilepsy evaluation. Neurosurg. Rev. **25**(3), 141–59; discussion 160-1 (2002)
5. J.R. Wolpaw, Brain-computer interfaces as new brain output pathways. J. Physiol. **579**(Pt 3), 3–9 (2007)
6. W. Speier, I. Fried, N. Pouratian, Improved P300 speller performance using electrocorticography, spectral features, and natural language processing. Clin. Neurophysiol. **124**(7), 1–8 (2013)
7. S. Silvoni et al., Amyotrophic lateral sclerosis progression and stability of brain-computer interface communication. Amyotroph Lateral Scler Frontotemporal Degener **14**(5–6), 3–6 (2013)

8. Z.R. Lugo et al., A vibrotactile p300-based brain-computer interface for consciousness detection and communication. Clin. EEG Neurosci. **45**(1), 14–21 (2014)
9. J.E. Huggins, P.A. Wren, K.L. Gruis, What would brain-computer interface users want? Opinions and priorities of potential users with amyotrophic lateral sclerosis. Amyotroph Lateral Scler **12**(5), 18–24 (2011)
10. J.L. Collinger et al., Functional priorities, assistive technology, and brain-computer interfaces after spinal cord injury. J. Rehabil. Res. Dev. **50**(2), 45–60 (2013)
11. J. Viventi, J.A. Blanco, Development of high resolution, multiplexed electrode arrays: opportunities and challenges. 2012 IEEE Conference on Proceedings of Engineering in Medicine and Biology Soceity (2012), p. 1394–1396
12. J. Viventi et al., Flexible, foldable, actively multiplexed, high-density electrode array for mapping brain activity in vivo. Nat. Neurosci. **14**(12), 599–605 (2011)
13. Y. Zhao et al., Implanted miniaturized antenna for brain computer interface applications: analysis and design. PLoS ONE **9**(7), e103945 (2014)
14. B. Rubehn et al., A MEMS-based flexible multichannel ECoG-electrode array. J. Neural Eng. **6**(3), 036003 (2009)
15. C. Henle et al., First long term in vivo study on subdurally implanted micro-ECoG electrodes, manufactured with a novel laser technology. Biomed. Microdevices **13**(1), 59–68 (2011)
16. H. Toda et al., Simultaneous recording of ECoG and intracortical neuronal activity using a flexible multichannel electrode-mesh in visual cortex. Neuroimage **54**(1), 3–12 (2011)
17. E.C. Leuthardt et al., Microscale recording from human motor cortex: implications for minimally invasive electrocorticographic brain-computer interfaces. Neurosurg. Focus **27**(1), E10 (2009)
18. C.W. Anderson et al., A comparison of EEG systems for use with brain computer interfaces in home environments. Psychophysiology, 2013. **50** (Issue Supplement S1), p. S6
19. N.E. Crone, A. Sinai, A. Korzeniewska, High-frequency gamma oscillations and human brain mapping with electrocorticography. Prog. Brain Res. **159**, 75–95 (2006)
20. T. Ball et al., Signal quality of simultaneously recorded invasive and non-invasive EEG. Neuroimage **46**(3), 8–16 (2009)
21. N.J. Hill et al., Recording human electrocorticographic (ECoG) signals for neuroscientific research and real-time functional cortical mapping. J. Vis. Exp. **64** (2012)
22. T. Kim et al., Spatiotemporal compression for efficient storage and transmission of high-resolution electrocorticography data. 2012 IEEE Conference on Proceedings of Engineering in Medicine and Biology Soceity (2012), p. 1012–1015
23. S. Kellis et al., Classification of spoken words using surface local field potentials. 2010 IEEE Conference on Proceedings of Engineering in Medicine and Biology Soceity (2012), p. 3827–3830
24. S. Kellis et al., Decoding spoken words using local field potentials recorded from the cortical surface. J. Neural Eng. **7**(5), 056007 (2010)
25. J. Xiang et al., Noninvasive localization of epileptogenic zones with ictal high-frequency neuromagnetic signals. J Neurosurg Pediatr **5**(1), 13–22 (2010)
26. M.S. Hamalainen et al., Magnetoencephalography—theory, instrumentation, and applications to noninvasive studies of the working human brain. Rev. Mod. Phys. **65**, 13–97 (1993)
27. J. Mellinger et al., An MEG-based brain-computer interface (BCI). Neuroimage **36**(3), 81–93 (2007)
28. L.A. Farwell, E. Donchin, Talking off the top of your head: toward a mental prosthesis utilizing event-related brain potentials. Electroencephalogr. Clin. Neurophysiol. **70**(6), 10–23 (1988)
29. U. Volpe et al., The cortical generators of P3a and P3b: a LORETA study. Brain Res. Bull. **73** (4–6), 20–30 (2007)
30. P. Baudena et al., Intracerebral potentials to rare target and distractor auditory and visual stimuli III. Frontal cortex. Electroencephalogr. Clin. Neurophysiol. **94**(4), 51–64 (1995)

31. E. Halgren et al., Intracerebral potentials to rare target and distractor auditory and visual stimuli. II. Medial, lateral and posterior temporal lobe. Electroencephalogr. Clin. Neurophysiol. **94**(4), 29–50 (1995)
32. E. Halgren et al., Intracerebral potentials to rare target and distractor auditory and visual stimuli. I. Superior temporal plane and parietal lobe. Electroencephalogr. Clin. Neurophysiol. **94**(3), 191–220 (1995)
33. M.E. Smith et al., The intracranial topography of the P3 event-related potential elicited during auditory oddball. Electroencephalogr. Clin. Neurophysiol. **76**(3), 35–48 (1990)
34. C. Mulert et al., The neural basis of the P300 potential. Focus on the time-course of the underlying cortical generators. Eur. Arch. Psychiatry Clin. Neurosci. **254**(3), 1–8 (2004)
35. I. Kiss, R.M. Dashieff, P. Lordeon, A parieto-occipital generator for P300: evidence from human intracranial recordings. Int. J. Neurosci. **49**(1–2), 3–9 (1989)

A Brain-Computer-Interface to Combat Musculoskeletal Pain

N. Mrachacz-Kersting, L. Yao, S. Gervasio, N. Jiang, T.S. Palsson, T.G. Nielsen, D. Falla, K. Dremstrup and D. Farina

Abstract Over the past several years, our group has conceived a completely new technological approach toward BCIs aimed at reversing the maladaptive plasticity induced by musculoskeletal pain. The EEG activity patterns of participants with chronic pain (tennis elbow) were differentiated from those of healthy, age and sex matched controls during real-time movement performance. Our results showed a dominance of power in the alpha frequency range only that was significantly correlated with the intensity of pain (visual analogue scale scale—VAS). Based on this novel finding, a neurofeedback system was developed allowing real-time monitoring of alpha power during idle time and movement execution (wrist extensions). Two bars were shown to the patient on a feedback screen—one containing continuous alpha power, the other only alpha power during the preparation phase of movement execution. The goal of the participant was to maintain the alpha power below the initial baseline value during movement execution. Three patients were tested using this system and their pain intensities were monitored. All participants were successful in decreasing their alpha power across days. This was accompanied by a reduction in their perceived pain VAS scores. In summary, we have developed

N. Mrachacz-Kersting (✉) · S. Gervasio · K. Dremstrup
Department of Health Science and Technology, Center for Sensory-Motor Interaction, Aalborg University, 9220 Aalborg, Denmark
e-mail: nm@hst.aau.dk

L. Yao · N. Jiang
Department of Systems Design Engineering, University of Waterloo, Waterloo, Canada

T.S. Palsson · T.G. Nielsen
Faculty of Medicine, Department of Health Science and Technology, Center for Neuroplasticity and Pain (CNAP), SMI, Aalborg University, Aalborg, Denmark

D. Falla
School of Sport, Exercise and Rehabilitation Sciences, University of Birmingham, Edgbaston, Birmingham B15 2TT, UK

D. Farina
Department of Bioengineering, Imperial College London, London SW7 2AZ, UK

C. Guger et al. (eds.), *Brain-Computer Interface Research*,
SpringerBriefs in Electrical and Computer Engineering,
DOI 10.1007/978-3-319-57132-4_10

a neurofeedback system for musculoskeletal pain that is capable of providing rapid, accurate and reliable neurofeedback in dynamic conditions, allowing the users to train their brain to reduce the pain.

Keywords Brain computer interface · Musculoskeletal pain · EEG

1 Introduction

Since the initial proposition by Daly and colleagues [1], Brain Computer Interfaces (BCIs) have increasingly been developed for the restoration of lost motor function by inducing neuromodulation (for a recent review see [2]). Typically, the participants have suffered from a central nervous system lesion, leading to abnormal movement control. Depending on lesion type, approximately 8–80% of these patients will also present with central neuropathic pain accompanied with a specific EEG signature [3, 4] that is positively correlated with the degree of somatosensory reorganization [5, 6]. Such patients require a different approach to rehabilitation through a BCI, since e.g. spinal cord injured patients present with reduced event-related desynchronization during motor imagery and a decreased power in the resting state [3], ultimately leading to a decreased classification accuracy. We have also shown that the peak negative amplitude of the movement related cortical potential (MRCP) is enhanced in this patient group; however, classification remains around 65%, likely due to its greater variability specifically in the rebound phase [4].

Similar to neuropathic pain conditions, musculoskeletal pain originating at the periphery has a significant central component [7–9] leading to reorganization within the cerebral cortex [10]. Using non-invasive transcranial magnetic stimulation (TMS) to map the motor cortical (M1) representation of two wrist extensor muscles (extensor carpi radialis brevis (ECRB) and extensor digitorum), patients with chronic elbow pain (lateral epicondylalgia) presented with an increased overall excitability and a closer proximity to their respective centers of gravity. These alterations were significantly correlated with the severity of pain, indicating that they are maladaptive [10]. Human experimental pain models, which mimic chronic pain states, reveal that significant maladaptive plasticity (i.e. negative alterations in the connections within the brain) occurs in the chronic musculoskeletal pain state that may lead to unfavorable alterations in the way the central nervous system controls the musculoskeletal system [11–13]. In an attempt to further understand the central changes in the chronic condition, we have quantified this reorganization during the transition from acute to sustained (chronic) pain using a novel model capable of inducing progressive muscle soreness, mechanical hyperalgesia, and temporal summation of pressure pain that can last up to 14 days [14, 15]. Nerve growth factor (NGF) was administered as a bolus injection of 5 μg (0.2 mL) into the right ECRB on Days 0 and 2. Corticomotor excitability and maps were assessed on Day 0, 2, 4 and 14. We demonstrated that the cortex commences its adaptation process already at day 4 of the induced pain and more importantly, at day 14 when the pain has

subsided, some of these changes persisted [16]. The above studies underline that even though musculoskeletal pain may appear as a localized event, central nervous system structures play a key role in its development and experience [17].

A recent review has highlighted several non-pharmacological treatments designed to restore normal brain function concomitantly with a reduction of chronic musculoskeletal pain [18]. These include repetitive transcranial magnetic stimulation (rTMS), transcranial direct current stimulation (tDCS) and neurofeedback. The central idea behind restoring brain activity patterns rather than relying on pharmacological treatments that reduce the pain symptom, is to avoid maladaptive alterations that may lead to secondary problems (i.e. altered movement patterns when performing a task that will induce pain in other areas thus adding to the problem rather than relieving it). In order to retrain the brain, and induce a relearning of the correct movement patterns and thereby reverse the maladaptive cortical reorganization, the mechanisms behind learning need to be satisfied. The current belief is that appropriate induction of plasticity requires the correlated activation of the relevant neural structures ("neurons that fire together, wire together") [19]. Treatments targeting the final output stage of the brain that activates the muscles that produce the movement (e.g. the motor cortex), need to satisfy this principle. In neurofeedback approaches, the user imagines performing a specific task (also called motor imagery (MI)) that normally produces pain (e.g. reaching movement in patients with tennis elbow) while the EEG activity is continuously monitored. The EEG signals associated with the pain are extracted in real time using mathematical algorithms, and provide continuous visual feedback to the user. In this way, the user learns to modify the brain waves to reduce the painful sensation, and an association is formed between the experience of pain and the neurofeedback.

For the user to learn to associate negative brain activity with the painful sensation and its opposite, the positive brain activity with a state of no pain, it is imperative to extract relevant signals affected during chronic musculoskeletal pain. To date, there is no clear consensus on this topic. Several studies have investigated EEG oscillations in central neuropathic pain [3, 20] and musculoskeletal pain [21], although these have been restricted to either resting state or motor imagery (MI). While both types of pain exhibit a frequency specific signature in their EEG patters, when a person is performing a motor task, the effect on the EEG waves may be different. Current neurofeedback for pain treatment seeks to reduce beta (13–35 Hz) oscillations while increasing alpha (8–12 Hz) or theta (4–7.5 Hz) oscillations [22]. However, this is heuristically determined based on previous experience rather than known mechanisms [3]. A further complication with current neurofeedback is that MI enhances pain and thus may not be as useful when treating patients with chronic pain such as tennis elbow. Performing the movement may, in these cases, be more appropriate specifically when using neurofeedback as a treatment modality.

Currently, little is known on the EEG signatures of musculoskeletal pain. Past studies have investigated alterations in the power of various frequency bands following the artificial induction of this pain using hypertonic saline injections [21].

These have been restricted to the resting state. However, it is well known that pain interacts with movement, and thus the patterns are likely different than in the resting state.

As a next step, we therefore sought to obtain a deeper understanding of this type of pain during movement performance. Since the enormous indirect socioeconomic costs due to chronic musculoskeletal pain far exceed those estimated for heart disease, cancer and diabetes [23] and new non-pharmacological treatment approaches [18] are highly desirable, our proposed neurofeedback system has the potential to be one of the new exciting approaches for BCIs in the future.

2 EEG Signatures of Musculoskeletal Pain

Several preliminary studies have been completed that characterize the alterations in EEG parameters induced by pain either in patients (n = 10, 38 ± 11 years) or in healthy participants (n = 19, 26 ± 4 years) prior to (HnP) and following (HwP) injections of hypertonic saline. During the experimental session, participants were seated in a chair in an upright position with the elbow joint extended at 170 ± 10°, the upper arm and shoulder fixated with Velcro tape and the forearm fully pronated. Following assessments of pressure pain thresholds (PPT) and the visual analog scale (VAS) for pain, participants had to complete four movement tasks with at least a 5-min rest interval between them, as follows: 1. Three maximum isometric voluntary contraction (MIVC) of the wrist extensors with a 1 min rest period between trials; 2. 30 index finger extensions; 3. 30 palmar grips and 4. 30 dynamic wrist extensions. Participants were asked to perform the tasks at a self-selected pace, but at a minimum frequency of 0.8 Hz and the order of tasks 2–4 was randomized. PPTs and VAS measures were repeated following each movement task. For healthy participants, all measures and tasks were performed either without pain or following a bolus injection of 5.7% hypertonic saline into the ECR of the dominant arm.

Monopolar EEG signals were recorded using an active EEG electrode system (g. GAMMAcap^2, Austria) and g. USBamp amplifier (gTec, GmbH, Austria) from FP1, F3, Fz, F4, FC5, FC1, FC2, FC6, T7, C3, Cz, C4, T8, CP5, CP1, CP2, CP6, P3, Pz and P4 according to the standard international 10–20 system. The channel selection was based on the large Laplacian with C3 or C4 (depending on the affected side) as the central channel [24]. The reference electrode was placed on Fz and the ground on the left earlobe. A single channel surface electromyography (EMG) was recorded from the extensor carpi radialis (ECR) muscle to control for the subject's movement. All signals were sampled at a frequency of 256 Hz (16 bits accuracy) and hardware filtered from 0 to 100 Hz. Power was calculated using 1 s Hamming windows with 1 sample increment within the alpha, beta, theta and gamma band from continuous EEG (256 Hz) at all electrode locations.

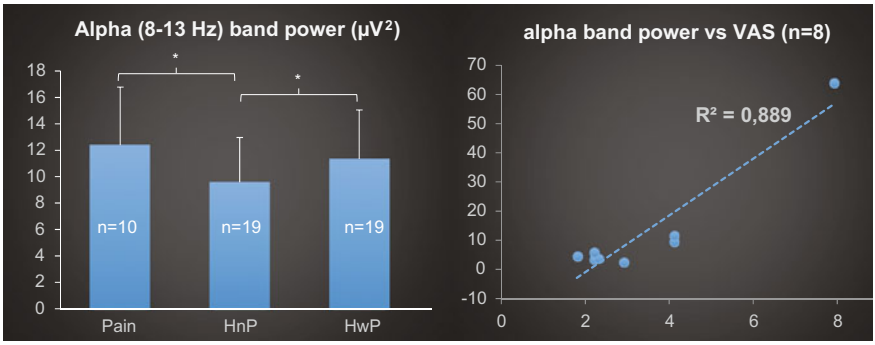

Fig. 1 Absolute power in the alpha band and its relation to the VAS scale

Figure 1 shows Alpha power from electrode location C3 across all subjects. Alpha power was significantly increased in the pain patients compared to HnP ($p < 0.05$), while induced pain (HwP) showed a similar trend (Fig. 1). This was correlated with the participants' perceived pain (VAS).

3 The Neurofeedback System

Figure 2 outlines our proposed approach for a neurofeedback system to reduce musculoskeletal pain, as well as the preliminary results from $n = 1$ pain patient. For the first 20 trials, participants were asked to perform wrist extensions with a light weight held in their hand. The power within the alpha frequency was subsequently calculated and served as the baseline value in the following trials, during which the alpha band power was continuously displayed to the participant in the left panel of the feedback screen. A green bar indicated a decrease in power (a desynchonization) while a red bar referred to an increase in power (a synchronization). Participants were asked to try to keep the bars green. Upon movement performance, the system fed back to the participant the power within the same band, but only for the preparation phase of the movement (right bar of the feedback screen, Fig. 2). A successful trial meant that this bar was green, and thus that power was maintained below the baseline value.

The first of three blocks of 50 trials were performed, and the percentage displayed on the screen indicated to the participant how many successful trials were completed. During the second block, the baseline values were adjusted based on those obtained for the previous block. For the third block, the baseline values were adjusted based on the second block. In this way, the task difficulty increased for each block, ensuring the participants were trained appropriately. To date, three patients have been exposed to this neurofeedback system. Results from one patient are shown in the two right hand graphs of Fig. 2. The change in sensory-motor-rhythm (SMR) during the movement execution was evident. The

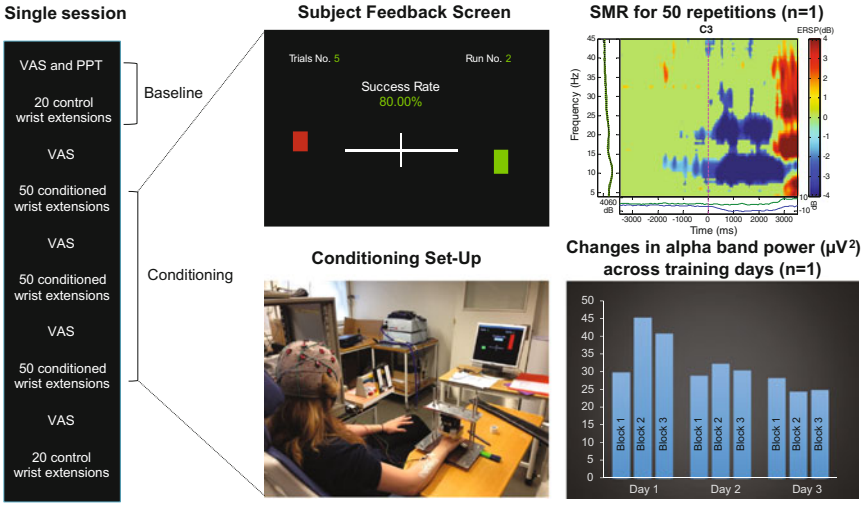

Fig. 2 Experimental protocol for the neurofeedback session, set-up and preliminary results from n = 1

alpha power was decreased within a session but also across the three sessions (performed on separate days). More importantly, these decreases in power were accompanied by decreases in the VAS scale (from 5.6 after session one to 0 at the end of session three), indicating that the patient felt less pain by session number three.

4 Discussion and Long-Term Perspectives

The field of BCI has been expanding rapidly over the past decade, with researchers seeking to widen the application to a larger patient population. BCI systems designed for neuromodulation in patients suffering from a central nervous system lesion provide a prime example of such an endeavor. Here, we propose an application with even wider and deeper impact, since musculoskeletal pain affects between 13.5 and 47% of the general population. Our recent evidence has shown that this condition is accompanied by significant reorganization in cortical plasticity that even outlasts the experience of pain. The future challenge is to reverse this maladaptive process, and a BCI approach is ideally suited to meet these demands.

Acknowledgements We wish to acknowledge our participants and all of the students from the laboratory, both past and present.

References

1. J.J. Daly, N. Hogan, E.M. Perepezko, H.I. Krebs, J.M. Rogers, K.S. Goyal, M.E. Dohring, E. Fredrickson, J. Nethery, R.L. Ruff, Response to upper-limb robotics and functional neuromuscular stimulation following stroke. J. Rehabil. Res. Dev. **42**, 723–736 (2005)
2. S.R. Soekadar, N. Birbaumer, M.W. Slutzky, L.G. Cohen, Brain-machine interfaces in neurorehabilitation of stroke. Neurobiol. Dis. **83**, 172–179 (2015)
3. A. Vuckovic, M.A. Hasan, M. Fraser, B. A. Conway, B. Nasseroleslami, D.B. Allan, Dynamic oscillatory signatures of central neuropathic pain in spinal cord injury. J Pain (2014)
4. R. Xu, N. Jiang, A. Vuckovic, M. Hasan, N. Mrachacz-Kersting, D. Allan, M. Fraser, B. Nasseroleslami, B. Conway, K. Dremstrup, D. Farina, Movement-related cortical potentials in paraplegic patients: abnormal patterns and considerations for BCI-rehabilitation. Front. Neuroeng. **7**, 35 (2014)
5. P.J. Wrigley, S.M. Gustin, P.M. Macey, P.G. Nash, S.C. Gandevia, V.G. Macefield, P. J. Siddall, L.A. Henderson, Anatomical changes in human motor cortex and motor pathways following complete thoracic spinal cord injury. Cereb. Cortex **19**, 224–232 (2009)
6. S.M. Gustin, P.J. Wrigley, P.J. Siddall, L.A. Henderson, Brain anatomy changes associated with persistent neuropathic pain following spinal cord injury. Cereb. Cortex **20**, 1409–1419 (2010)
7. T. Graven-Nielsen, L. Arendt-Nielsen, Peripheral and central sensitization in musculoskeletal pain disorders: an experimental approach. Curr. Rheumatol. Rep. **4**, 313–321 (2002)
8. L. Arendt-Nielsen, T. Graven-Nielsen, Muscle pain: sensory implications and interaction with motor control. Clin. J. Pain **24**, 291–298 (2008)
9. T. Graven-Nielsen, L. Arendt-Nielsen, P. Madeleine, P. Svensson, Pain mechanisms in chronic musculoskeletal conditions. Ugeskr. Laeger **172**, 1824–1827 (2010)
10. S.M. Schabrun, P.W. Hodges, B. Vicenzino, E. Jones, L.S. Chipchase, Novel adaptations in motor cortical maps: the relation to persistent elbow pain. Med. Sci. Sports Exerc. **47**, 681–690 (2015)
11. S.M. Schabrun, P.W. Hodges, Muscle pain differentially modulates short interval intracortical inhibition and intracortical facilitation in primary motor cortex. J. Pain. **13**, 187–194 (2012)
12. S.M. Schabrun, E. Jones, J. Kloster, P.W. Hodges, Temporal association between changes in primary sensory cortex and corticomotor output during muscle pain. Neuroscience **235**, 159–164 (2013)
13. T. Graven-Nielsen, L. Arendt-Nielsen, Assessment of mechanisms in localized and widespread musculoskeletal pain. Nat. Rev. Rheumatol. **6**, 599–606 (2010)
14. K. Hayashi, S. Shiozawa, N. Ozaki, K. Mizumura, T. Graven-Nielsen, Repeated intramuscular injections of nerve growth factor induced progressive muscle hyperalgesia, facilitated temporal summation, and expanded pain areas. Pain **154**, 2344–2352 (2013)
15. M.J. Bergin, R. Hirata, C. Mista, S.W. Christensen, K. Tucker, B. Vicenzino, P. Hodges, T. Graven-Nielsen, Movement evoked pain and mechanical hyperalgesia after intramuscular injection of nerve growth factor: a model of sustained elbow pain. Pain Med. **16**, 2180–2191 (2015)
16. S. Schabrun, S.W. Christensen, N. Mrachacz-Kersting, T. Graven-Nielsen, Motor cortex reorganization and impaired function in the transition to sustained muscle pain. Cereb. Cortex (2015)
17. B.K. Coombes, L. Bisset, B. Vicenzino, A new integrative model of lateral epicondylalgia. Br. J. Sports Med. **43**, 252–258 (2009)
18. M.P. Jensen, S. Hakimian, L.H. Sherlin, F. Fregni, New insights into neuromodulatory approaches for the treatment of pain. J Pain. **9**, 193–199 (2008)
19. D.O. Hebb, *The Organization of Behavior: A Neuropsychological Theory* (Lawrence Erlbaum Associates Inc, Mahwah, NJ, 1949)

20. L. Michels, M. Moazami-Goudarzi, D. Jeanmonod, Correlations between EEG and clinical outcome in chronic neuropathic pain: surgical effects and treatment resistance. Brain Imag. Behav. **5**, 329–348 (2011)
21. P.F. Chang, L. Arendt-Nielsen, T. Graven-Nielsen, A.C.N. Chen, Psychophysical and EEG responses to repeated experimental muscle pain in humans: pain intensity encodes EEG activity. Brain Res. Bull. **59**, 533–543 (2003)
22. M.P. Jensen, C. Grierson, V. Tracy-Smith, S.C. Bacigalupi, S. Othmer, Neurofeedback treatment for pain associated with complex regional pain syndrome type I. J. Neurother. **11**, 45–53 (2007)
23. J. Christensen, L. Bilde, A. Gustavsson, Socio-economic consequences of pain-intensive diseases in Denmark. (2011)
24. D.J. McFarland, L.M. McCane, S.V. David, J.R. Wolpaw, Spatial filter selection for EEG-based communication. Electroencephalogr. Clin. Neurophysiol. **103**, 386–394 (1997)

Recent Advances in Brain-Computer Interface Research—A Summary of the BCI Award 2015 and BCI Research Trends

Christoph Guger, Brendan Allison and Junichi Ushiba

1 The 2015 Winners

The preceding chapters presented work from projects nominated for the 2015 BCI Research Award. Being nominated is a significant achievement, and thus the nominees and the audience were excited to learn who won first, second, and third place during the Gala Awards Ceremony.

The BCI Award 2015 Winner Is

Guy Hotson[1], David P McMullen[2], Matthew S. Fifer[3], Matthew S. Johannes[4], Kapil D. Katyal[4], Matthew P. Para[4], Robert Armiger[4], William S. Anderson[2], Nitish V. Thakor[3], Brock A. Wester[4], Nathan E. Crone[5] ([1]Department of Electrical and Computer Engineering, Johns Hopkins University, US, [2]Department of Neurosurgery, Johns Hopkins University, US, [3]Department of Biomedical Engineering, Johns Hopkins University, US, [4]Applied Neuroscience, JHU Applied Physics Laboratory, US, [5]Department of Neurology, Johns Hopkins University, US).

C. Guger (✉) · B. Allison
14 Sierningstraße, 4521 Schiedlberg, Austria
e-mail: guger@gtec.at

B. Allison
e-mail: allison@gtec.at

J. Ushiba
3-14-1 Hiyoshi, Kohoku-Ku, 223-8522 Yokohama, Kazagawa, Japan
e-mail: ushiba@bio.keio.ac.jp

C. Guger et al. (eds.), *Brain-Computer Interface Research*,
SpringerBriefs in Electrical and Computer Engineering,
DOI 10.1007/978-3-319-57132-4_11

Fig. 1 Christoph Guger (*left*, organizer), Guy Hotson (Winner of 2015), Kenji Kato (*3rd place*), Ron Hogri (*2nd place*), Brendan Allison (*right*, moderator)

Individual Finger Control of the Modular Prosthetic Limb using High-Density Electrocorticography in a Human Subject

Junichi Ushiba, chair of the 2015 jury, called the winning idea "A creative and well-executed project that could lead to improved prosthetic control for patients" (Figs. 1 and 2).

The BCI Award 2015 2nd Place Winner Is

Roni Hogri[1,3], Simeon A. Bamford[2,4], Aryeh H. Taub[1,5] ([1]Psychobiology Research Unit, Tel Aviv University, IL, [2]Complex Systems Modeling Group, Istituto

Fig. 2 The flyer for the 2016 BCI Research Award

Superiore di Sanità, IT, [3]Department of Neurophysiology, Medical University of Vienna, AT, [4]Inilabs Gmbh, CH, [5]Department of Neurobiology, Wiezmann Institute of Science, IL).

De novo experience-based learning in rats interfaced with a "cerebellar chip"

The 3rd Place Winner Is

Kenji Kato, Masahiro Sawada, Tadashi Isa, Yukio Nishimura (National Institute for Physiological Sciences, Aichi, JP).

Restoration for the volitional motor function via an artificial neural connection

At the Gala Award Ceremony, Dr. Guger also thanked the experts in the 2015 jury:

Junichi Ushiba (chair of the jury 2015)

Masayuki Hirata

Nuri Firat Ince

Zachary Freudenburg

José del R. Millán

Sydney Cash

Tomasz M. Rutkowski.

2 Directions and Trends Reflected in the Awards

The four components of a BCI presented in the introduction have provided a solid framework for categorizing the BCI Research Award submissions to analyze trends in BCI research. This year's 63 submissions are grouped across four tables according to these four components: sensors; signal processing algorithms; outputs; and interaction environments. We also summarize submissions from prior years. These four tables thus provide some data to explore how the four BCI components have evolved over the years. In the top row of each table, N shows the total number of submissions that year. The numbers in the cells below equal the percentage of submissions with that property.

Sensors: Table 1 explores the different types of input signals used in the submitted projects. As with previous years, the 2015 submissions focused primarily on EEG-based systems, similar to most BCI articles. 76.1% of all submissions used EEG, which is slightly higher than previous years but still close to the average of 72.1%. The submissions also reflected other non-invasive sensor systems, such as

Table 1 Type of input signal for the BCI system

Property	2015% (N = 63)	2014% (N = 69)	2013% (N = 169)	2012% (N = 68)	2011% (N = 64)	2010% (N = 57)
EEG	76, 1	72, 5	68, 0	70, 6	70, 3	75, 4
fMRI	4, 8	2, 9	4, 1	1, 5	3, 1	3, 5
ECoG	9, 5	13, 0	9, 4	13, 3	4, 7	3, 5
NIRS	–	1, 4	3, 0	1, 5	4, 7	1, 8
Spikes	4, 8	8, 7	7, 1	10, 3	12, 5	–
Other signals	4, 8	4, 3	13, 0	2, 9	1, 6	–
Electrodes	–	–	6, 5	1, 5	1, 6	–

Table 2 Real-time BCIs and off-line algorithms in projects submitted to the BCI Awards

Property	2015% (N = 63)	2014% (N = 69)	2013% (N = 169)	2012% (N = 68)	2011% (N = 64)	2010% (N = 57)
Real-time BCI	96, 8	87, 0	92, 3	94, 1	95, 3	65, 2
Off-line algorithms	3, 2	8, 7	5, 3	4, 4	3, 1	17, 5

fMRI, and invasive methods like ECoG and neural spikes. Other signals included MEG.

Signal processing: In 2015, almost all submissions presented a real-time BCI system, and only two of 63 submissions (neither of which were nominated) presented off-line work. This result indicates that real-world applications are approaching (Table 2).

Output/application: The third essential component of any BCI is the output. Table 3 shows the applications that the 2015 submissions controlled. Most of the submissions improved the technology by developing new hardware and software, developed new platforms, or developed control interfaces for wheelchairs, robots or prosthetic devices including exoskeletons. Many BCI systems were used for control or spelling applications. Interestingly, only 4.8% presented stroke or neural plasticity applications, which received more attention in previous years. These submissions did relatively well with the jury.

Environment/interaction: Table 4 shows the type of neural activity used for control. The most prevalent approach involves motor imagery. Over the past six years, motor imagery BCIs have consistently accounted for about a third of all submissions. P300 and N200 components are mostly used for spelling applications, and the P300 and other ERPs can be used to assess patients. In addition to these types of signals that BCIs read from the brain, some submissions over the years have presented work with brain stimulation or used broad band activity.

Table 3 Type of output system and application

Property	2015% (N = 63)	2014% (N = 69)	2013% (N = 169)	2012% (N = 68)	2011% (N = 64)	2010% (N = 57)
Control	11, 1	17, 4	20, 1	20, 6	34, 4	17, 5
Platform technology	15, 9	13, 0	16, 6	16, 2	9, 4	12, 3
Stroke neural plasticity	4, 8	13, 0	13, 7	26, 5	12, 5	7
Wheelchair robot prosthetics	15, 9	13, 0	11, 8	8, 8	6, 2	7
Spelling	12, 7	8, 7	8, 3	25	12, 5	19, 3
Internet or VR game	4, 8	2, 9	5, 9	2, 9	3, 1	8, 8
Learning	1, 6	5, 8	5, 3	1, 5	3, 1	–
Monitoring, DOC	4, 8	1, 4	4, 7	4, 4	1, 6	–
Stimulation	1, 6	1, 4	3, 6	1, 5		
Authentication speech assessment	4, 8	13, 0	3	–	9, 4	–
Connectivity	–	–	2, 4	1,5	–	–
Music, Art	1, 6	1, 4	1, 8	-	–	
Sensation		–	1, 2	–	1, 6	–
Vision	3, 2	1, 4	1, 2	1, 5		
Epilepsy, Parkinson, Tourette‘s	3, 2	2, 9	1, 2	-	–	–
Depression, Fatigue, ADHD, pain	4, 8	1, 4	–	1, 5	–	–
Neuromarketing, emotion	–	1, 4	–	1, 5	–	–
Ethics	–	1, 4	–	–	–	–
Mechanical ventilation	–	–	–	–	1, 6	–

Table 4 Type of signal used to control BCI

Property	2015% (N = 63)	2014% (N = 69)	2013% (N = 169)	2012% (N = 68)	2011% (N = 64)	2010% (N = 57)
P300/N200/ERP	28, 6	11, 6	11, 8	30, 9	25	29, 8
SSVEP/SSSEP/cVEP	14, 3	11, 6	14,2	16, 2	12, 5	8, 9
Motor imagery	36, 5	37, 7	25, 4	30, 9	29, 7	40, 4
ASSR	–	–	1, 8	–	1, 6	–

3 Conclusion and Future Directions

The Annual BCI-Research Awards have been successful in recognizing and encouraging high quality BCI research innovations. We are proud to announce the jury for 2016:

Mikhail A. Lebedev (chair of the jury 2016),
Alexander Kaplan,
Klaus-Robert Müller,
Ayse Gündüz,
Kyousuke Kamada,
Guy Hotson (winner 2015).

As with prior years, the first place winner from the preceding year is included among the top-notch jury. The jury again includes a strong international focus, led by a chair from a top BCI institute. Dr. Lebedev has been a Professor at Duke University for many years, with a strong emphasis on implantable BCIs. Our 2016 flyer presents more information about the 2016 BCI Research Award.

This year's deadline was March 1, 2016, and the nominees for 2016 have been announced. We have already begun planning next year's book with the new nominees. We are pleased to announce that our editorial staff for the book reviewing the 2016 BCI-Research Award will again include the CEO of G.TEC (Dr. Guger), Dr. Allison, and the chair of the jury, Dr. Lebedev. We hope you have enjoyed this book, and look forward to developing the book for the 2016 Award.